WEAK INTERACTIONS AT HIGH ENERGIES*

John Ellis

Stanford Linear Accelerator Center
Stanford University, Stanford, California 94305

and

CERN
Geneva, Switzerland

Contents

General Introduction

ABSTRACT

...

General Introduction

There is a Yiddish saying "May the Lord preserve you from an inter-
esting life," but we are probably not sorry that life in high energy
physics has been quite interesting lately. Indeed we seem to be passing
through an archetypal scientific revolution,[1] wherein gathering contra-
dictions dissolve into apparent chaos and confusion, and a new orthodoxy
emerges and defines a framework for the next phase of normal accumulative
scientific development. It is not yet clear whether the gauge revolution
will have any indirect effects outside fundamental physics, but its in-
fluence certainly colours the questions we now ask in our high energy
experiments. The purpose of these lectures is to review the phenomeno-
logical implications of the modern spontaneously broken gauge theories of
the weak and electromagnetic interactions,[2] and make some observations
about _which_ high energy experiments probe _what_ aspects of gauge theories.
It should be emphasized at the outset that the evidence in favour of gauge
theories is largely circumstantial--we have yet to find directly incrimi-
nating evidence for gauge ideas, and these lectures are presented in the
hope that they may furnish useful clues for future detective work. Almost

no reference will be made to alternatives to the gauge orthodoxy. This is not because I abhor heresy, but because of a personal feeling that the most fruitful way forward is to take the "standard model" at face value and use it as a paradigm for generating phenomenological questions and experimental tests. And the heretic cause is admirably served by the ingenuity and persistence of Bjorken.[3]

These lectures should be devoted to the weak interactions, but it would be disingenuous to ignore the "standard model" for the strong interactions--quantum chromodynamics or QCD.[4] On a philosophical level, it seems quixotic not to believe that if the gravitational, weak and electromagnetic interactions are described by gauge theories, then so also are the strong interactions--QCD is an unalienable part of the gauge package. On a practical level, many tests of gauge theories of the weak and electromagnetic interactions rely on the quark-parton model[5] for hadrons at large momentum transfers. We surely need some theoretical underpinning for the phenomenological parton model, as a way of exploring its domain of applicability and understanding how it may break down and need modification. On a sentimental level, it would be invidious to exclude the gluon from a shopping list of gauge-theoretical desiderata. Lecture 1 will review some basic QCD phenomenology, including momentum dependent effective quark distributions,[6] the demise of the p_T cutoff,[7] and the search for gluons as sources of hadron jets.[8]

We will then move on to the main business, the phenomenology of weak and electromagnetic interactions at high energies. Lecture 2 will review the status and prospects for the spectroscopy of fundamental fermions (quarks and leptons), and how fermions may be used to probe aspects of

the weak and electromagnetic gauge theory. Lecture 3 will deal with the pursuit, capture and investigation of the anticipated intermediate vector bosons.[9] Lecture 4 discusses miscellaneous possibilities suggested by gauge theories--ranging from the Higgs bosons,[10] which lie at the heart of the spontaneous symmetry breaking mechanism that is supposed to provide the masses of other particles and hence make massive vector boson theories renormalizable, to speculations about proton decay.[11]

The possibilities discussed in these lectures are generally rather conservative and minimal. For example, the simplest $SU(2)_L \times U(1)$ Weinberg-Salam model[12] is often used to illustrate tests of the unified theories of weak and electromagnetic interactions. It has the bare minimum of three massive intermediate vector bosons, one physical Higgs boson, and perhaps as few as six quarks. All other gauge models are more profligate in their generation of new particles and weak interactions. However, we will see that even in this model, the predictable discoveries alone amount to an enticing cornucopia.

1. __Will the Strong Interactions be Weak at High Energies?__

1.1 __Motivation__

Since these lectures are supposed to concentrate on the weak interactions, it may be necessary to present some additional apologia for first discussing the strong interactions.

The first reason is that it is difficult to discuss manifestations of weak interactions at high energies without relying on some background theory of the strong interactions. For example, in e^+e^- annihilation we need the parton model of Fig. 1 for total and jet cross sections,[13] for

calculating weak/electromagnetic interferences, estimating $W^{\pm}$ and Z^0 decay rates, and so on. In order for the parton model to be a reliable tool for incorporating hadrons into the calculation of weak amplitudes and cross sections, we need some way of estimating corrections to the naive parton calculations.[5,13] Such a systematic correction procedure can only come from a theory which explains the apparent weakness of strong interactions at high momentum transfers and the basic validity of the parton model in this limit. As another example, consider deep inelastic lepton-hadron scattering (Fig. 2), where Bjorken scaling[14] is a good first order approximation to the systematics of the data,[15] but where deviations from scaling seem to have a coherent pattern. We must seek some understanding of these scaling deviations if we are to disentangle the appearance of new quark thresholds from other effects in deep inelastic lepton-hadron scattering. Another process where it is important to understand whether the parton model of Fig. 3 is applicable is the Drell-Yan[16] process: hadron + hadron → lepton pair + anything. This process is being proposed[9] as a way to produce the intermediate vector bosons and Higgs particles in hadron-hadron collisions. We would like to know whether the naive parton cross section estimates of Fig. 3 should be regarded as reliable, or whether they may acquire large scaling deviations analogous to those observed in deep inelastic scattering.[15] We would also like to know whether the differential cross section might be expected to have a different shape from the naive expectations, for example whether the $\langle p_T \rangle$ of the produced boson should be $O(1)$ GeV as expected in a naive parton model,[5] or might be $O(m_W)$ as some field theories lead you to expect.[1]

Another reason for discussing the strong interactions was mentioned in the general introduction. All strong interaction field theories invoke some sort of bosonic gluon to hold quarks together (e.g., an octet of coloured vector gluons in QCD), and these are constituents of matter as fundamental as the $W^{\pm}$, Z^0 or photon. The experimental isolation of the gluon and determination of its properties (mass, spin, colour) is therefore of fundamental significance, and it would appear arbitrary and unfair to exclude the gluon from a list of gauge goodies to be studied. Present evidence for the existence and nature of the gluon is generally indirect--there is the classic assignment of the missing fraction of the nucleon momentum to gluon partons which do not interact directly with the lepton probes in deep inelastic scattering.[17] More recently, there has been some evidence from scaling violations in neutrino scattering[15] which also indicates indirectly that gluons are present in the nucleon,[18] and probably have spin 1. This evidence will be discussed later in this lecture, but the interested reader is referred to Don Perkins' lectures at this Summer School for a more detailed analysis. These pieces of evidence are welcome, but it would be nice to see more direct manifestations of gluons as hadronic constituents. One possibility for a gluon search is the conjectured gluon jet,[8] which might show up in a hard (high momentum transfer) process when a gluon is bremsstrahled at large angles as in Fig. 4. Other places to look include the decays $\Upsilon \to 3$ gluons[19] or 2 gluons + photon[20] which are expected in QCD (see Fig. 5). At the end of this lecture there will be a discussion of the phenomenological prospects of finding gluons in this way.

There is a final reason for discussing QCD at the outset of these lectures. It is that the author and most other theorists have a strong prejudice that QCD is the correct theory of the strong interactions, and this inevitably colours the way in which we discuss the phenomenology of weak and electromagnetic interactions. The reasons for this consensus are strong but not irresistible. The only[21] field theory which is[22] asymptotically free at high momenta, and hence has a chance of reproducing the gross features of the parton model,[5] is a gauge theory. Also, quarks are apparently not abundant as physical particles in the real world, and QCD is one field theory in which quarks are not obviously unconfined.[23] But as foreshadowed in the general introduction, the best reason for believing in QCD may just be that the gauge principle seems to be a common feature of the other fundamental interactions, and it is philosophically tempting to believe that the gauge principle is universal, although there is no cast-iron motivation for this application of Occam's razor. It should be emphasized that much of the appeal of QCD reflects the lack of a viable alternative, and that conclusive experimental evidence in its favour is still in short supply.[18] Nevertheless, no alternative to QCD will be brooked in these lectures.

The strong interactions result from the QCD lagrangian[4,22,24]

$$\mathcal{L} = -\frac{1}{4} F^a_{\mu\nu} F^{a\mu\nu} + \sum_q \bar{q} \left(i\gamma_\mu D^\mu - m_q \right) q \qquad (1.1)$$

where $F^a_{\mu\nu}$ is the non-Abelian field strength

$$F^a_{\mu\nu} = \partial_\mu A^a_\nu - \partial_\nu A^a_\mu + ig f^{abc} A^b_\mu A^c_\nu \qquad (1.2)$$

and D_μ is the gauge-covariant derivative

$$D_\mu \equiv \frac{\partial}{\partial x^\mu} - ig \frac{\lambda^a}{2} A^a_\mu \qquad (1.3)$$

The theory (1.1) is characterized by a unique, unknown coupling constant
g to be determined by experiment, and an unknown number of quark flavours
q, with their number and masses also undetermined by theory. QCD con-
tains eight gluons A_μ^a which form an adjoint representation of SU(3) acting
on the three colours of quark: red, yellow and blue. There are several
well known phenomenological motivations for the colour degree of freedom,
which include:

--The fact that the lowest-lying baryon octet and decuplet seem to
have wave functions which are symmetric s-waves in space and symmetric in
spin. For the quarks to have the Fermi statistics appropriate to spin
1/2 particles, they must have an internal degree of freedom wherein the
baryon wave function is antisymmetrized. In the colour theory, the
baryon wave function contains a factor $\epsilon_{RYB} q^R q^Y q^B$, and the symmetriza-
tion problem is solved.[25]

--The decay rate for $\pi^0 \to 2\gamma$. According to current algebra and PCAC,
the amplitude for this decay is given by the triangle diagrams of Fig. 6,
and is hence proportional to the number of colours.[26] The rate for the
decay is calculated to be

$$\Gamma(\pi^0 \to 2\gamma) = \frac{m_\pi^3}{64\pi} \left(\frac{\alpha}{\pi f_\pi} \frac{N}{3} \right)^2 \qquad (1.4)$$

where N is the number of colours. If we take N=3 and f_π = 94 MeV, Eq.
(1.4) yields $\Gamma(\pi^0 \to 2\gamma)$ = 7.91 eV, whereas the latest experimental decay
rate is 8.04 ± 0.55 eV.[27]

--A related reason for colour is the cancellation of anomalous
triangle diagrams like those in Fig. 6 which is required[28] to ensure
the renormalizability[29] of a gauge theory of weak and electromagnetic

interactions. In the "standard" $SU(2)_L \times U(1)$ Weinberg-Salam model[12]
this cancellation occurs between doublets, each of which contributes an
anomaly

$$S = \varepsilon_A \left(Q_\nu^2 - Q_i^2 \right) = \frac{1}{2} \left(0 - (-1)^2 \right) = -\frac{1}{2} \qquad (1.5a)$$

and quark doublets, each of which contributes an anomaly

$$S = N\varepsilon_A \left(\left(\frac{2}{3} \right)^2 - \left(-\frac{1}{3} \right)^2 \right) = \frac{N}{6} \qquad (1.5b)$$

If there were no colour factor of N=3 in Eq. (1.5b) we would need three
times as many leptons as quarks, which does not seem to be a good
approximation to the experimental situation!

   --The cross section ratio for $e^+e^- \to \gamma^* \to$ hadrons relative to
$e^+e^- \to \gamma^* \to \mu^+\mu^-$. In the naive parton model[5] this is calculated from
the simple quark loops[13] of Fig. 1 and should be

$$R \equiv \frac{\sigma(e^+e^- \to \gamma^* \to \text{hadrons})}{\sigma(e^+e^- \to \gamma^* \to \mu^+\mu^-)} = N \sum_q Q_q^2 \qquad (1.6)$$

In the absence of colour, this ratio would be 2/3 below charm threshold
and 10/9 above. Experimentally, the ratio is about 2-1/2 below charm
threshold and about 4-1/2 to 5 above.[30] Allowing for (10 to 20)% sys-
tematic experimental errors and the contribution of a heavy lepton above
charm threshold, these values are not inconsistent with the values of 2
and 3-1/3 expected for R if N=3.

   --A closely related prediction is the ratio of semihadronic decays of
the τ relative to purely leptonic decays. We would estimate[31]

$$\Gamma(\tau^- \to \mu^- \bar{\nu}_\mu \nu_\tau) : \Gamma(\tau^- \to e^- \bar{\nu}_e \nu_\tau) : \Gamma(\tau^- \to \text{hadrons} + \nu_\tau) \approx 1:1:N \qquad (1.7)$$

if the semihadronic decays could be calculated using a naive pointlike

coupling of the lepton decay currents to quarks as in Fig. 7. Experi-
mentally, the ratios of these decays are about[32] 1:1:0(4), but we would
not expect the pointlike approximation to quark couplings to be exact
at the low Q^2 involved in τ decay. The fact that the result (1.7) is
even approximately correct indicates that the couplings of the weak
current to the low mass hadronic resonances which dominate τ decay[31,32]
must somehow average out to look like the pointlike coupling to three
colours of quark. It indicates that resonance couplings have some sensi-
tivity to the number of colours.[33]

The above arguments indicate that quarks have a threefold colour
degree of freedom. QCD[4] certainly provides colour with something to do,
but is there some good reason why gluons should not couple to the flavour
group? The simultaneous consideration of strong, weak and electromag-
netic interactions provides a possible answer, in that parity and
strangeness conservation in $D(s)$ can only be guaranteed[34] if the strong
and weak symmetry groups are disjoint and commute. This condition is
satisfied by QCD with its couplings to colour rather than flavour. It
is an example that nontrivial constraints may be imposed on the theory
of the strong interactions by the requirement of consistency with our
ideas about gauge theories of the weak interactions.[2,12] Another such
interconnection arises from considerations of CP violation,[35] and we will
return to it in the fourth lecture. In the meantime we will concentrate
on purely strongly strong interaction problems.

1.2 The Parton Model and Corrections in Field Theory

In the naive parton model[5] of Fig. 2, the collision of a virtual
photon, Z^0 or $W^{\pm}$ with a hadron target is viewed in terms of incoherent

collisions with pointlike parton constituents to be identified as quarks. Because a point has no intrinsic scale, the deep inelastic cross sections would then exhibit naive Bjorken scaling behaviour,[14] and could be simply expressed in terms of quark parton distributions $q(x)$, where $x \equiv -q^2/2p\cdot q$ is the longitudinal momentum fraction of the quark in an infinite momentum frame. Thus we have the usual deep inelastic structure functions

$$W_1^{eN}(\nu,q^2) \to F_1^{eN}(x) = \frac{1}{2} \sum_{q=u,d,\ldots} e_q^2(q(x) + \bar{q}(x))$$

$$\nu W_2^{eN}(\nu,q^2) \to F_2^{eN}(x) = \sum_{q=u,d,\ldots} e_q^2 \, x(q(x) + \bar{q}(x))$$

$$\nu W_2^{\nu N}(\nu,q^2) \to F_2^{\nu N}(x) = 2x(d(x) + \bar{u}(x) + \ldots)$$

$$\nu W_3^{\nu N}(\nu,q^2) \to F_3^{\nu N}(x) = 2(\bar{u}(x) - d(x)) + \ldots \qquad (1.8)$$

Notice that in the naive parton model the Callan-Cross relation[36] applies:

$$2xF_1(x) = F_2(x) \qquad (1.9)$$

This relation and the scaling of deep inelastic structure functions apply only because the transverse momenta of the partons are cutoff arbitrarily[5] —probably to 0 (few hundred GeV). It is also supposed that struck partons fragment into final state hadrons with finite transverse momenta, producing jets in the final state,[13] as indicated in Fig. 8. An alternative way of expressing the scaling laws (1.8) is to allow for the possibility that the quark distributions may depend on the momentum transfer $Q^2 \equiv -q^2$ by defining

$$\nu W_2^{eN}(\nu,q^2) = \sum_{q=u,d,\ldots} e_q^2 \, x(q(x,Q^2) + \bar{q}(x,Q^2)) \qquad (1.10)$$

and then observing that the laws (1.8) correspond to

$$Q^2 \frac{\partial}{\partial Q^2} q(x,Q^2) = 0 \qquad (1.11)$$

We have introduced the logarithmic derivative $Q^2 \frac{\partial}{\partial Q^2}$ in order to keep the left-hand side of Eq. (1.11) dimensionless.

In a renormalizable field theory, the Bjorken scaling predictions (1.8) or (1.11) do not hold,[37] as can be seen by calculating any Feynman diagram. For example, the bremsstrahlung diagrams of Fig. 9(a) and the pair creation diagrams of Fig. 9(b) both depend logarithmically on the Q^2 with which the quark or gluon parton is struck. These diagrams therefore tell us that

$$0 \neq Q^2 \frac{\partial}{\partial Q^2} q(x,Q^2) = O\left(\frac{\alpha_s}{\pi}\right) + \ldots$$
$$0 \neq Q^2 \frac{\partial}{\partial Q^2} G(x,Q^2) = O\left(\frac{\alpha_s}{\pi}\right) + \ldots \qquad (1.12)$$

where α_s is the strong interaction coupling constant $\alpha_s = g^2/4\pi$ in QCD, $G(x,Q^2)$ is the effective gluon distribution, and the dots in Eq. (1.12) include possible higher order terms from more complicated diagrams. The naive parton model[5] assumes that $\alpha_s/\pi \to 0$ at large Q^2, so that the quarks and gluons can be regarded as essentially free in this kinematic limit. The same assumption underlies the parton calculation of the e^+e^- total cross section in terms of the free quark-parton loop[13] of Fig. 1.

It is easy to deduce some qualitative physical implications[38] from the character of the fundamental processes in Fig. 9. The effect of both bremsstrahlung and pair creation is to generate an increase in the density of partons at small x as the momenta of the parent quark-partons

are degraded. Therefore a typical deep inelastic structure function which is quite broad in x at moderately low Q^2 will move in towards x=0 as $Q^2 \to \infty$, decreasing at large x, and rising towards x=0 as indicated in Fig. 10(a). This process may be envisioned intuitively[39] by thinking of the virtual photon (or Z, or W) probe as a sort of microscope with spatial resolution $\Delta x = O(1/Q)$. Therefore a low Q^2 photon will have poor resolution, while a high Q^2 photon will have better resolution. Perhaps it will resolve a parton seen by the low Q^2 probe into a larger number of smaller constituents, each of which has a smaller longitudinal momentum fraction x, as illustrated in Fig. 11. For example, in $O(\alpha_s)$ in QCD, a quark may be resolved into a quark + gluon (corresponding to the bremsstrahlung of Fig. 9(a)) and a gluon may be resolved into a $q\bar{q}$ or gluon pair (corresponding to the pair creation of Fig. 9(b) in the gluon field of the hadron). The fundamental processes at the root of scaling violation are therefore seen to be radiative corrections analogous to those familiar from high energy electromagnetic showers in QED.

So far we have not made much use of the specific features of QCD--most field theories have some sort of gluon, and the basic Feynman diagrams and resulting qualitative picture (Fig. 10(a)) of scaling violations is common to many field theories.[37,38,39] Thus the observation[15,40] of this general trend as in Fig. 10(b) is not conclusive evidence in favour of QCD rather than any other field theory. However, there is one feature of QCD which is unique, yields a connection with the parton model and enables quantitative predictions -- as in Fig. 10(c) to be made--the property of asymptotic freedom.[22]

The point is that in a field theory the basic vertex g depends on the momenta q which are fed into it. In perturbation theory as in Fig. 12

$$g \to g + O(g^3 \ln q^2) + O(g^5 \ln^2 q^2) + \dots \qquad (1.13)$$

Fortunately, in QCD the leading logarithms can be summed exactly and give an effective constant which decreases to zero as $Q^2 = q^2 \to \infty$ (Ref. 22):

$$\alpha_s(Q^2) = \frac{g^2(Q^2)}{4\pi} \to \frac{12\pi}{Q^2 \to \infty} \frac{12\pi}{(33-2f) \ln\left(\frac{Q^2}{\Lambda^2}\right)} \qquad (1.14)$$

In formula (1.14) f is the number of quark flavours and Λ^2 is an a priori unknown scale which sets the scale of the Q^2 development of the coupling $\alpha_s(Q^2)$. The complication of a Q^2 dependent coupling does not concern us in QED because the rate of change---$O(\alpha \ln Q^2)$---is very small. In QCD the scale parameter Λ replaces the QED parameter as a way of specifying the strength of the interaction. The derivation[22] of (1.14) will not be discussed in these lectures, though we will see a tantalizing reflection of it later on in this lecture. Instead we will occupy ourselves with exploring the consequences of asymptotic freedom. The general effect will clearly be that perturbation theory for the strong interactions should become evermore applicable as the typical momentum transfer Q^2 of a process $\to \infty$. However, the relatively slow rate of decrease (1.14) of $\alpha_s(Q^2)$ means that one does not always recover the naive scaling expectations of the naive parton model, as we now see.

1.3 Scaling Violations in QCD

In the previous section we saw that naive scaling correspond to $Q^2 \frac{\partial}{\partial Q^2} q(x,Q^2) = 0$, as in the naive parton model, whereas one might expect $Q^2 \frac{\partial}{\partial Q^2} q(x,Q^2) = O\left(\frac{\alpha_s}{\pi}\right) + \ldots$ in an interacting field theory. In QCD where $\alpha_s(Q^2) \to 0$ as $Q^2 \to \infty$, we might hope that the $O\left(\frac{\alpha_s}{\pi}\right)$ approximation to the Q^2 evolution of $q(x,Q^2)$ might be very good. In this order, the only contributions in $O\left(\frac{\alpha_s}{\pi}\right)$ are the basic bremsstrahlung and pair creation processes of Fig. 9, and the rates for them are proportional to $\log Q^2$. The quark parton distribution is characterized by the longitudinal momentum fraction x, and the bremsstrahlung and pair creation probabilities may be written in terms of the longitudinal momentum fraction z carried by the final state parton as in Fig. 12. We therefore specify $P_{A \to B}(z)$ as the probability of parton A emitting a parton B with longitudinal momentum fraction z when Q^2 is changed by dQ^2: by dimensional analysis

$$dP \equiv \left(\frac{\alpha_s}{2\pi}\right) P_{A \to B}(z) \; dz \; \frac{dQ^2}{Q^2} \qquad (1.15)$$

The situation in QCD is analogous to that in QED, where in the Weizsäcker-Williams equivalent photon approximation[41] we talk in terms of the photon density inside an electron being

$$\left(\frac{\alpha}{2\pi}\right)\left(\frac{1 + (1-z)^2}{z}\right) \ln\left(\frac{E}{m_e}\right) \qquad (1.16)$$

corresponding to

$$P_{e \to \gamma} = \left(\frac{1 + (1-z)^2}{z}\right) \qquad (1.17)$$

The density of gluons in a quark is analogous, the only difference being a group theoretical factor from the colour coupling (1.3) of the gluon

field:

$$\frac{1}{N} \sum_a \left(\frac{\lambda^a}{2}\right) \left(\frac{\lambda^a}{2}\right) = \frac{N^2-1}{2N} = \frac{4}{3} \qquad (1.18)$$

so that the final "splitting function" for $q \rightarrow G$ of Fig. 13(a) is:

$$P_{q \rightarrow G}(z) = \frac{4}{3} \left[\frac{1 + (1-z)^2}{z}\right] \qquad (1.19)$$

We can[42] write down the "evolution equations" of the form (1.12) which apply in QCD, just by looking at the basic interactions of Fig. 13:

$$Q^2 \frac{\partial}{\partial Q^2} q(x,Q^2) \sim \left(\frac{\alpha_s}{2\pi}\right) \int_x^1 \frac{dy}{y} \left[q(y,Q^2)P_{q \leftarrow q}\left(\frac{x}{y}\right) + G(y,Q^2)P_{G \leftarrow q}\left(\frac{x}{y}\right)\right] \qquad (1.20)$$

for quarks and

$$Q^2 \frac{\partial}{\partial Q^2} G(x,Q^2) = \left(\frac{\alpha_s}{2\pi}\right) \int_x^1 \frac{dy}{y} \left[q(y,Q^2)P_{q \leftarrow G}\left(\frac{x}{y}\right) + G(y,Q^2)P_{G \leftarrow G}\left(\frac{x}{y}\right)\right] \qquad (1.21)$$

for gluons. Because of the slow logarithmic decline (1.14) of $\alpha_s(Q^2)$, the evolution equations (1.20) imply that the parton distributions $q(x,Q^2)$ and $G(x,Q^2)$ do not scale exactly.

The pattern of scaling violation in QCD is well known,[4,22,43] and usually expressed in terms of theoretically precise, but experimentally arcane, numbers called anomalous dimensions. The connection between our physical picture[38,39] and the academic formalism[4,43] is easily made.[42] Let us consider x moments of the structure functions such as

$$M_n^{(2)}(Q^2) \equiv \int_0^1 dx \, x^{n-2} \, F_2(x,Q^2) \qquad (1.22)$$

which is the type of quantity for which rigorous predictions of QCD are usually expressed.[43] QCD makes predictions[43] of logarithmic violations of scaling:

$$M_n^{(2)}(Q^2) \sim (\ln Q^2)^{-d_n} \qquad (1.23)$$

whereas other field theories[21] are expected to violate scaling by powers[38,39] of Q^2. From the parton expression (1.10) we see that generically

$$M_n^{(2)}(Q^2) = \int_0^1 dx \ x^{n-1} \ q(x,Q^2) \tag{1.24}$$

Let us first consider a flavour <u>nonsinglet</u> combination of quark distributions, such as $u(x,Q^2) - d(x,Q^2)$ which is relevant to the ep-en cross section difference, or $\bar{u}(x,Q^2) - d(x,Q^2)$ which is seen from Eq. (1.8) to be relevant to $F_3^N(x,Q^2)$. The gluon term in the evolution equation (1.20) does not contribute to such a nonsinglet quark distribution $q^{NS}(x,Q^2)$:

$$Q^2 \frac{\partial}{\partial Q^2} \ q^{NS}(x,Q^2) = \left(\frac{\alpha_s}{2\pi}\right) \int_x^1 \frac{dy}{y} \ q^{NS}(y,Q^2) \ P_{q \leftarrow q}\left(\frac{x}{y}\right) \tag{1.25}$$

If we take the moment $\int_0^1 dx \ x^{n-1}$ of this equation, the left-hand side is $Q^2 \frac{\partial}{\partial Q^2} M_n(Q^2)$ and the right-hand side of Eq. (1.25) factorizes neatly:

$$Q^2 \frac{\partial}{\partial Q^2} M_n(Q^2) = \frac{\alpha_s}{2\pi} A_n M_n(Q^2) \tag{1.26}$$

where

$$A_n \equiv \int_0^1 dz \ z^{n-1} \ P_{q \leftarrow q}(z) \tag{1.27}$$

The solution of Eq. (1.26) is quite simple: introducing the notation

$$\alpha_s(Q^2) \approx \frac{1}{b \ \ln \frac{Q^2}{\Lambda^2}} : b \approx \frac{33-2f}{12\pi} \tag{1.28}$$

from Eq. (1.14), we see that Eq. (1.26) implies

$$M_n(Q^2) \approx \tilde{M}_n \ (\ln Q^2)^{A_n/2\pi b} \tag{1.29}$$

Making the comparison with the conventional QCD prediction[4,43] (1.23) it clearly is possible to identify

$$d_n = -\frac{A_n}{2\pi b} \tag{1.30}$$

so that we are able to calculate the famous anomalous dimensions as soon as we determine the "splitting function" $P_{q \leftarrow q}(z)$.[42]

Before doing this, let us just discuss the singlet combinations of parton distributions, which obey somewhat more complicated evolution equations. If we introduce the singlet distribution

$$q^S(x,Q^2) \equiv \sum_{i=1}^{f} \left\{ q(x,Q^2) + \bar{q}(x,Q^2) \right\} \qquad (1.31)$$

it is apparent from Eqs. (1.20) and (1.21) that $q^S(x,Q^2)$ and $G(x,Q^2)$ obey a coupled pair of evolution equations. If we take the moments $\int_0^1 dx \, x^{n-1}$ of these equations we obtain[42] a set of matrix equations

$$Q^2 \frac{\partial}{\partial Q^2} \begin{pmatrix} S_n(Q^2) \\ G_n(Q^2) \end{pmatrix} = \left(\frac{\alpha_S}{2\pi} \right) \begin{pmatrix} A_n & 2f B_n \\ C_n & D_n \end{pmatrix} \begin{pmatrix} S_n(Q^2) \\ G_n(Q^2) \end{pmatrix} \qquad (1.32)$$

where S_n and G_n are the moments of the singlet quark distribution

$$S_n(Q^2) \equiv \int_0^1 dx \, x^{n-1} \, q^S(x,Q^2) \qquad (1.33a)$$

and gluon distribution

$$G_n(Q^2) \equiv \int_0^1 dx \, x^{n-1} \, G(x,Q^2) \qquad (1.33b)$$

respectively. On the right-hand side of Eq. (1.32) the matrix elements A_n were defined in Eq. (1.27), while we have introduced

$$B_n \equiv \int_0^1 dz \, z^{n-1} \, P_{G \leftarrow q}(z) \qquad C_n \equiv \int_0^1 dz \, z^{n-1} \, P_{q \leftarrow G}(z)$$

$$D_n \equiv \int_0^1 dz \, z^{n-1} \, P_{G \leftarrow G}(z) \qquad (1.34)$$

The solution of the coupled equations (1.32) is quite straightforward.
First you must diagonalize the matrices on the right-hand sides

$$
\begin{pmatrix} A_n & 2fB_n \\ C_n & D_n \end{pmatrix} \rightarrow \begin{pmatrix} A_n^+ & 0 \\ 0 & A_n^- \end{pmatrix}
\tag{1.35}
$$

which must be done separately for each moment n. Then the eigenvector
combinations of $S_n(Q^2)$ and $G_n(Q^2)$ evolve separately, with the result that
a singlet moment

$$
M_n^S(Q^2) \sim \tilde{M}_n^+ (\ln Q^2)^{d_n^+} + \tilde{M}_n^- (\ln Q^2)^{d_n^-}
\tag{1.36}
$$

where the singlet anomalous dimensions $d_n^{\pm}$ are determined similarly to the
nonsinglet anomalous dimension

$$
d_n^{\pm} = - \frac{A_{11}^{\pm}}{2\pi b}
\tag{1.37}
$$

Thus the scaling violations in singlet combinations of structure functions
(1.36) are somewhat more devious than those in nonsinglet combinations.
As an added complication, many physically observable structure functions
such as $F_2^{ep}(x, Q^2)$ or $F_2^{vN}(x, Q^2)$ are in fact combinations of singlet and
nonsinglet structure functions, so that all three terms (1.29) and (1.36)
are necessary to fit the data.

1.4 Calculation of the Anomalous Dimensions

We saw in the previous section how the calculation of the anomalous
dimensions reduces[42] to the determination of the splitting functions
$P_{A \rightarrow B}(z)$, and we now proceed to evaluate them. First note that there are
certain trivial constraints which must be satisfied by the splitting
functions. For example, quark number is conserved in the bremsstrahlung

process, so that

$$\int_0^1 dz \ P_{q \leftarrow q}(z) = 0 \qquad (1.38)$$

Also, since it is clear that if you have a quark with momentum fraction z you must have a gluon with momentum fraction (1-z):

$$P_{q \leftarrow q}(z) = P_{q \leftarrow G}(1-z) \qquad (1.39)$$

The relations (1.38) and (1.39) between them imply that the $P_{q \leftarrow q, G}(z)$ obey the momentum conservation condition

$$\int_0^1 dz \ z \left[P_{q \leftarrow q}(z) + P_{q \leftarrow G}(z) \right] = 0 \qquad (1.40)$$

and there is a corresponding condition for gluon momentum conservation

$$\int_0^1 dz \ z \left[P_{G \leftarrow q}(z) + P_{G \leftarrow G}(z) \right] = 0 \qquad (1.41)$$

Between them, the momentum conservation conditions (1.40) and (1.41) ensure that the total momentum of the hadron target is conserved:

$$Q^2 \frac{\partial}{\partial Q^2} \int_0^1 dx \ x \left[\sum_{i=1}^f \left(q_i(x,Q^2) + \bar{q}_i(x,Q^2) \right) + G(x,Q^2) \right] = 0 \qquad (1.42)$$

We will use the conditions (1.38) to (1.41) in a moment to determine the contribution to the splitting functions corresponding to partons which do not interact, corresponding to $\delta(z-1)$ pieces in $P_{q \leftarrow q}(z)$ and $P_{q \leftarrow q}(z)$.

To determine the $P_{A \leftarrow B}(z)$ we first recall the modified Weizsäcker-Williams[41] formula (1.19):

$$P_{q \leftarrow q}(z) = \frac{4}{3} \left[\frac{1 + (1-z)^2}{z} \right] \qquad \text{for } z>0$$

The reciprocity relation (1.39) immediately tells us that

$$P_{q \to q}(z) = \frac{4}{3} \left[\frac{1+z^2}{1-z} \right] \qquad \text{for } z < 1$$

which unfortunately has a singularity at z=1 which must be regularized. Altarelli and Parisi[42,44] choose to do this by replacing

$$\frac{1}{(1-z)} \to \frac{1}{(1-z)_+}$$

which is defined for f(z) regular at z=1 by

$$\int_0^1 dz \, \frac{f(z)}{(1-z)_+} \equiv \int_0^1 dz \, \frac{f(z) - f(1)}{1-z} \tag{1.43}$$

The regularized form of $P_{q \to q}(z)$ does not obey the sum rule (1.38) and must be supplemented by a suitably chosen piece $\propto \delta(z-1)$:

$$P_{q \to q}(z) = \frac{4}{3} \left[\frac{1+z^2}{(1-z)_+} + \frac{3}{2} \, \delta(z-1) \right] \tag{1.44}$$

An elementary calculation[45] of the $q \to q\bar{q}$ pair creation vertex yields

$$P_{q \to q}(z) = \frac{1}{2} \left[z^2 + (1-z)^2 \right] \tag{1.45}$$

which is symmetric between z and (1-z). Finally one can calculate the z<1 part of $P_{G \to G}$ to be

$$P_{G \to G}(z) = 6 \left(\frac{z}{1-z} + \frac{1-z}{z} + z(1-z) \right) \qquad \text{for } z < 1 \tag{1.46}$$

which regularization and the application of the momentum conservation condition (1.41) cause to become

$$P_{G \to G}(z) = 6 \left(\frac{z}{(1-z)_+} + \frac{1-z}{z} + z(1-z) + \left(\frac{11}{12} - \frac{f}{18} \right) \delta(z-1) \right) \tag{1.47}$$

It should be emphasized at this point that the form of the splitting functions (1.19, 1.44, 1.45, 1.47) depends sensitively on the spin of the

gluon. For example, if we had scalar gluons we would have

$$P_{q \leftarrow q}^{(S)} \propto (1-z) - \frac{1}{2}\delta(z-1) \tag{1.48}$$

at lowest order in the q-scalar gluon coupling. We will see in a moment that the forms (1.44) and (1.48) produce very different anomalous dimensions which can be distinguished experimentally.

We are now in a position to compute the anomalous dimensions by taking the moments of the $P_{A \leftarrow B}(z)$ (1.19, 1.44, 1.45, 1.47). We find

$$A_n \equiv \int_0^1 dz \ z^{n-1} P_{q \leftarrow q}(z) = \frac{4}{3}\left(-\frac{1}{2} + \frac{1}{n(n+1)} - 2\sum_{j=2}^{n}\frac{1}{j}\right) \tag{1.49a}$$

$$B_n \equiv \int_0^1 dz \ z^{n-1} P_{g \leftarrow q}(z) = \frac{1}{2}\left(\frac{2+n+n^2}{n(n+1)(n+2)}\right) \tag{1.49b}$$

$$C_n \equiv \int_0^1 dz \ z^{n-1} P_{q \leftarrow g}(z) = \frac{4}{3}\left(\frac{2+n+n^2}{n(n^2-1)}\right) \tag{1.49c}$$

$$D_n \equiv \int_0^1 dz \ z^{n-1} P_{g \leftarrow g}(z) = 3\left(-\frac{1}{6} + \frac{2}{n(n-1)} + \frac{2}{(n+1)(n+2)} - 2\sum_{j=2}^{n}\frac{1}{j} - \frac{f}{9}\right) \tag{1.49d}$$

which are the familiar results of more sophisticated field theoretical calculations.[4,43] Hopefully they have been demystified slightly!

How do the predictions of QCD for scaling violations in the moments of the deep inelastic structure functions compare with the experimental data?[15] This question is addressed in more detail by Don Perkins in his lectures, but let us just pick out a few important points here and now. Consider a nonsinglet structure function, such as $F_2^{ep} - F_2^{en}$, or $F_3^{\nu N}$. Then QCD predicts[41] that

$$M_n(Q^2) \qquad \bar{M}_n (\ln Q^2)^{-d_n} \tag{1.50}$$

with d_n given by (1.30) and (1.49a). The forms (1.30) imply that

$$\ln M_n(Q^2) \approx -d_n \ln Q^2 + (\text{constant})_n \qquad (1.51)$$

If we compare the logarithms of two moments M_n and $M_{n'}$ we should find[18] a straight line with slope

$$\frac{d_n}{d_{n'}} = \frac{A_n}{A_{n'}} = \frac{\left(-\frac{1}{2} + \frac{1}{n(n+1)} - 2\sum_{j=2}^{n}\frac{1}{j}\right)}{\left(-\frac{1}{2} + \frac{1}{n'(n'+1)} - 2\sum_{j=2}^{n'}\frac{1}{j}\right)} \qquad (1.52)$$

The BEBC[18] data for the n=3,4,5 and 6 moments of $F_3^{\nu N}$ agree very well with the QCD predictions (1.52) as shown in Fig. 14. The best fit values for $d_n/d_{n'}$ obtained from the data are compared with QCD in the table below:

TABLE I

	d_5/d_3	d_7/d_3	d_6/d_4
QCD	1.46	1.76	1.29
Scalar Gluon Theory	1.12	1.16	1.06
Experiment	1.50 ± 0.08	1.84 ± 0.20	1.29 ± 0.06

For comparison, we have also included the "predictions"[46] of a scalar gluon theory. If such a theory were to have a coupling g which went to some small fixed value g* as $Q^2 \to \infty$—the only possible way of fixing to get approximate scaling in such a theory—then the moments would scale approximately as

$$M_n(Q^2) \sim \tilde{M}_n(Q^2)^{-\delta_n} \qquad (1.53)$$

where

$$\delta_n \propto a_n \equiv \int_0^1 dz \; z^{n-1} \; P_{q \rightarrow q}^{(S)}(z) \tag{1.54}$$

$$= \left(-\frac{1}{2} + \frac{1}{n(n+1)} \right) \tag{1.55}$$

Plots of the logarithms of the moments should then be straight lines with slopes $\delta_n/\delta_{n'}$, which Eq. (1.55) reveals to be very different from $d_n/d_{n'}$, given by Eq. (1.52). Figure 14 shows that the BEBC[18] data disagree[47] emphatically with the scalar gluon "predictions" (1.55) while agreeing very well with the QCD predictions (1.52). This amounts to a convincing demonstration that the quarks are bremsstrahling vector gluons rather than scalars—the first determination that the gluon spin = 1?

Another important point about the BEBC[18] data is that they indicate a logarithmic, rather than power law variation of the moments with Q^2. If we consider the quantity $M_n(Q^2)^{-1/d_n}$, then QCD (1.50) predicts that it should vary linearly with $\ln Q^2$, and this is consistent with the data shown in Fig. 15. Suppose that the moments had in fact behaved as

$$M_n(Q^2) \sim \bar{M}_n(Q^2)^{-\delta d_n} \tag{1.56}$$

as might have been expected in a (Abelian or non-Abelian) vector gluon theory with a small fixed point coupling g^* as $Q^2 \to \infty$. Then the quantities

$$\ln M_n(Q^2) = -\delta d_n Q^2 + (\text{constant})_n \tag{1.57}$$

as before (1.51), and the theory would also have passed the QCD test in Fig. 14. However

$$\left[M_n(Q^2) \right]^{-1/d_n} \propto (Q^2)^{\delta} \tag{1.58}$$

which fails[47] the test in Fig. 15. Shown for comparison with the straight
line QCD fits to the moments are fits of the form (1.58) with the power
B chosen[47] so as to give similar scaling violations to the data between
$Q^2=1$ and 10 GeV^2. It is apparent that the data are not well fitted by
these curves, and we conclude that such fixed point vector gluon theories
are strongly disfavored.

So far we have only looked at nonsinglet combinations of structure
functions. When we look at singlet structure functions, we get contri-
butions to the scaling violations which come from the pair creation in
the gluon field of Fig. 9(b), as well as the bremsstrahlung of Fig. 9(a).
The BEBC[18] group have analyzed the $F_2^{\nu N}$ structure function using the
amount of bremsstrahlung indicated by their analysis of $F_3^{\nu N}$. They find
strong evidence for an extra contribution coming from pair creation.
The amount of it is sensitive to the gluon distribution assumed, and
they[18] find that the observed scaling violations are consistent with
about $\frac{1}{2}$ the nucleon's momentum being carried by gluons, as found previ-
ously by just looking at $\int_0^1 dx\ F_2^{eN,\nu N}(x,Q^2)$.[17] The interested reader
is referred to Ref. 18 and the lectures of Perkins for more details.

It seems that the QCD analysis of deep inelastic scaling violations
is in very good shape, and probably constitutes the best experimental
evidence to date in favour of the theory. Before abandoning completely
the topic of deep inelastic scaling violations, it may be worth drawing
attention to a few interesting aspects of the evolution equation for-
malism.

There are some important sum rules for deep inelastic scattering
which depend on fundamental properties of the quark model. One example

is the Adler sum rule[48]

$$\int_0^1 \frac{dx}{2x}\left(F_2^{\bar{\nu}p}-F_2^{\nu p}\right) - \int_0^1 dx\left[u(x,q^2) - \bar{u}(x,q^2) - d(x,q^2) + \bar{d}(x,q^2)\right]$$

(1.59)

The right-hand side should be 1 at all Q^2. If we compute $Q^2\frac{\partial}{\partial q^2}$ of the right-hand side we see that it is proportional to $\int_0^1 dx\ P_{q+q}(x) = 0$, since the right-hand side of (1.59) is the n=1 moment of a nonsinglet combination of quark distributions. Thus the "quark conservation" condition (1.38) ensures the validity of the Adler sum rule at all Q^2. A similar analysis applies to the Gross-Llewellyn Smith[49] sum rule

$$\int_0^1 dx\left(F_3^{\nu p}+F_3^{\bar{\nu}p}\right) - -2\int_0^1 dx\left[u(x,q^2) + d(x,q^2) - \bar{u}(x,q^2) - \bar{d}(x,q^2)\right] = -6$$

(1.60)

Another interesting sum rule, which is specific to QCD and unobtainable in the naive parton model, is the momentum sum rule.[43] Let us consider the n=2 moment of the F_2 structure function, which corresponds to combinations of $\int_0^1 dx\ x\ q(x,q^2)$. From Eq. (1.32) we have

$$Q^2\frac{\partial}{\partial q^2}\ S_2(Q^2) - \left(\frac{\alpha_s}{2\pi}\right)\left[A_2 S_2(Q^2) + 2f\ B_2 G_2(Q^2)\right]$$

(1.61)

Let us look for the possibility that $S_2(Q^2)$, the momentum fraction carried by quarks and antiquarks, is independent of Q^2: this will happen if

$$A_2 S_2(Q^2) + 2f\ B_2 G_2(Q^2) = 0$$

(1.62)

The condition (1.62) can be regarded as a relation for the quark and

gluon momentum fractions:

$$\frac{S_2(Q^2)}{G_2(Q^2)} = \frac{-2fB_2}{A_2} = \frac{3f}{16} \qquad (1.63)$$

Since momentum conservation (1.42) ensures that $S_2(Q^2) + G_2(Q^2) = 1$, the condition (1.63) is sufficient to ensure that the momentum fractions carried by both quarks and gluons are independent of Q^2. The condition (1.62) amounts to a sort of equilibrium condition that the amount of momentum that quarks lose to gluons by bremsstrahlung is the same as that which gluons give to quarks by pair creation. This equilibrium can be reached as $Q^2 \to \infty$, in which limit[43]

$$\int_0^1 dx \, F_2^{eN}(x,Q^2) = \int_0^1 dx \, x \sum_q \left[q(x,Q^2) + \bar{q}(x,Q^2) \right] e_q^2 \xrightarrow[Q^2 \to \infty]{} \frac{3f}{16+3f} \langle e_q^2 \rangle \quad (1.64)$$

where the average quark (charge)^2 $\langle e_q^2 \rangle$ is presumably equal to 5/18 because of equal numbers of charge 2/3 and charge -1/3 quarks. The experimental data are consistent with the asymptotic behaviour (1.64) applying for either f=4 or 6. This momentum equilibrium sum rule clearly cannot be derived in the naive parton model,[3] because it relies on the right-hand side of the evolution equation (1.61) being nonzero. In the absence of interactions it is never possible to reach equilibrium. One might wonder what the equilibrium conditions on the higher (n>2) moments of the quark and gluon moment S_n and G_n might be. It is easy to satisfy oneself that there are two independent equations for each such moment which are only satisfied if

$$S_n(Q^2) = G_n(Q^2) = 0 \qquad \text{for all } n > 2 \qquad (1.65)$$

The only solutions to the combined equations (1.63) and (1.65) are distributions with singular support at x=0, as suggested by our intuitive reasoning in Section 1.2. The conditions (1.63) and (1.65) are the ultimate fate of all hadrons at large Q^2: the quantum chromodynamic "heat death".

Before leaving the evolution equations[22] (1.20) and (1.21) it may be amusing to point out one intriguing feature of the gluon splitting function $P_{G \leftarrow G}(z)$ in Eq. (1.47). The coefficient of the $\delta(z-1)$ piece is directly proportional to the lowest order term in the renormalization of the QCD coupling constant (β function), the coefficient b in Eq. (1.14) or (1.28). Is this a coincidence or a profound truth? I don't know, but it would imply that a gluon--whose "gluon in a gluon" distribution $G(x,Q^2)$ would have a $\delta(x-1)$ piece--would become more "pure"--the $\delta(x-1)$ piece would increase as Q^2 --because of the positive value of the coefficient of $\delta(z-1)$ in $P_{G \leftarrow G}(z)$ (1.28) if the number of flavours f is ≤ 16. The increasing "purity" of the gluon wave function is perhaps a harbinger of asymptotic freedom--or perhaps not.

1.5 Search for the Smoking Gluon

So far we have only discussed indirect evidence for the gluon, such as the scaling derivations induced by bremsstrahlung of it and pair production from it. However, the gluon is a constituent of hadronic matter which is as basic as the quark. Therefore we would like to have equally direct evidence for the gluon's existence--from spectroscopy[50] and from jets,[8,13] for example. One effect of the gluons will be to induce scaling violations in the distribution of hadrons within a quark jet. The longitudinal momentum distribution will be softened at large Q^2 by

bremsstrahlung and pair creation in a manner analogous to the effects we
discussed for the deep inelastic structure functions. For example, if
we introduce moments of the inclusive hadron distributions in e^+e^-
annihilation

$$\sigma^n(Q^2) \equiv \int_0^1 dz \; z^{n-1} \frac{d\sigma}{dz} (z, Q^2) \qquad (1.66)$$

where $z \equiv 2E_{hadron}/Q$, then $\sigma^n(Q^2)$ will exhibit logarithmic violations of
scaling just like those (1.29, 1.36) found for deep inelastic leptopro-
duction, with "anomalous dimensions" simply related[31] to the traditional
results (1.40).

Another characteristic of the bremsstrahlung and other field-
theoretical processes is their large p_T tail.[7,39] Because the basic
field-theoretical vertices have no dimensional scale,

$$\langle p_T^n \rangle \sim 0\left(\frac{\alpha_s}{\pi}\right) \; Q^n \qquad (1.67)$$

Of course $\alpha_s \sim 1/b$ in Q^2 (1.14), but the $\langle p_T \rangle$ coming from (1.67) is much
larger than the finite $\langle p_T \rangle = 0(300)$ MeV usually observed in hadron-
hadron collisions. This means that jets in e^+e^- annihilation or lepto-
production are best[8] described by angular cutoffs rather than field p_T
cutoffs. For example, let us suppose in e^+e^- annihilation that the
fundamental quanta (q,G) in the final state produce hadrons with finite
momenta transverse to their momentum vectors. We can then calculate[52]
in perturbation theory from Fig. 4 the probability F_q that a fraction
$(1-\epsilon)$ of the total e^+e^- centre of mass energy Q will be contained in some
pair of oppositely directed cones of half angle δ:

$$F_q = 1 - \frac{\alpha_s(Q)}{\pi} \; 4 \left[\ln \; (2\epsilon) + \right] \frac{4}{3} \ln \; \delta + \text{terms with no logs} \qquad (1.68)$$

For sufficiently large energies almost all of the e^+e^- events will fall into two angular jets.[8]

On the other hand, a fraction $O\left(\frac{\alpha_s}{\pi}\right)$ of the events come from hard gluons radiated outside the angular cones. The usual discussion would then suggest that these should show up as three jet final states, the third jet emitting from the metamorphosis of a gluon into hadrons.[8] The cross section for hard gluon bremsstrahlung was easy to calculate:

$$\frac{1}{\sigma_{total}} \frac{d\sigma}{dx_q dx_{\bar{q}}} = \left(\frac{2\alpha_s}{3\pi}\right) \frac{x_q^2 + x_{\bar{q}}^2}{(1-x_q)(1-x_{\bar{q}})} + \text{higher orders} \qquad (1.69)$$

where $x_q = 2E_q/Q$ and similarly for $x_{\bar{q}}$. Such final states would be convincing evidence of the reality of the gluon. A possible strategy[53] for fitting such events might run as follows:

—First look for e^+e^- events where the final state hadrons are not highly collimated. This could be done by computing the thrust[54]

$$T \equiv \max \sum_{hadrons} \frac{|p_h^z|}{|p_h|} \qquad (1.70)$$

where the maximization is with respect to the choice of the thrust axis, along which the p_h^z are measured. The cross section $\frac{1}{\sigma}\frac{d\sigma}{dT}$ can be calculated reliably[51,54] in QCD perturbation theory, because it does not depend on the details of the infrared properties of the theory which we do not understand[53]:

$$\frac{1}{\sigma} \frac{d\sigma}{dT} \approx \left(\frac{2\alpha_s}{3\pi}\right) \left[\frac{2(3T^2-3T+2)}{T(1-T)} \ln\left(\frac{2T-1}{1-T}\right) - \frac{3(3T-2)(2-T)}{(1-T)} \right] \qquad (1.71)$$

—In such events, find a plane containing the thrust axis which maximizes the sum of the moduli of the hadron momenta out of the plane. Events with only three fundamental quanta $(q,\bar{q},G)$ should define an event plane quite nicely.

—Orient even: in the plane by setting $\theta=0°$ to be along the thrust axis and heading into the hemisphere with smaller $\sum |p_T^h|$. Define the angular range $0<\theta<\pi$ to be the half of the event plane which has the larger amount of hadron energy.

—The events should now be oriented as in Fig. 16, and given any luck there should be a well-defined jet around $\theta=0$, another in the angular range $\frac{\pi}{2}<\theta<\pi$, and another in the range $\pi<\theta<\frac{3\pi}{2}$. To see whether the hadrons really come into three jets, it is first advisable to look at the half-plane $-\frac{\pi}{2}<\theta<\frac{\pi}{2}$, and check that the hadrons there have finite p_T relative to the thrust axis. If so, remove these hadrons and boost[53] the rest by an amount ζ:

$$\text{sh } \zeta = \frac{T}{2\sqrt{1-T}} \quad , \quad \text{ch } \zeta = \frac{2-T}{2\sqrt{1-T}} \qquad (1.72)$$

The remaining hadrons should now have been boosted back to the centre-of-mass of the two putative jets in the half-plane $-\frac{\pi}{2}<\theta<\frac{\pi}{2}$ as in Fig. 17. Given any luck, an axis can be defined for the boosted hadrons relative to which their p_T are finite, and this axis will define the directions of the second and third jets.[55]

It will be interesting to see whether three jet events show up when this analysis is applied. One potential complication is that the $<p_T>$ of hadrons in a gluon jet may be larger than the $<p_T>$ for a quark jet. As emphasized above, the jets seen so far have a finite $<p_T>$ which is not perturbative, and the relevance of the perturbative analysis is not obvious. Nevertheless, one can compute[56] that for a gluon jet the fraction F_G of events with $1-\epsilon$ of the total energy E inside two oppositely

directed cones of half angle δ is

$$F_G \approx 1 - \frac{\alpha(E)}{\pi}\left\{12\ln(2\epsilon) - \left(11 - \frac{2}{3}f\right)\right\}\ln\delta + (\text{finite terms}), \quad (1.73)$$

The perturbative width for small ϵ and δ is wider than that of (1.68) for a quark jet, but it is not clear whether this is relevant to the gluon jets to be looked for at presently accessible energies. An amusing aspect of the formula (1.73) is that the piece finite as $\epsilon\to 0$ is again (cf. Eq. (1.47)) proportional to the renormalization (1.14) of the strong coupling constant $\alpha_s(Q^2)$. Coincidence or ...?

Finally, we should note that another good place[19] to look for gluon jets, besides the obvious e^+e^- annihilation and leptoproduction[57] reactions, is in the decay of a heavy quark-antiquark vector resonance such as the Υ. According to the charmonium model, the dominant decay mode should be into three gluons as in Fig. 5, with a differential cross section[17]

$$\frac{1}{\Gamma_{3G}}\frac{d\Gamma}{dx_1 dx_2} \approx \frac{1}{\pi^2 - 9}\left\{\frac{(1-x_1)^2}{x_2^2 x_3^2} + \frac{(1-x_2)^2}{x_1^2 x_3^2} + \frac{(1-x_3)^2}{x_1^2 x_2^2}\right\} \quad (1.74)$$

This would be an especially pure place to look for gluon jets, using the same jet-finding strategy[53] outlined above. The thrust distribution should be

$$\frac{1}{\Gamma_{3G}}\frac{d\Gamma}{dT} \approx \frac{3}{\pi^2-9}\left[\frac{4(1-T)}{T^2(2-T)}(5T^2-12T+8)\ln\frac{2-2T}{T} + \frac{2(3T-2)(2-T^2)}{T^3(2-T)^2}\right], \quad (1.75)$$

and orienting events along the thrust axis should give distributions of hadron energy in the event plane like those shown in Fig. 18. Preliminary evidence from DORIS[58] suggests that the final states in Υ decay are not exactly the same as in the e^+e^- continuum. However, it is premature

to think that evidence for the 3-gluon decay yet exists. It will probably be much easier to see gluon jets in the decay of the "topsilon" $t\bar{t}$ vector meson, which presumably has a considerably larger mass $\gtrsim 15$ GeV, yielding much more phase space for the gluon jets to identify themselves. Other promising ways of looking for gluon jets in onium spectroscopy include $T \rightarrow GG\gamma$,[20] and radiative decays to intermediate states which may decay predominantly into 2 gluons.[53,59]

2. Fermions for Fun and Profit

2.1 Weak Interaction Issues

In this first of three lectures devoted to studies of weak interactions at high energies, it seems appropriate to make some introductory suggestions as to what are the important physics issues which one is trying to resolve. Up till now, no one has ever found any deviation from the pointlike four-fermion form of the weak interactions, whether charged or neutral.[60] In the regime where the pointlike approximation is applicable, a generic fermion-fermion scattering cross section will rise linearly with the centre-of-mass invariant s, as in Fig. 19(a):

$$\sigma(f_1 f_2) \sim s \times 0\left(\frac{G_F}{\pi}\right) \tag{2.1}$$

The rise (2.1) cannot continue indefinitely, because there is a unitarity limit of 1 on each partial amplitude. In the case of the naive form (2.1) of cross section this limit will be attained when $\sqrt{s} \sim$ a few hundred GeV.[61] At this juncture, the cross section may either saturate at a constant $0(1)$, or else fall again, as indicated in Fig. 19(b). It is generally supposed that the latter occurs, thanks to the presence of intermediate vector bosons. It is theoretically appealing that the

turnover energy $\sqrt{s}$ should be rather smaller than the unitarity limit of a few hundred GeV. This is because it is attractive to unify weak and electromagnetic interactions with couplings which are $O(\alpha)$. In an intermediate vector boson theory.[62] G_F is related to the boson couplings and masses:

$$G_F = O\left(\frac{g^2}{m^2}\right) \qquad (2.2)$$

and weak electromagnetic unification suggests

$$m^2 = O\left(e^2 \, C_F\right) \qquad (2.3)$$

and one is naturally led to contemplate vector boson masses of order (50 to 200) GeV. There are empirical reasons for liking intermediate vector bosons, such as the factorization and universality of weak couplings. One of the theoretical reasons for the introduction of intermediate vector bosons is that it helps to make higher order radiative corrections to weak interactions finite and calculable. This happens because such radiative corrections typically involve sums over virtual intermediate states which will diverge if weak cross sections do not fall at high energies roughly as $O\left(\frac{1}{s}\right)$. Unfortunately, just sticking in intermediate vector bosons does not cure all problems. First, it is necessary to include some self-couplings (Fig. 20) between the vector bosons, and it has been shown[63] that essentially the only way of doing this which yields cross sections falling sufficiently fast at high energies is to make these couplings those found in a gauge theory. Such a theory will be based on a non-Abelian gauge group with a charged $W^{\pm}$ or neutral Z^0 boson corresponding to each generator of the group.[64] Fermions (quarks and leptons) must be put into suitably chosen representations of the gauge group. Unfortunately, just using gauge vector bosons with masses acquired in an ad hoc manner does not give a

sensible (renormalizable) theory either. The only known way of making such a massive gauge boson theory renormalizable[29] is by breaking the gauge symmetry spontaneously[12] using scalar Higgs fields.[65] A theory of this type seems inevitable to possess at least one physical scalar Higgs boson.

The road to a sensible renormalizable theory[2] of the weak interactions is therefore quite a long one, as indicated in Table 2. Finding an intermediate vector boson is only a small part of establishing the validity of any spontaneously broken unified gauge theory of the weak and electromagnetic interactions such as the Weinberg-Salam[12] model.

TABLE 2. The Road to a Gauge Theory

Physical Input	Experimental Test	Discussed in Lecture
Weak cross sections fall at high energies	Do high energy e^+e^- or ep scattering, look for $W^\pm$, Z^0	3
Interactions described by a gauge theory	Look at 3- and 4- vector boson inter- actions	3
Choose a gauge group	Look at low energy weak interactions;	2
	Do $W^\pm$, Z^0 spectros- copy	3
Choose spectrum of fer- mions and their group representations	Look for fermions	2
Break gauge symmetry with Higgs fields	Look for Higgs particles	4

The strategy of these remaining lectures will be to survey this road with a view to the experimental confrontation of these theoretical

ideas. Finally, at the end of the last lecture 4 we will examine a few
speculative possibilities that go beyond this orthodoxy and help keep our
lives interesting. We start with fermiology.

2.2 How Much Do We Know Already?

We have so far established[66] unassailably the existence of 10 funda-
mental fermions:

$$4 \text{ quarks } - u, d, s, c$$
$$6 \text{ leptons } - e, \nu_e; \ \mu, \nu_\mu; \ \tau, \nu_\tau \tag{2.4}$$

and the existence of a fifth quark is not seriously questioned. So far
it has only been seen[64,68] bound with its antiquark into the T family
of meson resonances. There are some indirect indications that this new
heavy quark has charge $-\frac{1}{3}$. They are the smallish coupling of the T
to leptons ($\Gamma_{e^+e^-} = (1.3\pm0.4)$ keV [68]), the rumoured small branching ratio
of $T \to \mu^+\mu^-$, shaky arguments about the relative production rates of T
and T' in hadron-hadron collisions,[69,70] and speculative calculations of the
next charge $= -\frac{1}{3}$ quark mass in the context of grand unified gauge theo-
ries.[71,72] We will henceforth assume that the fifth quark has charge
$-\frac{1}{3}$ and call it b or bottom.[73]

We know quite a lot about some weak interactions of these fermions.
The following left-handed charged weak interactions are by now completely
classical[66]:

$$\checkmark: \ \begin{pmatrix} u \\ d \end{pmatrix}_L \sim \cos^2 \vartheta_c; \ \begin{pmatrix} u \\ s \end{pmatrix}_L \sim \sin^2 \vartheta_c; \ \begin{pmatrix} \nu_e \\ e^- \end{pmatrix}_L \sim 1; \ \begin{pmatrix} \nu_\mu \\ \mu^- \end{pmatrix}_L \sim 1. \tag{2.5}$$

Recently established but apparently quite reliable are the left-handed
charged couplings[21,66,74]

$$\checkmark? \ \begin{pmatrix} c \\ s \end{pmatrix}_L \text{ large}; \ 0 < \begin{pmatrix} c \\ d \end{pmatrix}_L \ll 1; \ \begin{pmatrix} u \\ b \end{pmatrix}_L \ll 1; \ \begin{pmatrix} \nu_\tau \\ \tau \end{pmatrix}_L \text{ dominant} \tag{2.6}$$

At the present time there is no good evidence for the existence of any right-handed charged currents. The following are excluded at anything approaching unit ($\sim G_F$) strength:

$$x: \quad \binom{u}{d}_R ; \quad \binom{u}{s}_R ; \quad \binom{c}{d}_R ; \quad \binom{\nu}{e}_R ; \quad \binom{\nu}{e}_R \qquad (2.7)$$

Plausibly excluded at anything approaching unit strength by observations of charge-changing charm production[74] and of τ decays[32] are

$$x? \quad \binom{c}{s}_R ; \quad \binom{\nu}{\tau}_R \qquad (2.8)$$

There is no time here to discuss in depth the present status of neutral current phenomenology which is admirably reviewed in the talk of Barnett at this Summer Institute.[75] Suffice to say that the following right-handed currents cannot[76] be large:

$$x: \quad \binom{u}{b}_R ; \quad \binom{?}{d}_R \qquad (2.9)$$

The following current is strongly disfavoured by the recent polarized eD scattering data[77]

$$x? \quad \binom{N^0_e}{e^-}_R \qquad (2.10)$$

To the best of my knowledge the following left- and right-handed currents are not yet severely constrained by experiment:

$$\binom{c}{b}_{L,R} ; \quad \binom{N^0_\mu}{\nu^-}_R ; \quad \binom{N^0_\tau}{\tau^-}_R \qquad (2.11)$$

As far as the neutral currents of the fermions (2.4) are concerned, we only have information at present on those of u, d, e, ν_e and ν_μ all of

which seem to agree[75,78] very well with the $SU(2)_L \times U(1)$ Weinberg-
Salam[12] model. On the other hand, we have as yet no useful information
on the diagonal neutral currents of s, c, b, μ, τ and v_τ. We do however
have information on the off-diagonal neutral current d$\leftrightarrow$s, which is
observed[27] to be $O(G_F^2)$, and we have a constraint[66,79] on the $\Delta C=2$ transi-
tion $D^0 \leftrightarrow \bar{D}^0$ which is related to the $\Delta C=1$ neutral current u$\leftrightarrow$c, and tells
us it is also at most $O(G_F^2)$. These small couplings are just as expected
in the Weinberg-Salam model, and indeed the smallness of the s$\leftrightarrow$d neutral
current was the motivation of Glashow, Iliopoulos and Maiani (GIM)[80] for
giving the charmed quark[81] a well-defined role in weak interaction
physics, by causing cancellations like that in the diagram of Fig. 21.

With the important exception of certain atomic physics experiments,[82]
all present data agree with the Weinberg-Salam model[12] with $\sin^2 \theta_W \sim 0.20$
to 0.25.

It is almost universally expected that there will be at least one
more quark, with charge $e = 2/3$ to be called t or top. Some reasons for
its existence are as follows:

--Aesthetics: perhaps we should parallel the (so far)

$$\text{three lepton doublets} \begin{pmatrix} v_e \\ e \end{pmatrix}_L, \begin{pmatrix} v_\mu \\ \mu \end{pmatrix}_L, \begin{pmatrix} v_\tau \\ \tau \end{pmatrix}_L$$

with (2.12)

$$\text{three quark doublets} \begin{pmatrix} u \\ d' \end{pmatrix}_L, \begin{pmatrix} c \\ s' \end{pmatrix}_L, \begin{pmatrix} t \\ b' \end{pmatrix}_L$$

where the primes on the charge $-\frac{1}{3}$ quarks indicates that they are (gen-
eralized) Cabibbo mixed, in a manner to be discussed later. It was just
such an aesthetic argument that led to the postulation of charm[81] when
only three quarks and four leptons were known. It was only much after

this original arbitrary introduction that charm was given[80] a raison d'être in suppressing strangeness-changing neutral currents. Perhaps some similar role will eventually be found for t and b--a possibility is CP violation[35] which will be discussed later in this lecture.

--Anomaly cancellation: The above prescription for constructing a renormalizable gauge theory of the weak interactions is in fact slightly incomplete. The falling high energy cross sections depend on tricky cancellations between different Born diagrams. The relations between these diagrams can be upset[28] by the so-called "anomalies" of perturbation theory which arise from the fermion loops of Fig. 6. The anomalies must be cancelled if the strict renormalizability[29] of the theory is to be preserved. Each triangle diagram makes a contribution $\propto g_A^f e_f^2$. As mentioned in Lecture 1, thanks to colour these anomalies are cancelled if there are equal numbers of left-handed lepton and quark doublets.

$$A_q = \sum_{i=1}^{n} \left(-\frac{1}{2}\right)\left[(-1)^2 - (0)^2\right] = -\frac{1}{2}\sum_{i=1}^{n},$$

$$A_q = \sum_{i=1}^{n} 3\left(\frac{1}{2}\right)\left(\left(\frac{2}{3}\right)^2 - \left(-\frac{1}{3}\right)^2\right) = +\frac{1}{2}\sum_{i=1}^{n} \qquad (2.13)$$

Nature has so far endowed us with three left-handed lepton doublets: it is natural to want to supplement the b with a t quark so as to get a third left-handed quark doublet to cancel the anomalies. However, other ways of cancelling the anomalies are in principle possible, and it has even been argued[83] that the requirement of anomaly cancellation is not to be taken seriously because it only destroys renormalizability in higher orders of perturbation theory which are not phenomenologically relevant.

--Flavour conservation by neutral currents: As mentioned above, $\Delta S=2$ and $\Delta C=2$ transitions all seem to be suppressed to $O(G_F^2)$. This was explained in the GIM[80] charm model through cancellations involving loop diagrams with charmed quarks (Fig. 21). When more heavy quarks are introduced, the cancellations are no longer automatic whatever the masses and couplings of the new quarks, unless these are chosen to occur in representations of the weak gauge group identical with those of the lighter quarks.[84,71] This would suggest that left-handed quarks should always be in doublets of $SU(2)$, and that right-handed quarks should always be in singlets. Therefore, given a b quark we should need a t quark to partner it.

The above arguments are suasivious, but not rigorous. Nevertheless we will assume that at least one new t quark is yet to be discovered. Unfortunately, I know of no stringent constraint on its mass or guarantee that it will be accessible to the next generation (PETRA/CESR/PEP) of e^+e^- machines.

What constraints are there on the possible existence of other fundamental fermions? We start with the supposedly massless neutrinos. In fact, high energy physics does not even determine them to be massless, but gives upper limits[27]

$$m_{\nu_e} < 60 \text{ eV} , \quad m_{\nu_\mu} < 0.57 \text{ MeV} , \quad m_{\nu_\tau} < 250 \text{ MeV} \qquad (2.14)$$

and does not yet seriously restrict the number of "massless" neutrinos. For example the $K^\pm \to \pi^\pm \nu\bar{\nu}$ branching ratio is expected[85] to be

$$B(K^\pm \to \pi^\pm \nu\bar{\nu}) = O(10^{-10})N_\nu \qquad (2.15)$$

whereas the experimental upper limit[27] is 6×10^{-7} corresponding to

$$N_\nu \lesssim 6000 \qquad (2.16)$$

In time a better constraint may be available from the decays of heavy $q\bar{q}$ vector mesons.[86] One can estimate

$$\frac{\Gamma(V \to Z^0 + \nu\bar{\nu})}{\Gamma(V \to \gamma^* + e^+ e^-)} = \frac{G_F^2}{64\pi^2\alpha^2} \frac{m_V^4}{e_q^2} \left(1 - 4|e_q| \sin^2 \theta_W\right)^2 \qquad (2.17)$$

$$\approx 0.2 \times 10^{-8} \times m_V^4 \times N_\nu \quad \text{for } e_q = \frac{2}{3} \qquad (2.18)$$

For the J/ψ, a guessed limit of 1 on the quantity (2.18) implies that $N_\nu \lesssim 5 \times 10^6$. However, the ratio (2.18) is $O(10^{-2})$ for $m_V \gtrsim 30$ GeV, so that a sensitive search for the decay toponium $\to \nu\bar{\nu}$ should be very interesting. One way to do it may be to look for events of the form

$$e^+ e^- \to (t\bar{t})' \to (t\bar{t}) + \pi\pi$$
$$\qquad\qquad\qquad \hookrightarrow \text{nothing}$$

There are however much more restrictive constraints[87] on neutrinos than (2.14) and (2.18) if one accepts the standard "big bang" cosmology.[89] Very light neutrinos would have been produced in great profusion during the big bang, and would now have slowed to being nonrelativistic if their masses were not exceedingly small. They would then contribute to the mass density of the Universe and cause its expansion rate to slow down by an experimentally unacceptably large amount unless[87] (see Fig. 22)

$$\sum_\nu m_\nu < 50 \text{ eV} \qquad (2.19)$$

which bound can be strengthened to $\lesssim 3$ eV by considering the dynamics of clusters of galaxies. If the neutrino masses obey the constraint (2.19) then they would have been in thermodynamic equilibrium and present in vast numbers at very early stages of the Universe when the temperature

$\gtrsim \frac{1}{2}$ MeV. Increasing the number of "massless" neutrinos increases the early Universe's expansion rate, which increases the n/p ratio when the weak interactions drop out of equilibrium, which in turn increases the primordial abundance of Helium. It is currently believed that the primordial Helium abundance was less than 25%, indicating as shown in Fig. 23 that there can be at most one more "massless" neutrino after the ν_τ (an improvement on the limit (2.16)!).

There are also cosmological limits on the possible existence of heavy stable neutral leptons L^0.[89] Figure 22 shows that the upper limit on the mass density of the Universe requires $M_{L0} > 2$ GeV which can be improved to $\gtrsim 10$ GeV by considering the dynamics of clusters of galaxies. A complete display of the allowed ranges of masses and lifetimes is shown in Fig. 24. The important constraints on semistable L^0 production come from upper limits on distortions of the 3°K microwave background, and on the γ-ray background. We see that L^0 particles of arbitrary mass are allowed if their lifetimes are $< 5 \times 10^3$ seconds. An L^0 with a roughly unit strength weak interaction making it decay would obey this lifetime constraint if its mass were $\gtrsim O(1)$ MeV. Hence the cosmological constraints on massive neutral leptons are not really very useful except in models[90] where some selection rule impedes their decay.

Let us now return to high energy physics to see the constraints it yields on the possible existence of very heavy fermions (either neutral or charged, leptons or quarks). Such objects could have an indirect effect on our low energy phenomenology. One such effect is on the ratio of intermediate vector boson masses.[91,92] In the simplest Weinberg-Salam model with only $I=1/2$ Higgs doublet fields, there is a zeroth

order prediction:

$$\frac{m_W^2}{m_{Z0}^2} = \cos^2 \theta_W \qquad (2.20)$$

This prediction gets renormalized by any massive fermion loop to become

$$\frac{m_W^2}{m_{Z0}^2} = \cos^2 \theta_W \left[1 - \left(\begin{array}{c}1\\ \text{or}\\ 3\end{array}\right) \frac{\alpha_2}{8\sqrt{2}\pi} \left(\frac{2m_1^2 m_2^2}{m_1^2 - m_2^2} \ln \frac{m_1^2}{m_2^2} - m_1^2 - m_2^2 \right) \right] \qquad (2.21)$$

where m_1 and m_2 are the masses of the fermions in the loop, and the factors of 1 and 3 apply to leptons and quarks respectively. Experimentally, low energy neutral to charged current ratios are sensitive to the boson mass ratio:

$$\frac{\sigma(NC)}{\sigma(CC)} \propto \frac{m_W^4}{m_Z^4} \qquad (2.22)$$

The present data agree very well with the naive Weinberg-Salam prediction (2.20): Sehgal[78] finds

$$\frac{m_W^2}{m_{Z0}^2 \cos^2 \theta_W} = 0.98 \pm 0.05 \qquad (2.23)$$

This apparent success of the I=1/2 Higgs assumption leads to interesting constraints on m_1 and m_2. For example, for a lepton doublet with $m_2 \sim$ the limits (2.23) imply

$$m_1 < 400 \text{ GeV} \qquad (2.24)$$

It is possible to imagine possible future experiments with e^+e^- machines[93] which might determine the Z^0 mass with an accuracy of 0.1%, in which case Eq. (2.21) would be sensitive to all $m_i \gtrsim 100$ GeV. In this way future e^+e^- experiments could successfully determine the entire fermion

mass spectrum, by finding all fermions with mass < 100 GeV and excluding by their indirect effects fermions with larger masses.

In passing, we should note[9c] one unaesthetic aspect of very heavy fermions. Since their couplings to Higgs particles in the naive Weinberg-Salam model are

$$\delta f_{fH} = \frac{6m_f}{m_f}$$ (2.25)

the Higgs-fermion system becomes strongly interacting if m_f is sufficiently large. Indeed, lowest order perturbation theory violates partial wave unitarity[92] for

$$m_{quark} \sim 550 \text{ GeV}, \quad m_{lepton} \sim 1.2 \text{ TeV}$$ (2.26)

indicating the presence of bound states or other nonperturbative effects. For this reason, one might interpret the values (2.26) as plausible upper bounds on fermion masses, though there is no rigorously logical reason to exclude such strongly-interacting fermions.

2.3 Finding Heavy Leptons

Let us now turn from indirect evidence on heavy fermions to the phenomenological problems of identifying them in future high energy experiments. We start with:

2.3.1 Charged Leptons

The principles for locating one of these are strongly suggested by the saga of the discovery of the τ.[94,32,66] The decay modes and branching ratios are well-defined in the framework of conventional weak-electromagnetic and strong (pattern, QCD) interaction ideas.[31] Assuming a conventional, sequential (V-A) heavy lepton ℓ^- with a mass in the range $6 \text{ GeV} \sim m_\tau \sim m_{\ell} \sim m_b \sim 10 \text{ GeV}$, Tsai[95] has calculated the diagrams

of Fig. 7(a) and found the dominant decay modes

$$B(\lambda^- \to e^- \bar{\nu}_e \nu_\lambda) : B(\lambda^- \to \mu^- \bar{\nu}_\mu \nu_\lambda) : B(\lambda^- \to \tau^- \bar{\nu}_\tau \nu_\lambda) : B(\lambda^- \to d\bar{u}\nu_\lambda) : B(\lambda^- \to s\bar{c}\nu_\lambda)$$

$$\approx 1 : 1 : (\tfrac{1}{2} \text{ to } 1) : 3 : (2 \text{ to } 3) \qquad (2.27)$$

The leptonic decay modes $\lambda^- \to e^- \bar{\nu}_e \nu_\lambda$ and $\lambda^- \to \mu^- \bar{\nu}_\mu \nu_\lambda$ each have branching ratios $\gtrsim 10\%$ and should therefore be identifiable. On the other hand, exclusive semihadronic decay modes such as $\lambda^- \to \pi^- \nu_\lambda$ or $\rho^- \nu_\lambda$ should each have branching ratios $<2\%$, which would therefore be very difficult to detect. In contrast to the τ, the dominant semihadronic decay modes are expected to be multiprong, as exemplified by the last two branching ratios in the set (2.27). For sufficiently heavy heavy leptons with masses $\gtrsim 10$ GeV, these multiparticle semihadronic decays should show up as two jets.[96] A possible signature for $\lambda^+ \lambda^-$ production--which has the cross section

$$\sigma(e^+ e^- \to \lambda^* \to \lambda^+ \lambda^-) \approx \beta \left(\frac{3-\beta^2}{2} \right) \cdot \frac{4\pi\alpha^2}{3s} \qquad (2.28)$$

would then be a lepton (from one leptonic decay) plus two jets plus missing energy from neutrinos.[96] It seems likely that such an object could be found in $e^+ e^-$ collisions if it exists.

2.3.2 Neutral leptons

Heavy neutral leptons are expected in many theories, and even in the Weinberg-Salam[12] model doublets like

$$\begin{pmatrix} E^0 \\ e^- \end{pmatrix}, \quad \begin{pmatrix} M^0 \\ \mu^- \end{pmatrix} \quad \text{or} \quad \begin{pmatrix} T^0 \\ \tau^- \end{pmatrix}$$

cannot yet be excluded.[97] Lower limits on their masses come from the absence of $K^+ \to E^0 e^+$ decay, which tells us that $m_{E^0} > 0.4$ GeV. Improved lower limits on $m_{E^0} \sim 1$ GeV come from τ or F decays.[98] An object

Σ^0 can be produced singly in e^+e^- annihilation by W^- exchange as in fig. 25: $e^+e^- \to \nu_e \Sigma^0$, $\bar{\nu}_e \bar{\Sigma}^0$. The total cross sections are calculated[99] to be

$$\sigma(e^+e^- \to \nu_e \Sigma^0) \approx \frac{G_F^2}{2\pi}\left(1 - \frac{m_{\Sigma^0}^2}{s}\right)^2 s \left(1 + \frac{s - m_{\Sigma^0}^2}{m_W^2}\right)^{-1} \quad \text{for a}$$

right-handed e-Σ^0 coupling

$$\approx \frac{G_F^2}{2\pi}\frac{s}{3} \quad \text{for } m_{\Sigma^0}^2 \ll s \ll m_W^2 \quad \text{and a}$$

left-handed e-Σ^0 coupling $\qquad$ (2.29)

One can also produce pairs $\Sigma^0 \bar{\Sigma}^0$ or $M^0 \bar{M}^0$ in e^+e^- collisions through a direct channel Z^0 as in Fig. 26. In the Weinberg-Salam model, massive left-handed neutral lepton[100] pairs would be produced with cross sections[98]

$$\sigma(e^+e^- \to \Sigma^0 \bar{\Sigma}^0) = \frac{G_F^2}{32\pi} s \bar{\beta}\left[4 \sin^4 \theta_W\left(1 + \frac{\beta^2}{3}\right) + \left(2 \sin^2 \theta_W - 1\right)^2 \left(1 - \frac{\beta^2}{3}\right)\right]$$

$$\text{for } s \ll m_Z^2 \qquad (2.30)$$

The cross sections (2.29) and (2.30) exhibit the linear rise with s characteristic of the pointlike four-fermion interaction (2.1). They are rather small for the SPEAR/DORIS generation of e^+e^- machines, but would be substantial at the highest PETRA/PEP energies. Thus one would have

$$\sigma(e^+e^- \to \nu_e \bar{\Sigma}^0) = O\left(\frac{1}{10}\right) \sigma(e^+e^- \to \mu^+\mu^-) \qquad (2.31)$$

and

$$\sigma(e^+e^- \to \Sigma^0 \bar{\Sigma}^0) \approx O\left(\frac{1}{100}\right) \sigma(e^+e^- \to \mu^+\mu^-) \qquad (2.32)$$

for beam energies $\approx$ 15 to 20 GeV.[99] At higher energies near and beyond the Z^0 pole (or poles) the ratios (2.31) and (2.32) would be $O(1)$. If an M^0 exists with a mass of a few GeV, visible cross sections for $\nu p \to M^0 + X$

could be expected for FNAL or CERN SPS beams. Very substantial cross sections for ep → $\Xi^0 X$ are found for ep colliding rings with centre-of-mass energies $\sqrt{s} \gtrsim 100$ GeV and $m_{\Xi^0} \lesssim \frac{1}{2}\sqrt{s}$.[111]

As for Ξ^0 decays, one might expect[45,44] that for 2 GeV $\lesssim m_{\Xi^0} \lesssim 15$ GeV the decay branching ratios

$$B(\Xi^0 \to e^- e^+ \nu_e \quad \lesssim 11\% \text{ each} \qquad (2.33)$$
$$\mu^+ \nu_\mu$$
$$\tau^+ \nu_\tau$$

with corresponding $\mu^- X$, $\tau^- X$ branching ratios for M^0, T^0. Similarly to (2.27) one would also expect

$$B(\Xi^0 \to e^- (u\bar{d})) \sim 30\% \text{ each} \qquad (2.34)$$
$$(c\bar{s})$$

The decay modes (2.33) would have characteristic signatures like $e_\mp$ final states with low invariant mass[45]:

$$m_{e^-e^+} \sim \begin{cases} 0.5 \ m_{\Xi^0} & \text{(left-handed)} \\ 0.6 \ m_{\Xi^0} & \text{(right-handed)} \end{cases} \qquad (2.35)$$

The decay modes (2.34) yield the exciting prospect of a peak in an invariant mass distribution $e^- + $ hadrons[?]. Unfortunately, as mentioned earlier heavy heavy leptons probably[45] have very small exclusive semi-hadronic decay modes, so such a peak might be difficult to track down.

Possible signatures[89] for single production $e^+ e^- \to \mu^\pm \Xi^\mp$ would be $(e^\pm \mu^\mp)$ final states with the μ spectrum having a forward-backward asymmetry, with the $e^+ \mu^-$ collinearity angle peaked towards $\theta \approx 0$, and with low $e^+ \mu^-$ invariant masses as mentioned above and as indicated in Fig. 27(a). Possible signatures[?] for double production $e^+ e^- \to \Xi^0 \bar{\Xi}^0$ events would include events with $e^+ e^- \mu^+ \mu^-$ and missing energy as in Fig. 27(b), and $e_\mp + $ hadrons events with the $e_\mp$ collinearity angle

small, so that the pair recoiled against a hadron jet as in Fig. 27(c).

In ep collisions[???] one could get events with

$$ep \to (\mu e) \to hadron\ jet^+ \qquad (Fig.\ 27(d))$$

or

$$ep \to (e+hadrons) \to hadron\ jet^+ \qquad (Fig.\ 27(e))$$

It seems likely that neutral heavy leptons will have sufficiently distinctive signatures to be discernible in e^+e^- or ep collisions at high energies.

2.4 Heavy Quarks

As was discussed in Section 1.2, we know there is a fifth quark b, and generally assume there will be a sixth quark t. In this section we will discuss some of the possible phenomenology of these quarks and of possible successors. In view of its successes to date, we will assume the Weinberg-Salam model in discussing the weak interactions of the b and t quarks. We therefore have (at least) 3 quark doublets of $SU(2)_L$, which will in general mix.

$$\begin{pmatrix} u \\ d' \end{pmatrix}_L \quad \begin{pmatrix} c \\ s' \end{pmatrix}_L \quad \begin{pmatrix} t \\ b' \end{pmatrix}_L \qquad (2.36)$$

The charge-changing weak interactions can be described in terms of an $N_q \times N_q$ unitary matrix U, where N_q is the

$$U = \begin{pmatrix} & & \\ & & \\ & & \end{pmatrix} \qquad (2.37)$$

number of quark doublets. The matrix U would appear to need N_q^2 parameters for its characterization, but $(2N_q-1)$ of these are relative phases between different quark fields, which are unobservable. The matrix U therefore has $(N_q-1)^2$ observable parameters. If N_q were 1, U would have no parameters as is immediate in physically obvious. If $N_q=2$, one would

expect 1 parameter, which is just the Cabibbo angle θ_c:

$$U_2 = \begin{pmatrix} \cos\theta_c & \sin\theta_c \\ -\sin\theta_c & \cos\theta_c \end{pmatrix} \qquad (2.38)$$

If $N_D=3$, one has 4 observable parameters.[?] Not all of these can be absorbed as the Euler angles of a 3x3 orthogonal matrix. The unitary matrix U has one extra observable complex phase δ:

$$U_3 = \begin{pmatrix} c_1 & -s_1 c_3 & -s_1 s_3 \\ s_1 c_2 & c_1 c_2 c_3 - s_2 s_3 e^{i\delta} & c_1 c_2 s_3 + s_2 c_3 e^{i\delta} \\ s_1 s_2 & c_1 s_2 c_3 + c_2 s_3 e^{i\delta} & c_1 s_2 s_3 - c_2 c_3 e^{i\delta} \end{pmatrix} \qquad (2.39)$$

where the θ_i, $i=1,2,3$ are generalized Euler-Cabibbo angles, and

$$c_i \equiv \cos\theta_i, \quad s_i \equiv \sin\theta_i, \quad (i=1,2,3) \qquad (2.40)$$

If the complex phase δ is nonzero, it will generate CP violation, as pointed out by Kobayashi and Maskawa (KM).[?] It is not at all clear whether the observed CP violation in the K^0-$\bar K^0$ system comes from this source—another favoured source of CP violation is a complicated, non-minimal Higgs system[105]--but we will return later to review some predictions of the KM mechanism for CP violation.

First we should take account of the phenomenological successes of the Weinberg-Salam model and the GIM[84] mechanism, which tells us that the observed weak interactions are approximately as described by the 2x2 coupling matrix U_2 (2.38). The new mixing angles in (2.39) must obey certain constraints, with

$$\theta_1 \approx \theta_c, \quad \theta_3, \theta_2 \ll \theta_c \qquad (2.41)$$

The best constraint on θ_1 seems to come[?] from the usual Cabibbo universality for quarks (which it was called in days gone by).

on nuclear β-decay and neutron decays indicate that[10]

$$s_{1-\lambda}^2 \quad \text{and} \quad s_{1-\lambda}^2 + s_{q-\lambda}^2$$

differ by $0.25 \pm 0.23\%$. However, there should be modifications to
universality due to axis radiative corrections. In the standard
Weinberg-Salam model these are[10]

$$\frac{\alpha}{5\pi} \left[3 \ln \left(\frac{m_W}{m_p} \right) + \ln \left(\frac{m_Z^2}{m_A^2} \right) \right] \tag{2.42}$$

If we take $m_W \approx 74$ GeV, corresponding to $\sin^2 \theta_W = 0.22$, and the axial
vector form factor parameter $m_A \approx 1.0$ GeV, then Eq. (2.42) gives a vio-
lation of u-quark universality of 0.20%. The net discrepancy between
Cabibbo-Weinberg-Salam[10] theory and experiment is therefore
$0.05 \pm 0.23\%$, so that we estimate the "leakage" of the u quark's weak
coupling to the b quark to be

$$s_2^2 s_3^2 < 0.0023 \tag{2.43}$$

Since $s_2^2 \approx \sin^2 \theta_c$, this result gives an upper limit[10] on s_3^2 of

$$s_3^2 < 0.06 \tag{2.44}$$

indicating that s_3 is at most the same order of magnitude as the Cabibbo
angle.

The best limit on s_2 probably[10] comes from the success of calcula-
tions[95] of the charmed quark mass from the observed K^0-$\bar{K}^0$ mixing. In
the SU[2] model utilized in Ref.[95] one uses diagram of Fig. 21 to
estimate

$$\frac{m_c^2}{m_W^2} \quad \approx \quad \sin^2 \theta_c \tag{2.45}$$

and the experimental value of m_c is approximately 1.5 to 2 GeV.

as subsequently confirmed by experiment. If we now include t quarks[104] in the loop the equation (2.45) factor

$$\sin^2\theta_c \cos^2\theta_c \, m_c^2 + s_1^2 c_1^2 c_3^2 \left[c_2^2 4m_c^2 + s_2^2 4m_t^2 + \frac{2s_2^2 c_2^2 m_c^2 m_t^2}{m_t^2 - m_c^2} \ln\left(\frac{m_t^2}{m_c^2}\right) \right] \quad (2.46)$$

The phenomenological success of the formula (2.45), and the fact that presumably $m_t > 7$ GeV since otherwise toponium would have been seen in the $pp \to \mu^+\mu^- + X$ experiments,[67] gives us a constraint on s_2^2:

$$s_2^2 < 0.1 \quad \text{if} \quad m_t < 7 \text{ GeV} \quad (2.47)$$

Once again, it seems phenomenologically that this generalized Cabibbo angle cannot be much larger in magnitude than the original Cabibbo angle, though there is no fundamental understanding of this fact.

Armed with the constraints (2.41, 2.44, 2.47) we are now in a position to make some educated guesses about the decay modes expected for bottom and top particles.[69] It is generally felt likely that heavy quarks in new heavy mesons will decay essentially as if they were free into light $q\bar{q}q$ combinations as in Fig. 28. These rates can then be calculated by scaling up the μ-decay formula

$$\Gamma(f \to f_1 f_2 \bar{f}_3) \approx \frac{G_F^2 m_f^5}{192\pi^3} \times \begin{pmatrix} \text{mixing} \\ \text{angle} \\ \text{factor} \end{pmatrix} \times \begin{pmatrix} \text{phase space} \\ \text{suppression} \\ \text{for } m_{f_1} \neq 0 \end{pmatrix} \times \begin{pmatrix} \text{colour} \\ \text{factor} \end{pmatrix} \quad (2.48)$$

From the weak coupling matrix (2.39) we should anticipate[69]

$$\frac{\Gamma(b \to c+X)}{\Gamma(b \to u+X)} \approx \left(\frac{s_2^2 + s_3^2 + 2s_2 s_3 \cos\delta}{s_1^2 s_3^2} \right) \times O\left(\frac{1}{3}\right) \quad (2.49)$$

where we have used $m_b \sim 5$ GeV, $m_c \sim 2$ GeV to estimate the phase space suppression factor $O(1/3)$. Assuming, as is consistent with the

constraints (2.44) and (2.47), that

$$s_2^2 + s_3^2 + 2s_2 s_3 \cos \delta \sim O\left(s_3^2\right)$$

and using $s_i^2 \sim \frac{1}{20}$, we obtain from formula (2.49) the general expectation[69] that

$$\frac{\Gamma(b \rightarrow c+X)}{\Gamma(b \rightarrow u+X)} \gtrsim O(6) \qquad (2.50)$$

Thus the dominant decays of bottom particles should probably be to charmed particles. Analogously to (2.49) we find for top particles that

$$\frac{\Gamma(t \rightarrow b+X)}{\Gamma(t \rightarrow s+X)} \gtrsim \frac{1}{\left(s_2^2+s_3^2+2s_2 s_3 \cos \delta\right)} \times O\left(\frac{1}{3}\right) \qquad (2.51)$$

for a randomly guessed $m_t \sim 12$ GeV. With the constraints (2.44) and (2.47) it seems probable that

$$\frac{\Gamma(t \rightarrow b+X)}{\Gamma(t \rightarrow s+X)} > 1 \qquad (2.52)$$

though this may not be the case if m_t is close to its lower limit of 7 GeV.

From the expectations (2.50) and (2.52) it seems very likely that multiple cascades of the form

$$T \rightarrow L + X$$
$$\quad \hookrightarrow c + X$$
$$\qquad \hookrightarrow s + X \qquad (2.53)$$

could well dominate the decays of heavy quark mesons. At each stage in the cascade, the emitted system X may include an (ev) or (μv) pair, probably each with a branching ratio O(10 to 20)%. (This comes from counting lepton versus coloured quark degrees of freedom, and the belief that nonleptonic decays of heavy quarks are not strongly enhanced.[107,66] The cascades (2.53) could therefore yield spectacular multilepton signatures in neutrinoproduction or e^+e^- annihilation.

It is also worth thinking what the lifetime of a top or bottom particle might be. Using the standard formula (2.48) and multiplying it by 5 to take account of all the possible semileptonic and nonleptonic decay modes, we find[69]

$$\tau(\text{bottom}) \gtrsim 10^{-14} / (s_1^2 + s_3^2 + 2s_1 s_3 \cos \delta) \gtrsim 10^{-13} \text{ sec} \qquad (2.54)$$

if we use the bounds (2.44) and (2.47). This suggests that bottom particles may live long enough to leave detectable tracks in emulsions or high resolution spark chambers or bubble chambers. How long could the bottom lifetime be? If the KM mechanism[102] is responsible for the CP violation observed in the K^0–$\bar{K}^0$ system,[104] then as discussed in greater detail later

$$s_2 s_3 \sin \delta \sim 10^{-3} \qquad (2.55)$$

This gives us a very weak lower bound

$$s_2^2 \text{ or } s_3^2 > 10^{-6} \qquad (2.56)$$

which combined with (2.54) suggests that the bottom lifetime should be $< 10^{-8}$ seconds. On the other hand, the KM mechanism may not lie at the root of the observed CP violation, in which case it becomes interesting to look for longer-lived bottom particles. Indeed, it has been suggested that bottom particles might be absolutely stable ($s_3 = 0$).[108] This possibility can probably be excluded now, since two FNAL experiments[109] exclude the existence of any heavy hadrons with $\tau > 5 \times 10^{-8}$ sec and a production cross section as large as that of the Υ in 400 GeV proton-nucleus collisions, as would be expected for bottom particles. If the bottom lifetime is $\gtrsim 10^{-12}$ sec, as is perfectly consistent with all the constraints mentioned above, then experiments to measure it at $e^+ e^-$ machines become imaginable.[110]

What about the production of new heavy quark particles? The three most promising mechanisms would seem to be:

Production in νN collisions. The prospects here are unfortunately not very good,[69] largely because of the severe constraints (2.44) and (2.47) on the mixing angles. These imply that at present energies, where there is a threshold suppression of heavy quark production,[111] one probably has

$$\frac{\sigma(\text{heavy})}{\sigma(\text{total})} \lesssim O(10^{-3}) \tag{2.57}$$

so the total cross section will not show an effect and one must look for distinctive signatures. These might include dilepton events, with one lepton coming from a cascade decay (2.53) and having large p_T because of the large energy release in the decay or tri- or tetralepton events. Unfortunately, these probably occur--because of (2.57) and the less-than-total acceptance of present neutrino scattering apparatuses--at observable rates

$$\frac{\sigma(3\mu)}{\sigma(\text{total})} \lesssim O(10^{-5}), \quad \frac{\sigma(4\mu)}{\sigma(\text{total})} \lesssim O(10^{-6}) \tag{2.58}$$

Present experiments are perhaps sensitive to the rates (2.58), but most observed 3μ events[112] seem to have a radiative origin, and the two published tetralepton events[113] are difficult to assess.

Production in eN collisions. One expects the production of heavy quarks to be relatively small at low Q^2, but that the sea of heavy $q\bar{q}$ pairs should gradually build up as Q^2 increases, with distributions approaching SU(f) symmetry as $Q^2 \to \infty$. The evolution of the heavy sea can be estimated in QCD using evolution equations of the form (1.20, 1.21)[101] corresponding to Fig. 9(b). Ideally, one should include in

these equations the finite mass of the heavy quark.[114] Neglecting it,[101] one finds production cross sections for c and b quarks in high energy ep colliding rings which are several % at low x, being within a factor of 2 or 3 of the SU(f) symmetry predictions.

Production in e^+e^- collisions. The situation here is most favourable, since the production of heavy quarks is expected to be $\sim 3e_q^2 \times \sigma(e^+e^- \to \mu^+\mu^-)$ above threshold, and there may be a threshold enhancement because of an analogue of the $\psi(4.03-4.16)$ just above charm threshold. Unfortunately, even SU(f) symmetry does not give a large increase in the cross section, or large signal-to-background ratio. One finds

$$
\left.
\begin{aligned}
\frac{R_{b\bar{b}}}{R_{total}} &\approx \frac{\frac{1}{3}}{\frac{10}{3} + \frac{1}{3}} \approx 9\% \\[2ex]
\frac{R_{t\bar{t}}}{R_{total}} &\approx \frac{\frac{4}{3}}{\frac{11}{3} + \frac{4}{3}} \approx 27\%
\end{aligned}
\right\}
\tag{2.59}
$$

which makes the experimental location of a new threshold nontrivial,[93] and identification of naked top or bottom particles very difficult. Several ways have been proposed for finding distinctive t or b signatures. One of them is suggested[93,53] by the expected dominance of t (or b) → $q\bar{q}q$ decays, which should populate top or bottom meson final states with 3 very embryonic "jets" for each b or t, making a total of 6 embryonic "jets" in an $e^+e^- \to t\bar{t}$ or $b\bar{b}$ final state as in Fig. 29. It is very unlikely that these multiple jets could be disentangled except if one were at extremely high energies and the t quark mass were very large. Close to threshold, one would expect the hadronic final states to be essentially isotropic,[93] rather like phase space. Above threshold

one would expect this isotropy to fade away gradually, so that for the thrust[53]

$$\langle 1-T \rangle_{heavy} = \frac{1}{2} \left\langle \frac{Q_0^2}{Q^2} \right\rangle \qquad (2.60)$$

where Q_0 is the heavy threshold energy as shown in Fig. 30. One could imagine locating a new ($t\bar{t}$) threshold by doing a relatively coarse energy scan looking for a jump in the fraction of events with high sphericity which should persist some way above threshold. Once the general location of such a threshold had been found, one could do a more conventional fine scan. A similar idea could be used to enhance the signal-to-background ratio for heavy $q\bar{q}$ final states by making cuts in sphericity or acoplanarity. Suppose you make a standard sphericity[13] analysis of each final state and identify the three eigenvalues λ_i ($i=1,2,3$) of the sphericity tensor:

$$\lambda_1 \geq \lambda_2 \geq \lambda_3 \qquad (2.61)$$

One may then define quantities

$$Q_i \equiv 1 - \frac{2\lambda_i}{\lambda_1 + \lambda_2 + \lambda_3} \qquad (2.62)$$

for which different classes of events have the following characteristic values:

	Q_1	$(Q_3 - Q_2)$
sphere	$\frac{1}{3}$	0
circular disc	0	0
2 jets	0	1
phase space	$\neq 0$	$\neq 0$

$$(2.63)$$

It is apparent from (2.63) that $(Q_3 - Q_2)$ is a measure of "jeticity",

while Q_1 is a measure of acoplanarity. One could imagine selecting heavy $q\bar{q}$ events either by making a "jeticity" cut, or by an acoplanarity cut, or by some more sophisticated combination of the two. To see how this procedure might work in practice, I have taken the distributions in Q_3-Q_2 and in Q_1 measured by PLUTO[58] in the e^+e^- continuum close to the Υ, and compared them with a phase space Monte Carlo[115] to mimic $b\bar{b}$ events in Fig. 31. Clearly the distributions are very different, and it appears that one may make cuts:

$$\text{Jeticity:} \qquad Q_3\text{-}Q_2 \lesssim \frac{1}{2} : \begin{cases} 7/8 \text{ of } b\bar{b} \\ 1/4 \text{ of 2 jet continuum} \end{cases} \begin{matrix} \text{survive} \\ \text{(Fig. 31(a))} \end{matrix} \quad (2.64a)$$

$$\text{Acoplanarity:} \qquad Q_1 \gtrsim \frac{1}{18} : \begin{cases} 7/8 \text{ of } b\bar{b} \\ 1/3 \text{ of 2 jet continuum} \end{cases} \begin{matrix} \text{survive} \\ \text{(Fig. 31(b))} \end{matrix} \quad (2.64b)$$

Thus it seems that the $b\bar{b}$ signal-to-background ratio may be enhanced by a factor of at least 3 by suitable cuts on the sphericity eigenvalues.

Another tactic may be to select single or multiple prompt lepton events.[32] If one uses the cascades (2.53) one has

$$\left.\frac{R_\mu}{R_e}\right|_b = \frac{1}{2} \; ; \qquad \left.\frac{R_{e^+e^-}}{R_{e^+e^-}}\right|_b = \frac{1}{2} \qquad (2.65)$$

where charm is expected to be the dominant background, while final states with $e^\pm e^\pm$, or 3 or 4 leptons could only come from $b\bar{b}$ production--until the $t\bar{t}$ threshold is reached. Such triggers suffer from two defects: they knock down the event rate by a factor of 5 to 10 for each semi-leptonic decay, and it is difficult to reconstruct an invariant mass peak when semileptonic decays are involved.

Before leaving the subject of $b\bar{b}$ production, it may be worthwhile to point out some intriguing aspects of b meson decays which would cast

strong light on the validity of the KM[102] model and CP violation.
These topics are treated in more detail in the talk by M. K. Gaillard[116]
at this Summer Institute. The subject of $K^0-\bar{K}^0$ mixing has been touched
on already, and is expected to be large in the GIM-KM model, as
observed experimentally. It is expected that $D^0-\bar{D}^0$ mixing should be
very small $O(10^{-3}$ to $10^{-4})$,[104] since it is sensitive to m_s^2 rather than
m_c^2, and comes from diagrams which are Cabibbo disfavoured by comparison
with the dominant $c \to s+X$ decays. In the case of $B^0(\equiv b\bar{d}) - \bar{B}^0(\equiv \bar{b}d)$
meson mixing, mixing is expected to be intermediate between that in the
$K^0-\bar{K}^0$ and $D^0-\bar{D}^0$ systems. The relevant mixing parameter is[69]

$$\left|\frac{\Delta m_B}{\Gamma_B}\right| \gtrsim \frac{m_t^2}{700 \text{ GeV}} \tag{2.66}$$

where the sensitivity to m_t^2 is intrinsic to the models while the precise
number in the denominator is rather uncertain. Since $m_t \gtrsim 7$ GeV, Eq.
(2.66) tells us that probably

$$D^0-\bar{D}^0 \text{ mixing} < B^0-\bar{B}^0 \text{ mixing} < K^0-\bar{K}^0 \text{ mixing}$$

and this could be the only route to a phenomenological estimate of m_t
before the t is found. Mixing would yield

$$e^+e^- \to B^0B^0X, \qquad B^0B^+X, \qquad \bar{B}^0B^-X, \qquad \bar{B}^0\bar{B}^0X \tag{2.67}$$

final states, whose primary decay leptons could give like-sign $e^\pm e^\pm$ sig-
natures. Unfortunately, these could also come from cascade decay con-
fusion, though this may be reduced by making a suitable lepton momentum
cut[117]: primary leptons should be harder.

Since the KM model has interesting results for CP violation in K
decays, it is natural to ask about its implications for bottom meson

systems. In the case of K^0 and D^0 meson decays, the KM[102] model gener-
ally reproduces the predictions of the superweak theory,[69,118] with the
usual CP violating parameters

$$|\varepsilon_K|, |\varepsilon_D| \approx O(2s_2 s_3 \sin \delta) \approx 2 \times 10^{-3} \qquad (2.68)$$

as foreshadowed in Eq. (2.55). The model also predicts a very small
neutron electric dipole moment, $\lesssim 10^{-28}$ cm and much smaller than the
present experimental limit $\lesssim 3 \times 10^{-24}$ cm.[119] For the $B^0-\bar{B}^0$ system the
corresponding CP violating parameter is much larger[69]:

$$|\varepsilon_B| \approx \tan 2\delta \gg 10^{-3} \qquad (2.69)$$

Thus the CP violation could be substantial. A characteristic signature
for it would be

$$\sigma(e^+ e^+) \neq \sigma(e^- e^-) \qquad (2.70)$$

in any region of $e^\pm$ phase space. The expected magnitude of the effect
(2.70) is strongly dependent on the values of the mixing angles and
m_t,[120] since both $|\varepsilon_B|$ (2.69) and $|\Delta m_B/\Gamma_B|$ (2.66) must be large to get
large effects.

The bottom may not be "just another quark" but may yield important
insight into the great unsolved problem of CP violation. Maybe that is
why we need the fifth and sixth quarks, which a fortiori is why we had
the third and fourth quarks and the muon!

3. The Intermediate Vector Bosons

3.1 Introduction

We now turn to that most characteristic aspect of gauge theories,
the intermediate vector bosons. We will be primarily interested in
their spectroscopy and couplings to elementary fermions, but as was

emphasized in section 2.1, the study of their interactions among them-
selves is also very important. This is, after all, the feature that
should make them gauge bosons rather than just any old intermediate vec-
tor bosons. We will start off by summarizing the masses and widths one
expects for charged and neutral vector bosons in a general weak inter-
action model, but will often use for illustration the Weinberg-Salam
model with $\sin^2 \theta_W \gtrsim 0.20$. This is the value found in the latest inclu-
sive νN[25] and polarized eD experiments.[77] It leads to rather higher
masses and widths for the $W^\pm$ and Z^0 than one had previously grown used
to contemplating.[9] After reviewing their properties,[93,121,127] we will
then move on to discuss how the $W^\pm$ and Z^0 may be discovered in hadron-
hadron collisions,[9] which seem likely to give our first glimpses of
them. We will look at backgrounds as well as cross sections, using as
a guide the scale-breaking and differential cross sections expected on
the basis of QCD.[123] Then we will study $W^\pm$ and Z^0 effects in ep colli-
sions.[101,124] It will transpire that these are not the best way to
produce the vector bosons directly, but they allow one to observe weak/
electromagnetic interference effects in regions of large Q^2 where they
are O(1). One should be able to see clear derivations from the pointlike
four-fermion weak interaction, and see the effects of the finite boson
masses. Next we will turn to e^+e^- experiments,[93,121,122] discussing in
particular the dramatic Z^0 peak with its prodigious event rate and the
opportunities it affords for precision weak interaction studies and
analyses of rare decays. The final section will examine phenomena away
from the Z^0 peak, including in particular the reaction $e^+e^- \to W^+W^-$,[125,126]
which affords a unique opportunity to see the gauge theoretic cancellation

of diagrams at work. The important possibility of seeing the three-point couplings between vector bosons will be mentioned.

It will be clear that while hadron-hadron collisions offer the most immediate prospects for exploratory experiments to find the $W^\pm$ and Z^0, detailed studies of them will only be possible with e^+e^- machines.

3.2 Properties of the Vector Bosons

3.2.1 Charged bosons

If we assume that a unique pair of charged vector bosons $W^\pm$ is responsible for the observed charge-changing weak interactions, then its decay width to $e^-\bar{\nu}_e$ is easily calculated[122] to be

$$\Gamma(W^- \to e^-\bar{\nu}_e) \approx \frac{G\alpha_W^3}{6\pi\sqrt{2}} \tag{3.1}$$

If we assume that all other fermions occur only in left-handed doublets, then decay rates are simply related to (3.1) by

$$\Gamma(W^- \to e^-\bar{\nu}_e):\Gamma(W^- \to \mu^-\bar{\nu}_\mu):\Gamma(W^- \to \tau^-\bar{\nu}_\tau):$$

$$\Gamma(W^- \to d\bar{u}):\Gamma(W^- \to s\bar{u}):\Gamma(W^- \to d\bar{c}):\Gamma(W^- \to s\bar{c}):\Gamma(W^- \to b\bar{c})$$

$$\approx 1:1:1:\approx 3 \cos^2\theta_c:\approx 3 \sin^2\theta_c:\approx 3 \sin^2\theta_c:\approx 3 \cos^2\theta_c:\approx 3 \tag{3.2}$$

where the factors of 3 come from colour, and we have neglected the generalized Cabibbo angles θ_2 and θ_3. If there are N_D doublets of quarks and leptons, each with the sums of their masses $\ll m_W$ then it is clear that the branching ratio

$$B(W^- \to e^-\bar{\nu}_e) \approx \frac{1}{4N_D} \tag{3.3}$$

and the minimal "known" three doublets of everything would imply

$$B(W^- \to e^-\bar{\nu}_e) \approx B(W^- \to \mu^-\bar{\nu}_\mu) = \frac{1}{12} \tag{3.4}$$

In order to fix the mass of the $W^{\pm}$ we will assume the Weinberg-Salam model in which

$$m_{W^{\pm}} = \sqrt{\frac{\pi\alpha}{\sqrt{2}\ G}}\ \frac{1}{\sin\ \theta_W} \tag{3.5}$$

If we take the latest experimental value of $\sin^2\theta_W \approx 0.20$, then we find

$$m_{W^{\pm}} \approx 84\ \text{GeV} \tag{3.6}$$

Armed with this mass estimate we return to Eq. (3.1) to find that

$$\Gamma(W^- \to e^-\bar{\nu}_e) \approx 230\ \text{MeV} \tag{3.7}$$

while Eq. (3.3) implies that

$$\Gamma(W^- \to \text{all}) \approx 900\ N_D\ \text{MeV} \tag{3.8}$$

and the minimal $N_D=3$, 6 quark, 6 lepton model would have

$$\Gamma(W^- \to \text{all}) \approx 2.7\ \text{GeV} \tag{3.9}$$

This is intriguingly wide so that one begins to wonder whether its width can be measured experimentally in hadron-hadron or e^+e^- collisions. Notice that according to high energy physics, $\Gamma(W^- \to \text{all})$ could be larger because of the paltry limit (2.16) on the number of "massless" neutrinos, and the lack of any other limits on the number of massive fermions in the mass range $\leq m_W$. Life would indeed be interesting if the W^- had too small a leptonic branching mode (3.3) to be detectable!

3.2.2 Neutral bosons

It is by no means universally accepted that a unique Z^0 boson is responsible for the observed neutral current phenomena,[75] so let us adopt a flexible parametrization[93] of the Z^0-f-$\bar{f}$ interaction

$$\mathscr{L}_Z = -m_Z \left(\frac{G_F}{\sqrt{2}}\right)^{1/2} Z^\mu \bar{f}\gamma_\mu \left(\frac{v_f - a_f\gamma_5}{\sqrt{2}}\right) f \tag{3.10}$$

In terms of the vector (v_f) and axial (a_f) couplings so defined, the Z^0 decay width is just

$$\Gamma(Z^0 \to \text{all}) \approx \frac{Gm_Z^3}{24\sqrt{2}\,\pi} \left[\sum_{\text{leptons}} \left(v_\ell^2 + a_\ell^2 \right) + 3 \sum_{\text{quarks}} \left(v_q^2 + a_q^2 \right) \right] \qquad (3.11)$$

In the Weinberg-Salam model[12] the couplings are specified as follows:

$$\left.
\begin{aligned}
a_e &= a_\mu = a_\tau = -1, & v_e &= v_\mu = v_\tau = -1 + 4\sin^2\theta_W \\
a_\nu &= 1 & v_\nu &= 1 \\
a_u &= a_c = a_t = 1, & v_u &= v_c = v_t = 1 - \tfrac{8}{3}\sin^2\theta_W \\
a_d &= a_s = a_b = -1, & v_d &= v_s = v_b = -1 + \tfrac{4}{3}\sin^2\theta_W
\end{aligned}
\right\} \qquad (3.12)$$

Inserting these couplings into Eq. (3.11) we find the following total Z^0 decay rate:

$$\begin{aligned}
\Gamma(Z^0 \to \text{all}) \sim \frac{Gm_Z^3}{24\sqrt{2}\,\pi} &\left\{ \left(1 + \left(1 - 4\sin^2\theta_W \right)^2 \right) N_e + 2N_\nu \right. \\
&+ 3\left(1 + \left(1 - \tfrac{8}{3}\sin^2\theta_W \right)^2 \right) N_{2/3} \\
&\left. + 3\left(1 + \left(1 - \tfrac{4}{3}\sin^2\theta_W \right)^2 \right) N_{-1/3} \right\} \qquad (3.13)
\end{aligned}$$

where we have been agnostic about the numbers of particles of each type. If we assume $\sin^2\theta_W \gtrsim 0.20$ as before, we find the relative decay rates

$$\Gamma(Z^0 \to \nu\bar{\nu}) : \Gamma(Z^0 \to \ell^+\ell^-) : \Gamma(Z^0 \to u\bar{u}) : \Gamma(Z^0 \to d\bar{d})$$

$$2 : 1.04 : 3.63 : 4.67 \qquad (3.14)$$

To go further, we need to estimate m_{Z^0}. If the Weinberg-Salam model only has $I=1/2$ Higgs multiplets, then as discussed in Lecture 2[127]

$$\frac{m_Z}{m_W} \approx \frac{1}{\cos\theta_W} \qquad (3.15)$$

and present data on neutral current cross sections suggest[78] that the mass formula (3.15) is correct to within $(1 \pm 2\frac{1}{2})\%$. Taking $\sin^2 \theta_w \gtrsim 0.20$ as before then yields

$$m_Z \approx 94 \text{ GeV} \qquad (3.16)$$

which is rather higher than the traditional guess[9,93] of 80 GeV. We then see from Eq. (3.13) that

$$\Gamma(Z^0 \to e^+e^-) \approx 82 \text{ MeV} \qquad (3.17)$$

and from Eq. (3.14)

$$B(Z^0 \to e^+e^-) \gtrsim \frac{1}{11N_D} \qquad (3.18)$$

Correspondingly the total Z^0 decay width

$$\Gamma(Z^0 \to \text{all}) \gtrsim 900 \ N_D \text{ MeV} \qquad (3.19)$$

and if there are the traditional minimal 3 doublets then

$$B(Z^0 \to e^+e^-) \gtrsim 3\% , \qquad \Gamma(Z^0 \to \text{all}) \gtrsim 2.7 \text{ GeV} \qquad (3.20)$$

Notice that in this case we really do have to worry about the number of "massless" neutrinos since the Z^0 will decay indiscriminately into all of them. If the cosmological bound[87] is disastrously wrong, the observable e^+e^- decay mode could have an embarrassingly small branching ratio.

Before leaving this section, it should be mentioned what general, model-independent bounds exist on the masses of the $W^\pm$ and Z^0. Bjorken[128] was able to show on reasonably general gauge theoretical assumptions that $m_{W^\pm}$ should be within about 20% of the Weinberg-Salam value (3.6), while m_{Z^0} was only constrained to be <200 GeV unless more stringent assumptions were made. Gauge theories generally seem to like to have their vector boson masses in the range up to 200 GeV. To my knowledge, the only indication that they really should have this mass scale comes from the

calculation[105] of radiative corrections to μ-quark universality (2.42),
which would come somewhat unstuck if the boson masses were as high as
the unitarity limit. It seems that a conservative hadron-hadron experi-
ment to search out vector bosons should have sensitivity up to $m_{W^{\pm}}$, m_{Z^0}
~ 200 GeV. On the other hand, the phenomenological successes and
aesthetic economy of the basic Weinberg-Salam make a gamble on a "Z^0
factory" e^+e^- machine with 50 or 60 GeV energy per beam look like a
reasonable bet.

3.3 Production in Hadron-Hadron Collisions

To estimate the cross sections for $W^{\pm}$ and Z^0 production in hadron-
hadron collisions we will use a cautious approach. First we will derive
conservative "lower bounds" from the CVC and scaling hypotheses, then
calculate the cross section using a naive parton Drell-Yan[9] mechanism
which incorporates these two assumptions. Finally, we will use QCD to
estimate the effects of scaling violations,[129] and the p_T distributions
which are expected to be rather broader than in the naive parton model.

In order to produce a $W^{\pm}$ or Z^0 it is necessary to bring together
to a point a quark and an anti-quark. But the same mechanism is needed
to produce a γ^* and hence a massive $\mu^+\mu^-$ (or e^+e^-) pair, so one should
be able to relate the cross sections. The $W^{\pm}$ may be produced by vector
or axial currents, so

$$\sigma_W = \left[\sigma_W\right]_V + \left[\sigma_W\right]_A \geq \left[\sigma_W\right]_V \qquad (3.21)$$

If one neglects s, c and heavier quarks, then the $W^{\pm}$ are produced by the I=1 current $\bar{u}d$, and one can use CVC in Eq. (3.21) to obtain

$$\langle \sigma_W \rangle \equiv \frac{1}{4}\left[\sigma_{W^+}(pp) + \sigma_{W^-}(pp) + \sigma_{W^+}(pn) + \sigma_{W^-}(pn) \right]$$

$$\geq \frac{3G \cos^2 \theta_c}{4\alpha^2 \sqrt{2}} m_W^4 \left[\frac{d\sigma}{dM^2}(pp \to \ell^+ \ell^- X) + \frac{d\sigma}{dM^2}(pn \to \ell^+ \ell^- X) \right]_{I=1}$$

(3.22)

Hence the W and $\ell^+ \ell^-$ continuum cross sections are related by the "conditional lower bound":

$$\langle \sigma_W \rangle \geq 0.22 \text{ GeV}^{-2} m_W^4 \left(\frac{d\sigma}{dM^2} (\ell^+ \ell^-) \right)_{I=1}$$

(3.23)

To use the bound (3.13) we must make a large extrapolation, because there are experimental data on $pN \to \ell^+ \ell^- X$ only at low values of s and M^2. But if the $\ell^+ \ell^-$ continuum is produced in a pointlike manner, the scaling law

$$M^4 \frac{d\sigma}{dM^2} = f\left(\tau \equiv \frac{M^2}{s} \right)$$

(3.24)

applies. Using the scaling law in the bound (3.23) and neglecting possible I=0 contributions one finally obtains

$$\left(\sigma_W \left(\frac{m_W^2}{s} = \tau \right) \right) \geq 0.22 \text{ GeV}^{-2} f(\tau)$$

(3.25)

As an example, let us take $\sqrt{s} = 540$ GeV, $m_W = 84$ GeV in which case experimental data on $pN \to \ell^+ \ell^- + X$ at $\sqrt{s} \sim 27$ GeV suggest

$$\left(\sigma_W \left(\frac{m_W^2}{s} = 0.024 \right) \right) \geq 2 \times 10^{-34} \text{ cm}^2$$

(3.26)

The above estimate is not very satisfactory, since it depends on assumptions about the neglect of I=0 contributions to the cross sections, and neglects production by axial currents. To go further, we use the

naive parton model which enables these contributions to be calculated, as well as obeying the CVC and scaling assumptions. The simple Drell-Yan[10] collision mechanism of Fig. 3 yields[9]

$$\frac{d\sigma}{dx} (a+b \rightarrow W+X) = G\pi \sqrt{2} \ H(\tau,x) \tag{3.27}$$

where $x \equiv 2p_\ell^W/\sqrt{s}$, $\tau \equiv m_W^2/s$ and

$$H(\tau,x) = \frac{x_a x_b}{\sqrt{x^2 + 4\tau}} W_{ab}^{\pm}(x_a, x_b) \tag{3.28}$$

where $W_{ab}^{\pm}(x_a, x_b)$ is the $q\bar{q}$ annihilation luminosity in ab collisions:

$$W_{ab}^{+}(x_a, x_b) \equiv \frac{1}{3} \left\{ u_a(x_a)\bar{d}_b(x_b) + \bar{d}_a(x_a)u_b(x_b) \right\} \cos^2 \theta_c$$

$$+ \ [s, c, \ldots] \ \text{contributions} \tag{3.29}$$

and $W_{ab}^{-}(x_a, x_b)$ is defined similarly to (3.29) by interchanging quarks and antiquarks. If one puts reasonable distributions of sea antiquarks into the formulae (3.27, 3.28, 3.29) one finds that for $m_W = 84$ GeV and $\sqrt{s} \sim 540$ to 800 GeV (see Fig. 32)

$$\sigma(pp \rightarrow W^+ + X) \sim 2 \times 10^{-33} \ cm^2$$

$$\sigma(pp \rightarrow W^- + X) \sim 1 \times 10^{-33} \ cm^2 \tag{3.30}$$

$$\sigma(pp \rightarrow W^\pm + X) \sim 3 \times 10^{-33} \ cm^2$$

In assessing the observability of the cross sections (3.30), one should not forget to fold in the branching ratio into a detectable final state such as $e^- \bar{\nu}_e$ or $\mu^- \bar{\nu}_\mu$, which the lower bound of 3 lepton and quark doublets implies will be $\leq 8\%$.

A precisely analogous calculation to the above can be done for Z^0 production to yield

$$\sigma(pp \rightarrow Z^0 + X) \sim 3 \times 10^{-33} \ cm^2$$

$$\sigma(\bar{p}p \to Z^o + X) \sim 2 \times 10^{-33} \text{ cm}^2 \qquad (3.31)$$

in the centre-of-mass energy $\sqrt{s} \sim 540$ to 800 GeV. The cross sections
(3.31) are somewhat smaller than for the $W^\pm$ (3.30), and the observable
leptonic decay modes $Z^o \to e^+ e^-, \mu^+ \mu^-$ are expected to have somewhat
smaller branching ratios, $\leq 3\%$ for ≥ 3 lepton and quark doublets.

The naive parton model makes predictions for the differential cross
sections as well as the total. Distributions for the decays $W^\pm \to \mu^\pm (+\nu)$
or $W^\pm \to$ hadron jets are also easy to calculate because the polarization
state of the $W^\pm$ is known. Representative calculations from the paper of
Quigg[9] are shown in Fig. 33. We see that there is a large charge
asymmetry violating forward-backward asymmetry in the distributions of
leptons from $W^\pm$ produced in $\bar{p}p$ collisions. Unfortunately, this effect is
likely to be very small in Z^o production which may lead the sceptic to
question how one knows that the "weak" Z^o is being produced, rather than
just any "strong" vector meson V. Paradoxically, the cross section for
such an hadron V is expected to be much smaller than that for a Z^o of
comparable mass, since the "charmonium" Zweig rule is expected to sup-
press $\Gamma(V \to \text{hadrons})$ to a few dozen keV, while $\Gamma(Z^o \to \text{hadrons})$ is $O(1)$
GeV, and the production rates are probably roughly proportional to the
hadronic decay widths.[130] A characteristic of the naive parton model[5]
is its p_T cutoff for partons, and hence the expected low $\langle p_T \rangle$ for the
produced $W^\pm$ and Z^o.[16] This prediction is presumably wrong, since the
p_T of observed $\ell^+ \ell^-$ pairs in hadron-hadron collisions seems to increase[131]
with M^2 if $\tau \equiv m^2/s$ is held fixed. Such behaviour is expected in QCD
(or any other field theory) where the pointlike nature of the funda-
mental interactions implies $\langle p_T \rangle = O(M) \sim \text{logs}$.[7,38,39] Field theories

also expect scaling violations in the cross sections, analogous to those predicted and observed (Fig. 10) in deep inelastic leptoproduction. Surely we would not expect scaling in $pp \to \ell^+\ell^-+X$ to be as resonant if it is violated in $\ell p \to \ell+X$.[19]

In QCD, modifications to the naive parton cross section formulae come from radiative corrections to the fundamental $q\bar{q}$ annihilation process, and from new processes such as $q\bar{q} \to W+q$, $G+q \to W+q$, etc. as in Fig. 34. The important changes in the $W^{\pm}$ or Z^0 cross section are three-fold. First, in the $q\bar{q}$ annihilation luminosity (3.29) one should use[132,133] the Q^2 dependent effective parton distributions[42] introduced in Lecture 1. Analysis of the logarithms of perturbation theory[51,132] shows that the leading Q^2 (or $M^2_{\ell+\ell-}$) evolution of the Drell-Yan cross section is correctly taken up by this substitution:

$$W^+_{ab}(x_a,x_b) \to \frac{1}{3}\left[u_a(x_a,M^2)d_b(x_b,M^2) + \bar{d}_a(x_a,M^2)u_b(x_b,M^2)\right]\cos^2\theta_c$$

$$+ \left[s,c,\ldots(M^2)\right] \text{ contributions} \qquad (3.32)$$

with $u_a(x_a,M^2)$, etc. obeying Eqs. (1.20, 1.21). There are also radiative corrections to the basic cross section formula (3.28) relating $H(\tau,x)$ to $W^+_{ab}(x_a,x_b)$. These will be $O(\alpha_s/\pi)$ and not very important relative to the effect of going from (3.29) to (3.32). More important is the third effect, which is to add to the $q\bar{q}$ annihilation subprocess essentially new subprocesses such as $q+G \to q+W$ as in Fig. 34. The cross section for these reactions will be superficially $O(\alpha_s/\pi)$ or $O(\alpha_s/\pi)^2$, but the effective luminosities analogous to (3.29) may be considerably larger, at least in pp collisions.[134] In this case the density of $\bar{q}$ is rather small, $O(\frac{1}{10})$ of the valence quarks, which can compensate for the (α_s/π)

suppression of other subprocess cross sections. In $\bar{p}p$ collisions both the q and $\bar{q}$ in (3.32) can be valence, so that the expected effect of these extra subprocesses is relatively smaller.

Figure 35 shows a typical QCD calculation[133] of the corrections to the naive parton formulae (3.27, 3.28, 3.29) due to the effective $q(M^2)$ subscitution (3.32). It transpires that the effects on the expected $W^{\pm}$ or Z^0 cross sections (3.30) and (3.31) are relatively small, because for the likely range of m_W^2/s there is a cross-over in the QCD scaling violation effects. This reflects the behavior of the QCD calculations of $F_2^{eN}(x,Q^2)$ shown in Fig. 10 (see also the experimental data), which indicate that for foreseeable values of Q^2 the structure function does not change much in the neighborhood of $x \approx 0.15$. On the other hand, the effects of QCD scaling violations are potentially rather serious at larger values of m^2/s. This may pose problems for the production of gauge bosons much more massive than 200 GeV in the presently discussed generation of $\bar{p}p$ and pp colliding ring machines, and is one reason why a low energy ($\sqrt{s} \lesssim 300$ GeV) pp collider was somewhat unappetizing. As mentioned above, the other QCD corrections to the formulae (3.27, 3.28, 3.32) are expected not to be very important in $\bar{p}p$ collisions. This is reflected in Fig. 36[133] which shows a calculation of the fractional modification of the cross section (3.27, 3.28, 3.32) expected in both $\bar{p}p$ and pp collisions. We notice that in the likely range of interest for $m^2/s \sim 0.01$ to 0.1 the modifications to the $q\bar{q}$ annihilation formulae are not even very big in pp collisions, though the effects at large m^2/s are again embarrassingly suppressive.

As mentioned earlier, it is expected that $<p_T>$ should be large for vector bosons produced in QCD. Generally one expects a typically brems-strahlung cross section with

$$\langle p_T^n \rangle = 0\left(\frac{\alpha_s}{\pi}\right)^n \quad \kappa_{W,Z}^n$$

A typical calculation[123] of $\langle p_T^2 \rangle$ is shown in Fig. 37. However, it should be emphasized that there is no solid indication yet that the p_T distribu-tions of Drell-Yan lepton pairs seen so far are well described by QCD. In line with the discussion of growing $<p_T>$ and jets in section 1.5, one would expect that $W^{\pm}$ or Z^0 production events with large p_T would be accompanied by an opposite side gluon or quark jet.[135]

So far we have said relatively little about how one might look for vector bosons in hadron-hadron collisions. The best prospects are appar-ently provided by $Z^0 \rightarrow e^+e^-$ or $\mu^+\mu^-$ decay, where one has an invariant mass peak to find superimposed on a continuum background which is expected to be very small. The large $<p_T>$ of the Z^0 should not disturb us, as long as we have a detector with sufficiently large lepton acceptance. The next most likely signature would appear to be $W^{\pm} \rightarrow \ell^{\pm}(\nu)$ decay. Here there is no invariant mass peak to be found, but the kinematics of $W^{\pm}$ decay give the $\ell^{\pm}$ spectrum quite a well-defined Jacobian peak in p_T as long as the $<p_T>$ of the $W^{\pm}$ is not too large. Figure 38 shows a cal-culation[123] of the spread of the $W^{\pm}$ Jacobian peaks expected in QCD. The smearing is not disastrous, despite the relatively large p_T (3.33) expected in QCD. The reason is apparently the characteristic bremsstrah-lung shape of the spectrum, which keeps a sharp peak at $p_T \sim 0$. Also shown in Fig. 38 is a calculation[123] of the lepton background expected in QCD which is two or three orders of magnitude below the peak. How-ever, it should be noticed that no experiment has ever found such a

nice Jacobian peak, and one could certainly imagine ways in which the
neat picture of Fig. 38 could be diluted.[136] For example $W^\pm \to \tau^\pm(\nu)$
would give prompt leptons which could start filling in the holes at
p_T=O(20) GeV, or there could be large numbers of prompt leptons coming
from heavy quark decays to push up the background levels. There are of
course features of the W decay leptons which could be used to suppress
background contamination. For one thing, the missing unobserved neu-
trino will cause lots of p_T to be missing, and this could be noticed by
a detector with sufficiently large acceptance. For another thing,
plausible backgrounds would not have the charge-symmetry violating
forward-backward asymmetry of W decay leptons in $\bar{p}p$ collisions shown in
Fig. 33. It therefore seems likely that the $W \to e\nu$ or $\mu\nu$ decays could
also be seen in hadron-hadron collision experiments.

Much more difficulty will be experienced with hadronic decays of
the vector bosons. These should give two jets with an invariant mass of
84 or 94 (?) GeV, but the background expected from QCD is very large.
The fundamental q-q, q-G and G-G scattering processes in QCD give a p_T^{-4}
hadron background,[137] which will mainly be in the form of pairs of jets
with a continuous mass distribution at a level considerably above the
$W^\pm$ and Z^0 production rates. Figure 39 shows a calculation[123] of the
pp $\to$ jet+X QCD background. (It also features guesses at the prompt γ
and μ spectrum which are useful in estimating backgrounds to the search
for leptonic decays of the vector bosons.) In the absence of a cunning
trick for suppressing the QCD background, it seems to me unlikely that
the vector bosons will e easy to find in their hadronic decay modes.

Before leaving the topic of vector boson production in hadron-hadron collisions, it may be worthwhile to remember[138] that the production of W^+W^- or Z^0Z^0 pairs is not totally negligible:

$$\frac{\sigma(pp \to W^+W^-X)}{\sigma(pp \to W^-X)} = O\left(\frac{1}{n}\right) \tag{3.34}$$

Some relevant graphs are shown in Fig. 40, and the results of a naive parton cross section calculation are[138] shown in Fig. 41. It seems that for pp collisions at $\sqrt{s} \sim 800$ GeV one might expect cross sections

$$\sigma(pp \to W^+W^-X) \sim 10^{-36} \text{ cm}^2$$
$$\sigma(pp \to Z^0Z^0X) \sim 10^{-37} \text{ cm}^2 \tag{3.35}$$

Given the luminosity $O(10^{33} \text{ cm}^{-2} \text{ sec}^{-1})$ expected at Isabelle, it should be possible to detect the processes (3.35). It is apparent from Fig. 40 that the W^+W^- production process is sensitive to the 3-boson vertex. However the measurement of it in this reaction seems much more tricky than in e^+e^- collisions because of the large backgrounds in hadron-hadron collisions.

3.4 Effects in ep Collisions

Let us first consider[101,124] the direct production of $W^\pm$ and Z^0 in ep collisions. The most important Feynman diagrams are those shown in Fig. 42. Production from the lepton vertex is generally larger than that from the hadron vertex because the hadron momentum is shared out between a number of quarks and gluons, only one of which can participate in any given reaction. Forms for the cross sections are rather complicated and not of intrinsic interest, so they will not be exhibited here.[101,124] In Fig. 43 are plotted the cross sections for ep → νWX and ep → eZX. We see that for immediately foreseeable centre-of-mass energies for ep

colliding rings ($E_e \sim 20$ to 30 GeV, $E_p \sim 250$ to 400 GeV, $\sqrt{s} \sim 150$ to 200 GeV) and reasonable $W^{\pm}$ and Z^0 masses the orders of magnitude of the cross sections are

$$\sigma(ep \to \nu W X) \sim 10^{-38} \; cm^2$$

$$\sigma(ep \to eZX) \sim 10^{-37} \; cm^2$$

(3.36)

so that with the projected[101] luminosities $O(10^{32} \; cm^{-2} \; sec^{-1})$ we are talking about very marginal event rates $O(1)$ per week or day at best. One asset of these reactions is that they are potentially very clean, with the final hadronic state X being a single proton about $\frac{1}{2}$ the time, and otherwise having a tendency to be a lightweight hadronic system, by the general standards of such a machine. However, it must be admitted that presently conceivable ep machines offer bleak prospects for detecting or studying intermediate vector bosons.

Much more interesting for this class of machines[101,124] is the study of indirect effects of the $W^{\pm}$ and Z^0 from their exchanges and interference with γ exchange in the case of the Z^0. The Q^2 accessible with such a machine range up to $O(10^4)$ GeV^2, where γ and Z^0 exchanges are of equal order of magnitude, and one can expect $O(1)$ charge asymmetries or parity violations, to be compared with the $O(10^{-4})$ effects detected in present experiments. Detailed formulae for the effects are given in the CHEEP report[101]: some representative calculations are shown in Fig. 44. Figure 44(a) shows the charge asymmetry

$$\frac{\sigma(e^- p)}{\sigma(e^+ p)} \neq 1$$

(3.37)

expected in ep collisions at $x = 0.25$, $s = 27,000$ GeV^2 and varying values of Y. The $SU(2)_L \times U(1)$ Weinberg-Salam model (A,B), $SU(2)_L \times SU(2)_R \times U(1)$ model (C)

and model with an $\begin{pmatrix} E^0 \\ e^- \end{pmatrix}_R$ doublet (D) can clearly be easily distinguished. We also see considerable sensitivity to the mass of the Z^0, which can be measured indirectly in this way. Figure 44(b) shows the parity violating effect

$$\frac{\sigma(e_L^- p)}{\sigma(e_R^- p)} \neq 1 \qquad (3.38)$$

which can be expected for similar values of the kinematic variables. All calculations are in the Weinberg-Salam model, but with m_Z adjusted arbitrarily while keeping identical neutral current cross sections near $Q^2=0$. You might wonder to what extent these calculations are independent of the strong interaction model used, which was the naive parton model. Figure 44(c) shows the effect on the parity-violating asymmetry (3.38) of including asymptotic freedom effects[101] which modify the quark distributions as discussed in Lecture 1. We see that the changes are minimal, indicating that strong effects do not confuse the weak effects. Figure 44(d) shows a comparison[101] of the scaling violations expected from asymptotic freedom compared with the apparent deviations from a point-like electromagnetic cross sections which would be exhibited by weak interference effects on $\sigma(e^-p) + \sigma(e^+p)$ in a variety of models. We see that strong scaling deviations are expected to be small in the range of large Q^2 where weak interferences are large. Conversely, the strong scaling violations are big when $Q^2 \lesssim O(1000)$ GeV^2 where the weak interference effects are relatively small. It seems that QCD and weak gauge theory effects can plausibly be disentangled in the reaction $ep \rightarrow e+X$.

Figure 45 shows the effect on the charged current reaction $ep \rightarrow \nu+X$ of asymptotic freedom and/or the finite mass of the $W^\pm$.[124] There is

clearly great sensitivity to deviations from the pointlike four-fermion interaction. With a luminosity of 10^{32} cm^{-2} sec^{-1} one would obtain several hundred events a day even in the most pessimistic case of a low $W^{\pm}$ mass.

3.5 The Z^0 Peak in e^+e^- Annihilation

Clearly the cleanest and most dramatic place to study the Z^0 is in e^+e^- collisions,[93,121,122] where it is produced alone and with a high rate. For comparison, let us normalize the cross sections of this and the subsequent section to

$$\sigma_{pt} \equiv \sigma(e^+e^- \to \gamma^* \to \mu^+\mu^-) = \frac{4\pi\alpha^2}{3s} \qquad (3.39)$$

At the centre-of-mass energy of order 94 GeV which we are interested in, $\sigma_{pt} \sim 10^{-2}$ nb corresponding to an event rate of 3.6 events per hour if the projected luminosity of 10^{32} cm^{-2} sec^{-1} is attained. The analysis of section 3.2.2 suggested that we should be prepared for a total Z^0 decay width of order 2 to 3 GeV. This is much wider than the e^+e^- beam energy evolution which is expected to be $O(10^{-3})$ of the beam energy itself, giving a an energy resolution $O(100)$ MeV. We can therefore discuss the Z^0 peak under the assumption

$$\Gamma(Z^0 \to \text{all}) \gg \Delta E_{\text{beam}} \qquad (3.40)$$

whereas the reverse situation applies to the J/ψ and Υ hadronic resonances. At the peak of the resonance, the condition (3.40) means that

$$\frac{\sigma(e^+e^- \to Z^0 \to \text{all})}{\sigma_{pt}} \approx \frac{9}{\alpha^2} B(Z^0 \to e^+e^-) \qquad (3.41)$$

Putting in $B(Z^0 \to e^+e^-) \sim 3\%$ as suggested in Eq. (3.20), we find

$$\frac{\sigma(e^+e^- \to Z^0 \to \text{all})}{\sigma_{pt}} \gtrsim 5000 \qquad (3.42)$$

corresponding to $O(5)$ Z^0 decays/second.[139] It should be emphasized that this rate is sensitive to the existence of unsuspected decays of the Z^0 (many neutrinos?) which could suppress $B(Z^0 \to e^+e^-)$ and the size of the peak. Nevertheless, experiments with $O(10^7)$ Z^0 decays become imaginable. This gives us many possibilities for precision measurements and/or studies of rare Z^0 decays.

Let us first discuss the shape[93] of total $e^+e^- \to f\bar{f}$ cross sections in the neighborhood of the Z^0 peak. The quantity

$$R_f \equiv \frac{\sigma(e^+e^- \to \gamma^*, Z^0 \to f\bar{f})}{\sigma_{pt}}$$

$$= Q_f^2 - \frac{2\rho Q_f v_e v_f}{\left(\left(\frac{u}{m_Z^2} - 1\right) + \frac{\Gamma_Z^2}{s - m_Z^2}\right)} + \frac{\rho^2 s^2 (v_e^2 + a_e^2)(v_f^2 + a_f^2)}{\left(\left(\frac{s}{m_Z^2} - 1\right)^2 + \frac{\Gamma_Z^2}{m_Z^2}\right)} \qquad (3.43)$$

where the vector and axial couplings v_e and v_f were defined in Eq. (3.10), and the Weinberg-Salam values are tabulated in Eq. (3.12). The quantity ρ appearing in Eq. (3.43) is defined by

$$\rho \equiv \frac{G_F}{8\sqrt{2}\,\pi\alpha} \qquad (3.44)$$

and sets the scale for the magnitude of weak interference effects. In the special case that $f\bar{f} = \mu^+\mu^-$, we have

$$R_\mu \approx 1 + 2v_\mu^2 + (v^2 + a^2)^2 \, \rho^2 \qquad (3.45)$$

if we neglect Γ_Z, and assume e-μ universality

$$v_e = v_\mu \equiv v, \qquad a_e = a_\mu \equiv a \qquad (3.46)$$

In Eq. (3.45), χ is defined by

$$\chi = \rho m_Z^2 \frac{s}{s - m_Z^2} \qquad (3.47)$$

In the special case of $m_Z \simeq 94$ GeV corresponding to $\sin^2 \theta_W = 0.20$, the expression (3.44) implies that $\rho_Z^2 \simeq 0.39$. The cross section ratio (3.45) goes through a minimum when

$$\frac{s}{m_Z^2} = \left(\frac{1}{m_{Z0}^2}\right) \frac{v^2}{(v^2 + a^2)^2} \qquad (3.48)$$

In the Weinberg-Salam model with $\sin^2 \theta_W = 0.20$ this occurs at $\sqrt{s} = 29$ GeV. The value of R_μ at the minimum is

$$R_\mu = 1 - \frac{v^4}{(v^2 + a^2)^2} \qquad (3.49)$$

Unfortunately, if $\sin^2 \theta_W = 0.20$ so that $v=0.2$, the minimum value of R_μ is 0.9985, which might be difficult to disentangle from 1. However, Eqs. (3.45), (3.48) and (3.49) show that the shape R_μ of the cross section is in principle sensitive to the ratio $|v/a|$. Figure 46 shows the behaviour of R_μ for some representative values[93] of the vector and axial couplings. The Weinberg-Salam model with $\binom{E^0}{e^-}_R$ and $\binom{M^0}{\mu^-}_R$ doublets would have $a=0$, which would certainly make the R_μ plot interesting!

Another measurement of interest is the charge violating forward backward asymmetry. In general one has, neglecting Γ_Z,

$$\frac{d\sigma(e^+ e^- \to f \bar{f})}{d \cos \theta} = \frac{\pi \alpha^2}{2s} \left\{ q_f^2 (1 + \cos^2 \theta) - 2Q_f \left[v_e v_f (1 + \cos^2 \theta) + 2a_e a_f \cos \theta \right] \right.$$
$$\left. + \chi^2 \left[(v_e^2 + a_e^2)(v_f^2 + a_f^2)(1 + \cos^2 \theta) + 8v_e a_e v_f a_f \cos \theta \right] \right\} \qquad (3.50)$$

where χ was previously defined in Eq. (3.47). The integrated asymmetry

$$A_f \equiv \frac{\int_0^1 d\sigma_f - \int_{-1}^0 d\sigma_f}{\int_0^1 d\sigma_f + \int_{-1}^0 d\sigma_f} \tag{3.51}$$

is readily calculated from Eq. (3.50) to be

$$A_f = \frac{\frac{3}{2}\chi\left(-Q_f a_e a_f + 2v_e a_e v_f a_f \chi\right)}{\left[Q_f^2 - 2Q_f \chi v_e v_f + \chi^2\left(v_e^2 + a_e^2\right)\left(v_f^2 + a_f^2\right)\right]} \tag{3.52}$$

There is bound on A_f from the combination of $L_z=0$ and 1 initial states:

$$|A_f| \leq \frac{3}{4} \tag{3.53}$$

and a nonvanishing effect clearly requires a_e, $a_f \neq 0$. If we first specialize to the low energy case where only the term linear in χ is retained:

$$A_f \approx \frac{-\frac{3}{2}\chi \, a_e a_f}{Q_f} \tag{3.54}$$

Since $|a_e| = |a_f| = 1$ for all fermions in the Weinberg-Salam model (3.12), if we set

$$\chi = \rho m_Z^2 \, \frac{s}{s - m_Z^2} \approx 0.07 \tag{3.55}$$

corresponding an e^+e^- centre-of-mass energy around 40 GeV, we see from (3.54) that

$$|A_\mu| \approx 10\% \ , \quad |A_{u,c,t}| \approx 7\% \ , \quad |A_{d,s,b}| \approx 14\% \tag{3.56}$$

with the differences being generated by the differences in the quark charges. This type of asymmetry measurement may be a good way of getting at the weak couplings of the s,c,... quarks which were not accessible in

neutral current experiments to data (c.f. section 2.2). The asymmetries get more exciting closer to the Z^0 pole. Specializing to $\mu^+\mu^-$ we have from Eq. (3.52)

$$A_\mu = \frac{3}{2}\chi \frac{(a^2 + 2v^2 a^2 \chi)}{\left(1 + 2\chi v^2 + \chi^2(v^2 + a^2)^2\right)}$$ (3.56)

which goes through a minimum at

$$\frac{s}{m_Z^2} = \frac{1}{1 + (\rho m_Z^2)(a^2 + 3v^2)}$$ (3.57)

where it attains the value

$$A_\mu = -\frac{3}{4} \frac{1}{\left(1 + \frac{2v^2}{a^2}\right)}$$ (3.58)

For comparison, the value at the peak of the resonance is approximately

$$A_\mu \approx \frac{3v^2 a^2}{(v^2 + a^2)^2}$$ (3.59)

while the asymmetry is a maximum at

$$\frac{s}{m_Z^2} = \frac{1}{1 - (\rho m_Z^2)(a^2 - v^2)}$$ (3.60)

where it attains the maximum value

$$A_\mu = +\frac{3}{4}$$ (3.61)

For orientation purposes, the values and positions of the asymmetries (3.57) to (3.60) have the following values in the Weinberg-Salam model with $\sin^2 \theta_W = 0.20$:

$$A_\mu^{min} = -0.69 \quad at \quad \sqrt{s} = 78 \text{ GeV}$$

$$A_\mu^{peak} = +0.11 \quad at \quad \sqrt{s} = 94 \text{ GeV}$$

$$\Lambda_\mu^{\max} = +0.75 \quad \text{at} \quad \sqrt{s} = 118 \text{ GeV} \tag{3.62}$$

In Fig. 47 we plotted[93] generic curves of the asymmetry A_μ (3.56) for a fixed $m_Z = 83$ GeV and an interesting collection of v and a couplings.

A third class of interesting measurements at and near the Z^0 pole concerns polarization and helicity-dependent effects. If we first consider the case of unpolarized e^+e^- beams, the dependence of the cross section on the helicity of the final state fermion is of the form:

$$\frac{d\sigma_f}{d\cos\theta} = \sigma_1 + h_f \sigma_2 \tag{3.63}$$

where $\sigma_1 = \frac{1}{2} \frac{d\sigma(e^+e^- \to f\bar{f})}{d\cos\theta}$ (cf. Eq. (3.50)) and

$$\sigma_2 \equiv \frac{\pi\alpha^2}{2s} \chi \left\{ Q_f \left[v_e a_f (1+\cos^2\theta) + 2a_e v_f \cos\theta \right] \right.$$
$$\left. - \chi \left[v_f a_f (a_e^2+v_e^2)(1+\cos^2\theta) + 2a_e v_e (a_f^2+v_f^2)\cos\theta \right] \right\} \tag{3.64}$$

with the mean fermion helicity

$$\langle h_f \rangle = -\langle h_{\bar{f}} \rangle = \frac{\sigma_2}{\sigma_1} \equiv H_f(\theta,s) \tag{3.65}$$

The dependence on initial e^- beam helicity h^+ is

$$\frac{d\sigma_f(h^+,h^-)}{d\cos\theta} = (1-h^+h^-)\sigma_1 + (h^- - h^+)\bar{\sigma}_2$$
$$= \sigma_1 \left[(1-h^+h^-) + (h^- - h^+)\bar{H}_f(\theta,s) \right] \tag{3.66}$$

where $\bar{\sigma}_2$ and $\bar{H}_f$ are obtained from σ_2 and H_f respectively by the substitutions $(a_e, v_e) \leftrightarrow (a_f, v_f)$. The integrated average final state fermion

helicities from unpolarized beams are

$$H^f(s) = -H^{\bar{f}}(s) = \frac{\int_{-1}^{1} \sigma_2 \, d\cos\theta}{\int_{-1}^{1} \sigma_1 \, d\cos\theta}$$

$$= \frac{2\chi a_f \left[Q_f v_e - \chi v_f \left(a_e^2 + v_e^2 \right) \right]}{Q_f^2 - 2Q_f \chi v_e v_f + \chi^2 \left(a_e^2 + v_e^2 \right) \left(a_f^2 + v_f^2 \right)} \tag{3.67}$$

It is clear the final state fermion helicity is sensitive to the product $a_f v_e$ at low energies, and $a_f v_f$ close to the Z^0 pole. A sample plot of (3.67) for the mean μ (or τ helicity) is shown in Fig. 48.[93] Unfortunately, if the Weinberg–Salam model with $\sin^2\theta_W = 0.20$ is correct, the average helicity is rather small. For example, if we specialize to the forward direction $\cos\theta = +1$ to maximize the effect,

$$H^{\mu^-} \text{ or } \tau^-(s,\cos\theta = +1) = \frac{4\chi \, av \left[1 + \chi(a^2 + v^2) \right]}{\left[1 + 2\chi(v^2 + a^2) + \chi^2 \left[(a^2 + v^2)^2 + 4a^2 v^2 \right] \right]} \tag{3.68}$$

which becomes 0.13 on the resonance peak. There is a similar effect on the cross sections of the initial state electron helicity, which is dependent on $a_e v_f$ at low energies and $a_e v_e$ near the Z^0 pole. Since the v_f are not necessarily small in the Weinberg–Salam model with $\sin^2\theta_W = 0.20$, unlike v_e, measurements of the dependence of cross sections on the $e^+ e^-$ helicity may perhaps be most interesting away from the Z^0 peak itself.

One reaction we have not discussed up to now is $e^+ e^- \to e^+ e^-$, where there are crossed channel exchanges as well as the direct channel γ and Z^0 diagrams. We are used to the differential cross section for this reaction being sharply peaked forward-backward because of the crossed

channel γ exchange. In the neighborhood of the Z^0 resonance this asymmetry may be sharply reduced. More details can be found in section 3 of the CERN e^+e^- report.[93]

Detailed measurements of the Z^0 peak will be useful for several things besides measuring $\sin^2 \theta_W$ to 3 decimal places. For example, a detailed measurements of m_{Z^0} enables us to exclude very massive fermions,[91,92] as discussed in section 2.2. On the other hand, a precise measurement of the width of the Z^0 peak or of the height (3.41), combined with a determined search for massive fermions with masses $< m_{Z/2}$, can tell us how many unobserved neutrinos there are. We should therefore be able to clear up fermion spectroscopy as well as boson spectroscopy. The possibility of precise measurements with 10^7 Z^0 decays should enable us to probe weak radiative corrections, which might for example give us a look at the effects of very massive Higgs systems.[140] As for rare Z^0 decays, one interesting possibility is $Z^0 \to$ Higgs $+ (\mu^+\mu^-$ or $e^+e^-)$, which looks to be a promising way of scanning for neutral Higgs particles with masses up to O(50) GeV as will be discussed in lecture 4. One might hope that the decay $Z^0 \to W^+e^{\pm}\nu$ or $\mu^{\pm}\nu$ would be a good way of looking for single $W^{\pm}$ production below the W^+W^- threshold. Unfortunately, the decay rate[125]

$$\Gamma(Z^0 \to W^+e^+\nu) \lesssim 10^{-2} \text{ GeV} \qquad (3.69)$$

which makes the prospects look bleak, even with 10^7 Z^0 decay experiments. Even above resonance the $e^+e^- \to W^{\pm}e$ cross section is unappreciably small, being

$$\sigma(e^+e^- \to W^+e^+\nu) = O(10^{-37} \text{ to } 10^{-36}) \text{ cm}^2 \qquad (3.70)$$

$$\text{for } \sqrt{s} \sim 110 \text{ to } 200 \text{ GeV}$$

It seems that the best prospects for $W^\pm$ production will be above the pair production threshold, to which we turn in the next section. For the moment, we just note that e^+e^- experiments are a source of Z^0 production and decays which enables studies many orders of magnitude more precise than any other machine.

3.6 e^+e^- Annihilation Beyond the Z^0 Pole

The next most obviously interesting reaction beyond the Z^0 pole is W^+W^- pair production.[125,126] This reaction is a showcase for gauge theories, since it enables one to search for, and hopefully observe, the cancellations between different crossed and direct channel exchanges which are needed[52] for the renormalizability of the theory. The diagrams involved should be the direct channel γ and Z^0, and the crossed channel neutrino and possible heavy lepton exchanges in Fig. 49. In particular, one would like to see evidence for the archetypical 3 boson interaction, either in the form of the γW^+W^- vertex which should have a specific value for the anomalous magnetic moment, or in the form of the $Z^0 W^+W^-$ vertex itself. A useful study of the $e^+e^- \to W^+W^-$ reaction has been made by Alles, Boyer and Buras,[125] who emphasize that the gauge theory cancellations are important even quite close to threshold.

Let us consider the Weinberg-Salam model,[141] where the differential cross section can be written in the form

$$\frac{d\sigma(e^+e^- \to W^+W^-)}{d\Omega} = \frac{\alpha^2}{2! \sin^4 \theta_W} \frac{\beta}{s} \sum_{i,j} M_{ij} \qquad (3.71)$$

where the M_{ij} are the distinct interferences and cross sections. They take the forms

$$M_{\gamma\gamma} = F_{\gamma\gamma}(s,\theta) \qquad M_{\gamma\gamma} = \sin^4 \theta_W F_{ZZ}(s,\theta)$$

$$M_{ZZ} = \left(\sin^4 \theta_W - \frac{1}{2} \sin^2 \theta_W + \frac{1}{8}\right) \frac{s^2}{(s-m_Z^2)^2} F_2(\theta,s)$$

$$M_{ZY} = 2 \sin^2 \theta_W \left(\frac{1}{2} - \sin^2 \theta_W\right) \frac{s}{s-m_Z^2} F_2(\theta,s)$$

$$M_{\gamma Z} = \left(\sin^2 \theta_W - \frac{1}{2}\right) \frac{s}{s-m_Z^2} F_3(\theta,s)$$

$$M_{\gamma\gamma} = -\sin^2 \theta_W F_3(\theta,s) \tag{3.72}$$

where the F_i are useful kinematic combinations

$$F_1(\theta,s) \equiv \frac{2}{a} + \frac{\sin^2 \theta}{2} \left\{\left(\frac{s}{K^2}\right)^2 + \frac{1}{4a^2}\right\} s^2$$

$$F_2(\theta,s) \equiv s^2 \left\{\frac{16}{a} + \left(\frac{1}{a^2} - \frac{4}{a} - 12\right) \sin^2 \theta\right\}$$

$$F_3(\theta,s) \equiv 16 \left(1 + \frac{m_W^2}{K^2}\right) + 9 s^2/a + s^2 \frac{\sin^2 \theta}{2} \left(\frac{1}{a^2} - \frac{2}{a} - \frac{4s}{K^2}\right) \tag{3.73}$$

The definitions of various quantities appearing in Eqs. (3.72) and (3.73) are

$$a = \frac{m_W^2}{s}, \qquad \beta = \sqrt{1-4a}, \qquad L = \ln\frac{1+\beta}{1-\beta}, \qquad K^2 = m_W^2 - \frac{s}{2} - \frac{s}{2} \beta \cos\theta \tag{3.74}$$

Meditation will reveal that $M_{\gamma\gamma}$ is sharply peaked forward-backward, while γ and Z exchanges are relatively isotropic. When we integrate (3.71) over the solid angle Ω to get the total cross section we find

$$\sigma(e^+e^- \to w^+w^-) = \frac{\pi\alpha^2}{8 \sin^4 \theta_W} \frac{\beta}{s} \sum_{ij} \bar{z}_{ij} = \sum_{ij} \bar{z}_{ij} \tag{3.75}$$

where corresponding to Eq. (3.72):

$$\bar{z}_{\gamma\gamma} = \bar{z}_1 \qquad \bar{z}_{\gamma\gamma} = \sin^4 \theta_W \bar{z}_2$$

$$\bar{\sigma}_{ZZ} = \left(\sin^4 \theta_W - \frac{1}{2} \sin^2 \theta_W + \frac{1}{3}\right) \frac{s^2}{\left(s - m_Z^2\right)^2} \; \bar{\sigma}_2$$

$$\bar{\sigma}_{Z\gamma} = 2\left(\frac{1}{4} - \sin^2 \theta_W\right) \sin^2 \theta_W \frac{s}{s - m_Z^2} \; \bar{\sigma}_2$$

$$\bar{\sigma}_{\gamma Z} = \left(\sin^2 \theta_W - \frac{1}{2}\right) \frac{s}{s - m_Z^2} \; \bar{\sigma}_3$$

$$\bar{\sigma}_{\gamma\nu} = -\sin^2 \theta_W \; \bar{\sigma}_3 \qquad\qquad (3.76)$$

with

$$\bar{\sigma}_1 = \frac{2}{a} + \frac{1}{12a^2} \, \varepsilon^2 + 4\left\{(1-2a)\frac{\varepsilon}{s} - 1\right\}$$

$$\bar{\sigma}_2 = \frac{16}{a} \, \varepsilon^2 + \frac{2}{3} \, \varepsilon^2 \left\{\frac{1}{2} - \frac{4}{a} + 12\right\}$$

$$\bar{\sigma}_3 = 16 - 32 \, \frac{L\varepsilon}{\varepsilon} + \varepsilon \, \frac{\varepsilon}{a} + \frac{\varepsilon^2}{3a^2} \, (1-2a) + 4(1-2a) - \frac{16La^2}{8} \qquad (3.77)$$

Getting it all together we finish up with

$$\sigma(e^+ e^- \to w^+ w^-) = \frac{-\pi^2 \bar{\sigma}_3}{2 \sin^2 \theta_W s} \left\{ (1+2a+2a^2) \frac{1}{3} - \frac{5}{4} \right.$$

$$+ \frac{m_Z^2 (1 - 2\sin^2 \theta_W)}{s - m_Z^2} \left[2a^2 \left(1 + \frac{2}{a}\right) \frac{1}{3} - \frac{1}{12a} - \frac{5}{2} - a \right]$$

$$\left. + \frac{m_Z^4 \left(3 \sin^4 \theta_W - 4 \sin^2 \theta_W + 1\right)}{48 \left(s - m_Z^2\right)^2} \frac{s^2}{a^2} (1 + 20a + 12a^2) \right\}$$

$$(3.78)$$

In Fig. 50 we have plotted[115] $\sigma(e^+ e^- \to w^+ w^-)$ from Eq. (3.78) for some (rather large) values of $\sin^2 \theta_W$ and (rather small) values of m_W. We see that the cross section has a rather neat peak about 40 GeV above

threshold, of height $O(10^{-35})$ cm^2 which could be observable given a
luminosity of 10^{32} cm^{-2} sec^{-1}, followed by a sharply falling cross sec-
tion at higher energies which is a few times σ_{pt} (3.39). The diagram-
matic cancellations are exhibited[125] in Fig. 51, and are very significant
even quite close to threshold. Therefore we may hope to see the famous
gauge theory cancellations even at low centre-of-mass energies $\sqrt{s} \leq 200$
GeV. The neutrino exchanges cause the W^+W^- angular distribution to be
sharply peaked forward-backward even relatively close to threshold.[125]
On the other hand, it is difficult[141] to disentangle the γ and Z^0
exchange effects because they are required by gauge theory to have simi-
lar structure, but even the determination of the γW^+W^- vertex would be an
interesting nontrivial check of gauge theory ideas.

Another interesting reaction is the process $e^+e^- \to Z^0 + \text{Higgs}$,[10]
which may be a good way of producing Higgs particles with masses above
50 GeV, and is more background-free than the $Z^0 \to \text{Higgs} + \ell^+\ell^-$ decay
mode mentioned earlier. This reaction will be discussed in more detail
in Lecture 4.

Mention should be made of the reaction $e^+e^- \to Z^0Z^0$.[139] In the
standard model, this only proceeds by lepton exchange in the crossed
channel. It is therefore less interesting than $e^+e^- \to W^+W^-$, since it
does not give us a window on the 3-boson vertex. However, the cross
section is quite big close to threshold (see Fig. 52), quite likely
being as large as for $e^+e^- \to W^+W^-$ around $\sqrt{s} = 200$ GeV. Is this reaction
useful for something?

It would be nice to measure the 4-boson vertex, perhaps in the two-
photon process $e^+e^- \to e^+e^-W^+W^-$, but... .

4. The Funny Farm

4.1 Introduction

This last lecture will be concerned with various aspects of gauge theories which are more controversial than the topics discussed so far. Most of the lecture will be devoted to Higgs bosons in some form or another. As was emphasized in the introduction to Lecture 2, the renormalizability of present gauge theories of the weak interactions[2,63] depends on the masses of particles being generated by spontaneous symmetry breaking. No fully satisfactory way has ever been found of generating masses by some dynamical mechanism which does not invoke elementary Higgs fields. Furthermore, all realistic spontaneously broken weak interaction models have at least one Higgs boson remaining in the physical spectrum. For example, the simplest $SU(2)_L \times U(1)$ Weinberg-Salam model has j   ne physical neutral Higgs boson if the symmetry is broken by just one $I=\frac{1}{2}$ multiplet, and there are additional charged and neutral bosons if more than one multiplet is used. It therefore seems very important to do experimental searches for Higgs particles.[10] Either they will be found, in which case the spontaneously broken gauge theory picture will finally be confirmed, or if they do not exist theorists will have to totally rethink their ideas. Much of the lecture will discuss empirical and theoretical constraints on the simplest Higgs system in the Weinberg-Salam model, and possible ways of doing experimental searches for neutral Higgs particles.

There will also be some discussion of more complicated Higgs systems, including possible charged bosons. One possible modification[142] of the Higgs system which has attracted much interest recently implies

the existence of a very light pseudoscalar Higgs boson, the axion,[143] which would play a role in preventing QCD from having a strong source of CP violation. In its simplest form, the axion would be very light with a mass $\leq O(1)$ MeV, but this possibility now seems to be phenomenologically excluded.[144,145,146] However, a more sophisticated, massive, axion could still exist. A search for it then becomes rather like the search for a neutral Higgs boson discussed earlier.

The last parts of the lecture will be concerned with much more speculative aspects of gauge theories. One possibility present in some gauge theories was the existence of a magnetic monopole,[147] with a mass $O(1)$ TeV. The phenomenology of monopoles is rather amusing. Unfortunately, they are not present in the Weinberg-Salam model, which is just as well since there are cosmological arguments[148] that exclude monopoles of the simplest type, as found[147] for example in the Georgi-Glashow model.[149] The Weinberg-Salam may possess other types of "extended" structure on a scale of 1 TeV or more, but they would not be strictly (topologically) stable. These include rotating dumb-bells[150] and vortex-like[151] solutions of the field equations. It is not at all clear whether such things do exist, or if they are stable even if they do exist, or if they are observable even if they are stable. But their existence would certainly make life interesting.

In the rest of the lectures, we have been relatively conservative in our theoretical models, only considering models that unify weak and electromagnetic interactions. However, we should clearly keep in mind the possibility of unifying them with strong interactions. The last part of this lecture will discuss this inspirational topic.[152,153]

focusing in particular on phenomenological tests of this grand unification concept. For example, the proton is generally unstable in grand unified theories, and may have a lifetime within a few orders of magnitude of the present experimental limit of 2×10^{30} years.[154,72] While not strictly speaking a weak interaction at high energies, an experiment to refine the limit on this fundamental quantity seems an encouragingly offbeat note on which to finish these lectures.

4.2 Higgs in the Weinberg-Salam Model

As was mentioned before, gauge theories[2] need Higgs bosons if they are to incorporate masses and remain renormalizable. Indeed, it has been shown that from analyses[63] of the Born diagrams that Higgs particles must not only be present, but must have interactions with fermions, bosons and each other which are essentially those specified in a spontaneously broken gauge theory. In the Weinberg-Salam theory one needs at least one I=½ Higgs multiplet $H \equiv \binom{H^+}{H^0}$ to give masses to the fermions through couplings of the form

$$\mathcal{L}_H \ni \bar{f}_R H^+ f_L \qquad (4.1)$$

(recall that right-handed fermions are SU(2) singlets, while left-handed fermions are SU(2) doublets[2]). As emphasized in Lecture 2, the apparent success[25,78] of the neutral current rate predictions resulting from the relation (2.20) strongly suggests that the vector bosons also get most of their masses from I=½ Higgs. We are therefore led to contemplate spontaneous symmetry breaking by I=½ Higgs alone, and the simplest possibility is to use just one multiplet. In this case the Higgs system

has just 4 degrees of freedom

$$\underset{\sim}{H} \equiv \begin{pmatrix} H^+ \\ H^0 \end{pmatrix}, \qquad \underset{\sim}{H}^- \equiv \begin{pmatrix} -H^{0*} \\ H^+ \end{pmatrix} \tag{4.2}$$

When the neutral Higgs acquires a vacuum expectation value v:

$$H^0 = \frac{1}{\sqrt{2}} \, (v + H + i\tilde{H}) \tag{4.3}$$

from the minimum (Fig. 53(a)) of a Higgs potential of the form

$$V(H) = \mu^2 \, H^+H + \lambda(H^+H)^2 \quad ; \quad \mu^2 < 0 \tag{4.4}$$
$$\lambda > 0$$

3 of the Higgs degrees of freedom (4.2), namely H^+, H^- and $\tilde{H}$, are eaten by the W^+, W^- and Z^0 respectively to become their longitudinal polarization states, while one degree of freedom H is left over as a physical, neutral Higgs particle.[10] The magnitude of v reflects the masses of the vector bosons:

$$v^2 = \frac{1}{\sqrt{2} \, G} \tag{4.5}$$

with

$$m_W^2 = \frac{g^2 v^2}{4} \, , \qquad m_Z^2 = \frac{g^2 v^2}{4 \cos^2 \theta_W} \tag{4.6}$$

where g is the non-Abelian SU(2) semiweak coupling constant. The W^+W^-H and Z^0Z^0H couplings are fixed to be large:

$$g_{W^+W^-H} = \frac{2m_W^2}{v} \, , \qquad g_{Z^0Z^0H} = \frac{2m_Z^2}{v} \tag{4.7}$$

On the other hand, the $f\bar{f}H$ couplings are generally small

$$\mathscr{L}_H \ni (H^0 + v) \, \bar{f}f \, g_{f\bar{f}H} \tag{4.8}$$

implying that

$$g_{f\bar{f}H} = \frac{m_f}{v} = \{2^{\frac{1}{2}} \, G\}^{\frac{1}{2}} m_f \tag{4.9}$$

which is small as long as m_f is in the range of presently known fermion masses. Some of the implications of fermions with very large masses[91,92] were discussed in section 2.2.

The parameters of the potential (4.4) are simply related to the value of v:

$$\lambda v^2 = -\mu \qquad (4.10)$$

and the resulting physical Higgs mass is

$$m_H^2 = -2\mu^2 \qquad (4.11)$$

It is apparent that none of the formulae (4.4 to 4.11) give us any way of fixing m_H, which is a priori totally unknown. Is it $O(m_f) \ll m_W$? or $O(m_W)$ like other bosons? or $\gg m_W$?

There are some theoretical considerations on the Higgs boson mass which come from considering radiative corrections[154] to the Higgs poten- tial (4.4). Effectively, they give a lower bound to the interaction term, which by an analogue of Eq. (4.10) for the simple interaction gives in turn a lower bound[155] on the Higgs mass. The extra potential term has the form

$$\Delta V_1(H) = \frac{1}{64\pi^2 v^4} \left[3 \sum_{W,Z} m_i^4 \right] (H^+ \cdot H)^2 \ln\left(\frac{H^+ \cdot H}{m_0^2} \right) \qquad (4.12)$$

and demanding that the gauge symmetry break spontaneously to the minimum value of the combined potential (4.4), (4.12) as in Fig. 53(b) yields the bound:

$$m_H^2 \gtrsim \frac{3\sqrt{2} G}{16\pi^2} \left[2m_W^4 - m_Z^4 \right] \qquad (4.13)$$

where we have neglected the fermion contribution in Eqs. (4.12 and 4.13) implying

$$m_H^2 \gtrsim \frac{3\alpha^2 \left(2 + \sec^4 \theta_W\right)}{16\sqrt{2} G \sin^4 \theta_W}$$ (4.14)

which for $\sin^2 \theta_W \gtrsim 0.20$ is

$$m_H \geq 7.1 \text{ GeV}$$ (4.15)

This bound is interestingly nontrivial, but some cautionary remarks should be made. The first is that the bound disappears[10] if there is any fermion with mass $O(m_W)$, because the fermions contribute to (4.13) with a minus sign. The second comment is that it is not strictly necessary that the Universe must lie in the lowest possible vacuum.[156] If one allows for the Universe to have chosen a nonminimal value of the Higgs potential as in Fig. 53(c), and demands only that the lifetime for quantum-mechanical tunnelling to the lowest vacuum be greater than the age of the Universe $\sim 10^{10}$ years, the bound (4.15) is greatly relaxed,[157] to

$$m_H > 260 \text{ MeV}$$ (4.16)

for $\sin^2 \theta_W = 0.33$, somewhat higher for $\sin^2 \theta_W \gtrsim 0.20$. However, it has been argued[157] that the nonminimal vacuum could only be chosen and the bound (4.16) attained only if the early Universe initially had enormous lepton number $L \gtrsim 10^8 B$. If there were no such large asymmetry, one would recover a bound of the same order as (4.14). It therefore seems that observation of a low-mass Higgs boson with a mass in the range between (4.16) and (4.15) would be cosmologically fascinating! Before leaving

the subject of the radiative correction bound (4.11), it should be emphasized that if there are more than one $I=\frac{1}{2}$ Higgs multiplet, while the bound (4.13) would apply to one of the neutral Higgs particles, some of the others could have lower masses.[156]

In view of the above remarks, it seems reasonable to ask for empirical constraints on the existence of low-mass Higgs bosons. The most substantial phenomenological bounds are 3 independent arguments[10] that $m_H > 0$ (15 to 20) MeV. One is the absence of light scalar Higgs bosons produced in $0^+ \rightarrow 0^+$ nuclear transitions, which exclude $m_H < 18$ MeV. Another is the absence of Higgs exchange effects in neutron-nucleus scattering, which suggest that m_H is probably >13 MeV. The third is muonic atom X-rays, which at one time showed anomalies which could be explained by the effects of exchanging a Higgs with mass 0 (10-20) MeV, but which have now become completely canonical.

The three empirical constraints above all come from nuclear physics, and reflect characteristic nuclear energy scales. One might expect some more stringent restrictions on the mass of the Higgs to come from high energy physics, but this does not seem to be the case. The closest high energy physics comes seems to be in K decay, where the branching ratio

$$B(K^+ \rightarrow \pi^+ + H) \simeq O(10^{-7}) \qquad (4.17)$$

was estimated[10] for $m_H = O(m_\pi)$, and there is an experimental upper limit

$$B(K^+ \rightarrow \pi^+ + H) \ B(H \rightarrow e^+e^-) < 0.4 \times 10^{-7} \qquad (4.18)$$

for 140 MeV $< m_H <$ 340 MeV. Only Higgs particles in the mass range up to 210 MeV are expected to have a substantial ($\geq 10\%$) branching ratio into e^+e^- (see the next section), but it seems that the bound (4.18) is not even sufficient to rule out 140 MeV $< m_H < 2m_\mu$.

There are some theoretical arguments[140,159,160] against the exist-
ence of a very heavy Higgs boson which, while not rigorously excluding
the possibility, emphasize the problems involved. As in the case of
massive fermions discussed in section 2.2, the point is that Higgs par-
ticles become strongly interacting if they are very massive, as is seen
immediately from Eqs. (4.10) and (4.11). Veltman[140] in particular has
suggested that the Higgs mass should be less than the value which makes
perturbation theory break down. This would require

$$\frac{g^2}{4\pi} \frac{m_H^2}{m_W^2} \lesssim 1 \qquad (4.19)$$

or $m \lesssim 300$ GeV. Lee, Quigg and Thacker[160] have done a detailed partial
wave analysis for WW, ZZ and HH scattering and conclude that partial wave
unitarity is violated by the Born diagrams unless

$$m_H^2 \lesssim \frac{8\pi\sqrt{2}}{3G} \approx 1 \text{ (TeV)}^2 \qquad (4.20)$$

If the Higgs mass tried to exceed this value, presumably perturbation
theory would not be applicable, but probably some sort of complicated
bound state would drop out on a mass scale $\lesssim 1$ TeV. One might expect that
the strong interactions of the Higgs particles would have some dramatic
lower energy manifestations. Unfortunately, no example of this has yet
been found, because the Higgs effects are always shielded by the rela-
tively small $f\bar{f}H$ or WWH couplings.

In view of all these inconclusive remarks about the mass of the
Higgs boson, even in the relatively tightly constrained Weinberg-Salam
model, it behooves us to consider almost any possible mass, and look for
the Higgs in many different places. We therefore turn to possible future
experimental probes.

4.3 Higgs Phenomenology

4.3.1 Decays

Before discussing experiments to find a Higgs boson, perhaps we should first think about what we should look for.[10] The decay modes of relatively light Higgs are simple to deduce from Eq. (4.9). In general, the favoured decay mode for a Higgs with mass $<2m_W$ will be into the heaviest available fermion pair as in Fig. 54(a):

$$\Gamma(H \rightarrow f\bar{f}) \backsimeq \frac{Gm_f^2}{4\sqrt{2}\,\pi}\, m_H \left[1 - \frac{4m_f^2}{m_H^2}\right]^{3/2} \left\{\begin{array}{c} \times 3 \text{ for} \\ \text{colour} \end{array}\right\} \qquad (4.21)$$

Thus $c\bar{c}$ decays should dominate H decays in the mass range 4 GeV $< m_H$ < 10 GeV, with $\tau^+\tau^-$ decays suppressed by a colour factor of 3. Between the top and bottom thresholds, $b\bar{b}$ decays should dominate by a factor of $O(10)$ compared with $c\bar{c}$ decays, and so on. The situation is less clear for light Higgs particles, because the quark-parton model cannot be used to estimate the hadronic decays. But estimates support the naive guess that strange particles will dominate H decays in the mass range of 1 to 4 GeV, while $\tau\tau$ final states should dominate for $2m_\tau < m_H < 1$ GeV, and $\mu^+\mu^-$ decays for $2m_\mu < m_H < 2m_\tau$. Higgs masses below the $\mu^+\mu^-$ threshold may be somewhat academic in view of the remarks of section 4.3, but it is possible that $H \rightarrow \gamma\gamma$ through virtual fermion and boson loops as in Fig. 54(b) could be important for $m_H \gtrsim 30$ MeV, with $H \rightarrow e^+e^-$ otherwise dominating when $m_H > 2m_e$. A compendium[13] of likely Higgs branching modes for 1 MeV $< m_H < 100$ GeV is shown in Fig. 55. Heavy Higgs bosons would[160]

decay into W^+W^- or Z^0Z^0 pairs:

$$\left.\begin{array}{c} \dfrac{\Gamma(H \rightarrow W^+W^-)}{m_H} \\[2ex] \dfrac{\Gamma(H \rightarrow Z^0Z^0)}{m_H} \end{array}\right\} = \left\{\begin{array}{c} 2 \\ 1 \end{array}\right\} \dfrac{Gm_H^2}{16\pi\sqrt{2}} \dfrac{\sqrt{1-x}}{x} (3x^2 - 4x + 4) \qquad (4.22)$$

where $x \equiv 4m_W^2/m_H^2$ or $4m_Z^2/m_H^2$ respectively.

The lifetimes for Higgs particles which result from these available decay modes are portrayed[10] in Fig. 56, becoming unobservably short 10^{-9} sec $> \tau_H > 10^{-21}$ sec for $2m_\pi < m_H < 100$ GeV. The dominant boson pair decays (4.22) of heavier Higgs bosons push up their decay rates to become comparable with their masses when $m_H \sim 1$ TeV. This corresponds to the strong interaction "bound" (4.20).

4.3.2 Production

We now run through a selection of possible Higgs production mechanisms.

Vector meson $\rightarrow$ H+γ

The radiative decay (Fig. 57) of a heavy $q\bar{q}$ vector meson, say $\Upsilon(b\bar{b})$ or the forthcoming toponium $t\bar{t}$ into a Higgs particle has a substantial[161] branching ratio:

$$\dfrac{\Gamma(V \rightarrow H+\gamma)}{\Gamma(V \rightarrow \mu^+\mu^-)} \approx \dfrac{Gm_V^2}{4\sqrt{2}\,\pi\alpha} \left(1 - \dfrac{m_H^2}{m_V^2}\right) F\left(\dfrac{m_H^2}{m_V^2}\right) \qquad (4.23)$$

where $F\left(m_H^2/m_V^2\right)$ is a known function[162] which is quite well approximated by

$$F\left(\dfrac{m_H^2}{m_V^2}\right) \approx \left(1 - \dfrac{m_H^2}{m_V^2}\right) \qquad (4.24)$$

For $m_H \sim \frac{1}{2}m_V$ the formulae (4.23, 4.24) yield

$$\frac{\Gamma(V \to H+\gamma)}{\Gamma(V \to \mu^+\mu^-)} \approx \begin{cases} 3 \times 10^{-3} & \text{for } \Upsilon \\ 3 \times 10^{-2} & \text{for } t\bar{t} \text{ if } m_t = 15 \text{ GeV} \end{cases} \tag{4.25}$$

Putting in the expected branching ratios

$$B(\Upsilon \to \mu^+\mu^-) \sim 3\% , \qquad B(t\bar{t} \to \mu^+\mu^-) \sim 8\% \tag{4.26}$$

we find the final branching ratios

$$B(V \to H+\gamma) \approx \begin{cases} 10^{-4} & \text{for } \Upsilon \\ 2 \times 10^{-3} & \text{for } t\bar{t} \text{ if } m_t = 15 \text{ GeV} \end{cases} \tag{4.27}$$

These branching ratios (4.27) are quite promising, and suggest that the decay $V \to H+\gamma$ may be a good way of looking for Higgs bosons with masses up to the as yet unknown mass of the $t\bar{t}$ bound state.

$Z \to H + \ell^+\ell^-$

This can proceed through the diagram shown in Fig. 58, where the $\mu^+\mu^-$ pair are produced by a virtual Z, and the relatively large Z^0Z^0H coupling (4.7) is being exploited to get a reasonable branching ratio. Bjorken[122] has calculated the decay rate

$$\frac{1}{\Gamma(Z^0 \to \mu^+\mu^-)} \frac{d\Gamma(Z^0 \to H\mu^+\mu^-)}{dx} = \frac{\alpha}{4\sin^2\theta_W \cos^2\theta_W} \frac{\left[1 - x + \frac{x^2}{12} + \frac{2}{3}\frac{m_H^2}{m_Z^2}\right]\left[x^2 - \frac{4m_H^2}{m_Z^2}\right]^{\frac{1}{2}}}{\left(x - \frac{m_H^2}{m_Z^2}\right)^2} \tag{4.28}$$

where $x \equiv 2E_H/m_Z$. In Fig. 59 is shown $\dfrac{\Gamma(Z^0 \to H\mu^+\mu^-)}{\Gamma(Z^0 \to \mu^+\mu^-)}$ as a function of m_H for $\sin^2\theta_W = 1/3$. We see that the relative decay rate is $\gtrsim \times 10^{-5}$ for $m_H \lesssim 40$ GeV. Taking the branching ratio for $Z^0 \to \mu^+\mu^-$ to be 3% gives a

total branching ratio

$$B(Z^0 \to H_\mu^+ \mu^-) \geq 10^{-6}$$

$$\text{or } \mu e^+ e^-$$

(4.29)

for $m_H < 40$ GeV. This should be accessible if one really can do experiments with $O(10^7)$ Z^0 decays, as seemed possible (section 3.5) with a Z^0 factory.

Another decay which may yield Higgs at a rate comparable to (4.29) is $Z^0 \to H\gamma$, which would proceed via virtual fermion and $W^\pm$ loops. An order of magnitude calculation suggests that $B(Z^0 \to H\gamma) \sim 10^{-6}$ also.

$e^+e^- \to Z^0 + H$

This is the complement of the $Z^0 \to H\mu^+\mu^-$ reaction. Again one uses the large Z^0Z^0H coupling (4.7) to bremsstrahl a Higgs. The only difference is that the process is now $Z^* \to Z + H$ instead of $Z \to Z^* + H$ as in Fig. 60. The cross section is[163]

$$\sigma(e^+e^- \to Z^0 + H) = \frac{\pi\alpha^2}{24} \left(\frac{2K}{\sqrt{s}}\right) \left(\frac{K^2 + 3m_Z^2}{(s - m_Z^2)^2}\right) \frac{\{1 - 4\sin^2\hat{\epsilon}_W + 8\sin^4\hat{\epsilon}_W\}}{\sin^2\hat{\epsilon}_W \{1 - \sin^2\hat{\epsilon}_W\}^2}$$

(4.30)

where K is the centre-of-mass momentum of the Z^0 or H. The cross section for $e^+e^- \to Z^0 + H$ relative to the QED $\sigma(e^+e^- \to \mu^+\mu^-) \equiv \sigma_{pt}$ (3.39) is plotted[164] in Fig. 61 for a range of centre-of-mass energies $\sqrt{s}$, and values of m_H. The "error bars" on the theoretical curves represent the uncertainty in varying $\sin^2\hat{\epsilon}_W$ from 0.22 to 0.29. We see that at $\sqrt{s} \approx 200$ GeV even a Higgs of mass close to 100 GeV could be produced with a cross section $\gtrsim 10^{-37}$ cm^2, corresponding to 1 event/day at a luminosity of 10^{32} cm^{-2} sec^{-1}. Furthermore, the event will be relatively "clean" and easy to pick out using a Z^0 trigger.

$pp \rightarrow H + X$

Three possible Higgs production mechanisms have been proposed for high energy hadron-hadron collisions. First there is a simple $pp \rightarrow H + X$, where the dominant production mechanism is probably via gluon-gluon collisions,[165] and the Higgs-GG coupling is estimated using virtual quark loops.[161] Calculations (see Fig. 62) indicate that

$$\sigma(pp \rightarrow H + X) \gtrsim 10^{-35} \text{ cm}^2 \text{ for } m_H \lesssim 30 \text{ GeV},$$
$$\sqrt{s} \gtrsim 400 \text{ GeV} \qquad (4.31)$$

depending somewhat how many quarks are put into the loops. This cross section certainly yields a sizeable event rate at a machine like Isabelle. Unfortunately, it is difficult to think of a signature which would enable the Higgs events to be separated from the less interesting events. One possible way of solving this problem is to look for $pp \rightarrow Q + \bar{Q} + H + X$, where Q is some heavy quark, and the Higgs is bremsstrahled from the heavy quark line. A naive order of magnitude estimate[166] suggests that the cross section for $pp \rightarrow b + \bar{b} + H + X$ might be comparable to (4.31), and the presence of heavy quark particles in the final state might serve as a useful signature. A still better signature would come from the reaction[167,1t--] $pp \text{ (or } \bar{p}p) \rightarrow W^{\pm} \text{ or } Z^0 + H + X$. Calculations[164] (see Fig. 63) indicate that

$$\frac{\sigma(p\,p \rightarrow W^{\pm}\ \text{or}\ Z^0 + H + X)}{\sigma(p\,p \rightarrow W^{\pm}\ \text{or}\ Z^0 + X)} \sim 10^{-4} \qquad (4.32)$$

for $m_H \lesssim$ 30 GeV and pp collisions at $\sqrt{s}$ = 800 GeV or $\bar{p}p$ collisions at $\sqrt{s}$ = 5.0 GeV. The cross section (4.33) might well be accessible at Isabelle, and the $W^{\pm}$ or Z^0 could provide a signature through decay leptons.

$\nu+N \rightarrow \mu+H+X$

In this reaction the dominant diagram is likely to be that where the Higgs is bremsstrahlung from the exchanged W line[10,168] as in Fig. 64. For light Higgs and neutrino energies which are not so large that $W^{\pm}$ propagator effects are important,

$$\frac{\sigma(\nu+N \rightarrow \mu+H+X)}{\sigma(\nu+N \rightarrow \mu+X)} \sim 3 \times 10^{-6} \times E_{\nu}(\text{GeV}) \qquad (4.33)$$

The cross section ratio (4.34) is probably too low to be usable, given the absence of a distinctive Higgs decay signature. The same remarks apply to high energy ep colliding rings,[101] where the Higgs cross section is plausibly $0(10^{-38})$ cm^2, compared with a possible luminosity of $0(10^{32})$ cm^{-2} sec^{-1}.

To summarize the above discussion, it seems that the most promising sources of the basic neutral Weinberg-Salam Higgs boson may be (in order of increasing m_H): T decays, toponium decays, Z^0 decays, $e^+e^- \rightarrow Z^0+H$, with pp $\rightarrow W^{\pm}$ or $Z^0 + H$ as the least unpromising alternative to e^+e^- colliding beam experiments.

4.4 More Complicated Higgs Systems

4.4.1 Charged Higgs particles

If the Weinberg-Salam model is modified very slightly to include more than one $I=\frac{1}{2}$ Higgs multiplet, then only one combination of the charged Higgs fields ($\phi_1^+, \phi_2^+ \ldots$) can be eaten by the W^+, and the remaining combination or combinations will show up as physical charged scalars. There is considerable freedom to adjust parameters, but one would expect a general correlation of the Higgs couplings with the masses of the fermions. Thus important decays of H^+ might be[169] $H^+ \rightarrow \tau^+\nu_{\tau}$, $c\bar{s}$, $t\bar{b}$, etc., depending on the mass of the H^+. An invariant mass peak in a

combination $(\bar{c}K)^+$ would be interesting! The cross section for producing H^+H^- pairs in e^+e^- collisions is just

$$\frac{\sigma(e^+e^- \to \gamma^* \to H^+H^-)}{\sigma_{\mu\mu}} = \frac{1}{4}\left(1 - \frac{4m_{H^+}^2}{s}\right)^{3/2} \qquad (4.34)$$

Such a charged pair would therefore not have a big threshold in e^+e^- collisions. However, if the H^+ were sufficiently massive, H^+H^- events would probably have high sphericity and acoplanarity close to threshold, and the sort of sphericity scan advocated in Lecture 2 for finding heavy quarks would also find an H^+H^- threshold. The H^+H^- threshold would then be distinguished by its pointlike structureless nature and the absence of resonances below threshold. If m_t (or m_b) and m_{H^+} are in the right relationship, decays like $t \to H^+ b$ or $b \to H^- c$ become kinematically accessible.[170] Bearing in mind the expected generic correlation of H^+ couplings with quark mass, one might expect

$$\Gamma(Q \to H^+ q) \approx \frac{G_F m_Q^3}{3\sqrt{2}} \times \binom{\text{angle}}{\text{factors}} \times \binom{\text{phase}}{\text{space}} \qquad (4.35)$$

for a heavy quark Q to decay into H^+ and a lighter quark q. In the case of Q=b a (generalized) Cabibbo angle factor might be present, so that

$$\Gamma(b \to H^- c) \approx 10^{-5} \, (\sin^2 \theta) \; \text{GeV}$$

$$\approx 1 \; \text{keV ?} \qquad (4.36)$$

This decay rate would certainly dominate conventional weak decays of b: it would even be a significant decay mode of $\Upsilon = b\bar{b}$,[171] giving final states $\Upsilon \to H^+ \bar{b} c X$! It should soon be possible to exclude such decays at the level of a branching $\approx 10\%$, which would militate against an H^+ with mass $\lesssim 2$ GeV, and similar searches could be made in the decays of mesons

made of heavier quarks. One can easily add decays like H^0 or $Z^0 \to \mu^+\mu^-$ to the list of possible places to look, but these are somewhat more distant prospects.

4.4.2 The axion

The axion[143] is a special type of neutral Higgs particle which was proposed as a way of solving certain problems concerning CP violation in QCD.[142,172] These are that when nonperturbative topological aspects of QCD are taken to account, it turns out that there may be an extra term

$$\mathcal{L}_\theta = \frac{\theta}{32\pi^2} \epsilon_{\mu\nu\rho\sigma} F^a_{\mu\nu} F^a_{\rho\sigma} \tag{4.37}$$

to be included in the QCD Lagrangian with θ an a priori unknown parameter. You can see from the form of $\mathcal{L}_\theta$ (4.32) that it has C even and P odd, and hence violates CP. In the real world, CP violation due to the strong interactions is extremely small. The best limit on it comes from the neutron electric dipole moment $\frac{D}{e}$, which is known experimentally[27] to be

$$\frac{D}{e} \lesssim 3 \times 10^{-24} \text{ cm} \tag{4.38}$$

This quantity violates CP and would be proportional to θ if it were nonzero but small. One calculation[173] gives

$$\frac{D}{e} \approx 4 \times 10^{-16} \theta \text{ cm} \tag{4.39}$$

so allowing for uncertainties in the theoretical calculation, θ must be $< 10^{-8}$. It would be nice to ensure that $\theta = 0$ automatically. This could be done[142] by giving the world's Lagrangian an extra $U(1)$ symmetry with an associated current J^5_μ. Similar anomalies to the ones we discussed in Lectures 1 and 2 cause the divergence of this current to be

nonzero:

$$\partial_\mu J^5_\mu \approx \frac{f_{\mu\nu\rho\sigma}}{16\pi^2} F^a_{\mu\nu} F^a_{\rho\sigma} \tag{4.40}$$

By making a chiral transformation of the J^5_μ type, one changes the Lagrangian by an amount proportional to $\partial^\mu J^5_\mu$ (4.40), and so may remove any possible term $\mathcal{L}_\theta$ (4.37) from the QCD Lagrangian. The next problem is to find a way of giving the Lagrangian this U(1) symmetry. One way would be if one of the quarks--probably the u quark--had zero mass. But this hypothesis, while not completely excluded, looks to be in bad shape when one looks at meson and baryon mass differences.[174] An alternative way of getting a U(1) symmetry is to introduce a pseudoscalar boson which is essentially massless. This can be done by extending the simplest Weinberg-Salam model to two or more Higgs multiplets, and restricting their interactions so that the combined QCD-modified Weinberg-Salam theory has the requisite U(1) symmetry. The low mass pseudoscalar boson introduced in this way is the axion (a).[143] Its mass is not strictly zero because of strong interaction symmetry breaking effects, which cause its mass to be generically of order

$$m_a = \sqrt{G_F} \times \mu^2 \tag{4.41}$$

where μ is some typical strong interaction scale--O(300) MeV?--so that one might expect $m_a = O(10^{2\pm1})$ keV. Being a Higgs particle, one would expect the couplings g_{aff} to be $O(gm_f/m_w)$, as for the basic Higgs boson (4.9).

To proceed further, we will turn to the simplest axion model,[143] which has just two $1\times\frac{1}{2}$ Higgs multiplets. The theory is then characterized

by a free parameter

$$\frac{v_1}{v_2} = \frac{\langle 0|H_1^0|0\rangle}{\langle 0|H_2^0|0\rangle} = \tan \alpha \qquad (4.42)$$

where in order to get the $W^{\pm}$ mass correct

$$v_1^2 + v_2^2 = \frac{1}{\sqrt{2} \, G} \qquad (4.43)$$

which should be compared with the single Higgs formula (4.5). In this model, the coupling to heavy quarks has a form analogous to (4.9):

$$\mathcal{L}_{aq} = 2^{\frac{1}{4}} \, G^{\frac{1}{2}} \, a \Big[m_c \bar{c} \gamma_5 c \, \tan \alpha + m_b \bar{b} \gamma_5 b \, \cot \alpha + \ldots \Big]$$
$$+ m_t \bar{t} \gamma_5 t \, \tan \alpha + \ldots \qquad (4.44)$$

On the other hand, the axion coupling to light quark systems goes predominantly through mixing with the π^0 and η which have the same quantum numbers ($C=+1$, $P=-1$) as the axion. The mixing is specified by parameters

$$\xi_\pi = \zeta \left[\left(\frac{3m_d - m_u}{m_d + m_u} \right) \tan \alpha - \left(\frac{3m_u - m_d}{m_u + m_d} \right) \cot \alpha \right]$$
$$\xi_\eta = \zeta \left[\sqrt{3} \, \tan \alpha + \frac{1}{\sqrt{3}} \cot \alpha \right] \qquad (4.45)$$

where $\zeta \simeq 2^{-5/4} \, G^{1/2} f_\pi \simeq 1.9 \times 10^{-4}$, and the axion mass in this simplest model is approximately

$$m_a \simeq \frac{f m_\pi f_\pi}{\sqrt{2}(m_u + m_d)^{\frac{1}{2}}} \left[\frac{m_u m_d m_s}{m_u m_d c + m_d m_s + m_s m_u} \right] \frac{2^{1/4} \, G^{1/2}}{\sin 2\alpha}$$
$$\simeq \frac{23 \pm f}{\sin 2\alpha} \text{ keV} \qquad (4.46)$$

where f is the number of quark flavours, as usual. The simplest axion described by the formulae (4.42) to (4.46) would presumably be lighter

than $2m_e$ and so decay mainly into 2γ with a lifetime $\gtrsim 10^{-4}$ sec. The mixings (4.45) would allow the axion to be produced at rates $O(10^{-7})$ of π^0 or η production in any hadronic process. The couplings (4.44) ensure its production in heavy vector meson decays[143,161] $V \to a+\gamma$ at a rate $\tan^2 \alpha$ (or $\cot^2 \alpha$) times the $V \to H+\gamma$ rate (4.23).

Can the axion exist? Probably not in the simplest form discussed above, but this is not totally excluded. Evidence against it comes from several sources.

Beam dump experiments

In experiments[175,176] at CERN, a proton beam has been dumped into a hadron target which absorbed hadronic secondaries before most of them decayed, and searches were made for events in neutrino experiment detectors downstream which could have been generated by neutral penetrating particles such as neutrinos or the axion as in Fig. 65. Axion-induced events would have shown up as apparent neutral current events with small missing p_T in the hadronic final state. It has been estimated[144] that

$$\frac{\sigma(p+p \to a+X)}{\sigma(p+p \to \pi^0+X)} \approx \xi_\pi^2 + \frac{1}{3}\xi_\eta^2, \qquad \frac{\sigma(a+p \to X)}{\sigma(\pi^0+p \to X)} \approx \xi_\pi^2 + \frac{2}{3}\xi_\eta^2 \tag{4.47}$$

implying a product of axion production and interaction cross sections

$$\sigma(p+p \to a+X)\sigma(a+p \to X) \approx (\xi_\pi^2 + \frac{1}{3}\xi_\eta^2)(\xi_\pi^2 + \frac{2}{3}\xi_\eta^2) \cdot 2 \times 10^{-31} \text{ cm}^4$$

$$\gtrsim 9 \times 10^{-66} \text{ cm}^4 \tag{4.48}$$

where the lower bound comes from the fact that ξ_π (4.45) cannot be switched off, even though ξ_η can be zero for uncooperative values of m_d/m_u and $\tan \alpha$. Various experimental limits on axion production in the CERN beam dump experiments[175,176] are $O(10^{-62})$ cm^4, indicating that the bound (4.48) is violated by about two orders of magnitude,[145] so that an axion with

mass $\lesssim$ 2 MeV cannot exist. An analysis[146] has also been made of a SLAC beam dump experiment which also finds an upper limit of an axion-induced events about two orders of magnitude less than would have been expected in the simple model discussed above.

Reactor neutrino experiments

Axions could show up in these experiments by being produced in nuclear transitions and then decaying into $\gamma\gamma$, or undergoing Compton scattering $a+e \to \gamma+e$, or by causing deuteron disintegration $a+d \to n+p$.[143] Unfortunately, theoretical estimates of axion production rates by nuclei are rather unreliable. Nevertheless, it has been conservatively[146] estimated that

$$N_{a \to 2\gamma} \simeq 10^3 \left(\frac{m_a}{100 \text{ keV}}\right)^6 \tag{4.49}$$

axion $\to \gamma\gamma$ decays should have been seen per day, compared with an experimental limit of (-160 ± 260) γ events/day. Also

$$N_{a+e \to \gamma+e} \sim \frac{10^3}{\tan^2 \alpha} \tag{4.50}$$

would have been expected. The deuteron disintegration rate is naively calculated to be $O(10^3)$ larger than the experimental limit, though this calculation is particularly sensitive to unreliable details of nuclear calculations. Despite the uncertainties[143,146] in the nuclear calculations, it seems likely that reactor neutrino experiments also rule out the simplest form of axion.

Cosmology and astrophysics

The best restriction on the axion from these sources comes from considerations on the evolution of red giant stars. It is apparently[177] required that $m_a > 200$ keV, but this is not inconsistent with the mass estimate (4.46).

$K^+ \to \pi^+ + a$
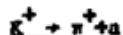
We believe that this decay rate should be comparable with that esti-
mated[101,178] for $K^+ \to \pi^+ + H \sim O(10^{-7})$ (4.17). The relevant experimental
limit is that on $K^+ \to \pi^+ \nu\bar{\nu} < 6 \times 10^{-7}$. We conclude that K decays do not
yet exclude the axion's existence.

The preponderance of the above evidence is against the existence of
an axion in the simple form given by Eqs. (4.42) to (4.46). However,
the existence of an axion cannot be totally excluded.[179] For example,
the parameter α (4.42) could be very small for some reason which may
seem unnatural in the context of this model, but might be made to look
less unreasonable in a more complicated model with more Higgs multiplets
and/or vector bosons.[179] When α is sufficiently small the axion decays
mainly into $e^+ e^-$, which it does too quickly to show up in beam dump or
reactor experiments. Its phenomenology would then resemble that of the
very light Higgs bosons discussed in sections 4.2 and 4.3, with the
exception that being a pseudoscalar, the various nuclear constraints
that $m_H > (15 \text{ to } 20)$ MeV would not apply to the axion.

What if there is no axion? No other totally satisfactory method of
ensuring $\theta = 0$ has yet been proposed. Even if $\theta = 0$ for the strong interac-
tions alone, the possibility exists that it may be renormalized by the
weak interactions and become unacceptably large. In the simplest
Weinberg-Salam model with one Higgs multiplet, if one sets $\theta = 0$ for the
strong interactions, the renormalization of θ due the CP violation in the
weak interactions generated by the Kobayashi-Maskawa model (2.39) is
zero in $O(\alpha)$, but nonzero and $O(10^{-16})$ in $O(\alpha^2)$.[180] There is another popular

model of CP violation which uses multiple Higgs multiplets,[103] which
has a larger renormalization of θ than allowed by experiment (4.38).
There is[181] another multi-Higgs model with θ renormalization which is
finite and $O(10^{-6}$ to $10^{-7})$, which is on the outskirts of phenomenological acceptability.[180] It seems that the problem of CP violation in QCD
and weak electromagnetic gauge theories is still very little understood,
and in particular we lack any good reason why θ should be zero or small
before weak renormalization.

4.5 Monopoles, etc.

We are now at the stage of the lectures where fantasy begins to take
over, and we examine some more speculative possibilities suggested by
gauge theories. In this section we would look into the possible existence
of heavy particles arising from extended solutions of the non-Abelian
field equations. The first example will be the monopole,[147] which is a
sort of topological knot tied in the Higgs system of a spontaneously
broken gauge theory. So far (cf. Eq. (4.5)) we have always discussed
situations where the Higgs vacuum expectation value was independent of x
as in Fig. 66(a):

$$\langle 0|H^0(x)|0\rangle = v \qquad (4.51)$$

but it could happen that $\langle 0|H^0(x)|0\rangle$ was x-dependent as illustrated in
Fig. 66(b). This could happen if there were an isotriplet of Higgs
particles:

$$\langle 0|H^i(x)|0\rangle \rightarrow v\left(\frac{x^i}{|x|}\right) \qquad (4.52)$$

as $|\underline{x}| \to \infty$ in all 3-space directions. Solutions like (4.52) exist in some gauge theories like the (phenomenologically defunct) Georgi-Glashow model,[152] but not in the Weinberg-Salam model with its left Higgs multiplets.

Nothing daunted, the generic properties of such monopoles are that they have masses

$$m_M \gtrsim \frac{1}{\alpha} m_{W,Z} \sim 1 \text{ TeV} \tag{4.53}$$

Their couplings to weak and electromagnetic fields are characteristically strong:

$$\frac{g_M^2}{4\pi} = O\left(\frac{1}{\alpha}\right) \tag{4.54}$$

and they presumably interact strongly with each other. Monopoles are guaranteed by their topological properties to be absolutely stable. Above the threshold $2m_M$, one would expect monopoles to be produced in pairs as in Fig. 67(a), but not by a single photon. The pair production cross section should be O(1) because of the strong coupling (4.54). The monopole pair could also annihilate into many photons and/or vector bosons as in Fig. 67(b). This process might be particularly important close to threshold, and have a dramatic signature in the form of very large γ showers. The motion of a monopole in a magnetic field is characteristically bizarre—its momentum tends to align itself parallel to any magnetic field as in Fig. 67(c). It should also be remembered that the monopole would find it very easy to lose energy by radiating photons (and W's and Z's)[101] as in Fig. 67(d).

Can monopoles exist? No one has ever been able to confirm seeing one. If one accepts the standard big-bang cosmology for the early

Universe, one can estimate[148] the density of monopoles which should have been formed then. The calculation of the monopole density today depends on how one believes the production model and estimates of the probability of mutual annihilation of the primordial monopoles. But it seems that monopoles with the properties (4.53, 4.54) should probably have been $O(10^6)$ more abundant than the experimental upper limit. But surely someone can come up with a theory containing more massive monopoles which would be cosmologically rarer and hence acceptable.

It was mentioned above that the Weinberg-Salam model does not have monopoles. Does it have any other sort of extended, heavy object? It has been proposed[150] that there may be quasi-stable string-like objects which somewhat resemble dumb-bells with a sort of monopole at each end as in Fig. 68(a). These would form Regge trajectories with an intercept and Regge slope of order 1 TeV^2. High spin "particles" on the leading trajectory--corresponding to rapidly rotating dumb-bells--would possibly be somewhat stable because of the angular momentum barrier. However, these objects would not be guaranteed stable by any topological conservation law, and their lifetimes are difficult to estimate. If these string-like solutions exist, so probably do other string configurations such as closed loops[151] which loosely resemble smoke rings or vortices as in Fig. 68(b). They would also have Regge trajectories, which would correspond to the Pomeron in normal Regge lore, and also have a mass-scale $O(1 \text{ TeV})$.

Unfortunately, it is not clear whether these string-like objects really exist in the Weinberg-Salam model, and if so how stable they are. Even if they do exist and are stable, it is not clear what their

production cross section is, except that it is probably very small.
They are in some sense coherent extended field configurations containing
$O\left(\frac{1}{\alpha}\right)$ vector bosons, and the overlap with the $O(1)$ vector boson state
produced, say, by e^+e^- collisions is probably very small.

The prospects for finding anything like a monopole in presently
conceivable weak interaction experiments seem rather dim. However, the
subject is still rather uncertain, and it is hoped that these remarks
may stimulate more serious theoretical thoughts, because objects of this
type would be very interesting if they exist.

4.6 Grand Unification Phenomenology

Up till now, we have been treating the strong and weak electromag-
netic interactions rather separately. With the exception of the discus-
sion of CP violation and the axion, which was not brilliantly successful,
we have not really addressed the theoretical interrelationship between
the different interactions. However, since we rather complacently
believe we have found the correct theory of the strong interactions,
namely QCD,[4] and think we are on the track of the right spontaneously
broken gauge theory of the weak interactions[2]--very possibly the Weinberg-
Salam model[16]—it is clearly high time to speculate on the next phase of
unification.[152,153] In the process of this grand unification, we may
hope first to find certain consistency conditions that must be imposed
on the individual strong, weak and electromagnetic interactions before
they can be unified. We may also hope to predict dramatic new types of
interaction, such as those violating baryon and lepton number and
causing the proton to decay.

Let us consider the type[152] of theory where a large group G is postulated which has a unique coupling constant, and which is broken somehow into component parts

$$G \rightarrow SU(3) \times SU(2)_L \times U(1) \times ?$$ (4.55)

for the different interactions. Clearly the grand unification symmetry[152] must be considerably broken, because the observed strong and weak coupling strengths are very different. However, after Lecture 1 and Eq. (1.14) we are used to the idea that coupling strengths depend on the scale at which they are measured. We believe that the strong interactions get weak at high momenta, so perhaps it is not[182] inconceivable that the strong and weak/electromagnetic coupling strengths may come together at some sufficiently high Q^2 as in Fig. 69(a). In the Weinberg-Salam model the $SU(2)_L$ and $U(1)$ couplings g and g' are independent, and the ratio

$$\sin^2 \theta_W = \frac{g'^2}{(g^2 + g'^2)}$$ (4.56)

is a number to be determined by experiment. A symmetry group G would make a prediction for g^2/g'^2, and hence for $\sin^2 \theta_W$. In the same way as the ratio α_s/α, the ratio g^2/g'^2 will be renormalized[182] if the G symmetry is only exact at very high momenta.

The simplest grand unification model is the SU(5) model of Georgi and Glashow,[152] which breaks down into exactly QCD × Weinberg-Salam. Simple application of the QCD evolution formula (1.14) for $\alpha_s(Q^2)$ shows that it will be O(α) only at very high Q^2. In fact, the best estimate of the momentum at which grand unification takes place in SU(5) is[72,183]

$$m_{GUM} = O(10^{15} \text{ to } 10^{16}) \text{ GeV}$$ (4.57)

Using this value, one can estimate the renormalization of $\sin^2 \theta_W$, which is 3/8 in the symmetry limit, to[72]

$$\sin^2 \theta_W \gtrsim 0.20 \qquad (4.58)$$

which is not in disagreement with the latest experiments. It is characteristic of grand unification models that they put quarks and leptons into the same multiplet of the grand unification symmetry group G. For example in $SU(5)$[152] there are multiplets

$$(\bar{d}_R, \bar{d}_Y, \bar{d}_B; e^-, \nu_e)_L; \ (\bar{a}_R, \bar{a}_Y, \bar{a}_B; \bar{u}, \nu_\mu)_L; \ (\bar{b}_R, \bar{b}_Y, \bar{b}_B; \ \ , \nu_\tau)_L \qquad (4.59)$$

which put meat on the often-discussed concept of quark-lepton universality that was discussed in section 2.2. Because of the large symmetry-breaking (4.57) inherent to this type of model, the quark-lepton symmetry will not be exact. But analogously to (4.58), the renormalizations of symmetry predictions may sometimes be calculable. Possible examples are quark and lepton masses.[71,72] The simplest $SU(5)$ representation of Higgs fields which can provide fermion masses is 5 dimensional, and it reduces to the usual $I=\frac{1}{2}$ doublet of Weinberg-Salam. The multiplet assignments (4.59) imply that in the symmetry limit

$$m_d = m_e; \qquad m_s = m_\mu; \qquad m_b = m_\tau \qquad (4.60)$$

Just as $\alpha_s(Q^2) > \alpha$ at present Q^2, so we also find that (4.60) gets renormalized to give $m_q > m_\mu$ as in Fig. 69(b). In fact one finds, using m_μ and m_τ as inputs, that[72,184]

$$m_s \sim 0.5 \ GeV, \qquad m_b \sim (5 \ to \ 5\frac{1}{2}) \ GeV \qquad (4.61)$$

where these masses are to be interpreted as approximately the masses of the lightest strange or bottom pseudoscalars respectively. (It is not possible to calculate m_d very reliably, but it does seem to be too small

by comparison with the usual current algebra estimates of m_d/m_s.) The predictions (4.58) and (4.61) of the SU(5) model are quite encouraging: it is unfortunate that in this model the masses of the charge 2/3 quarks cannot be calculated, so that there is no prediction for m_t. It should be mentioned that while the calculation of $\sin^2 \theta_W$ (4.58) is insensitive to the number of quark flavours, the quark mass calculations (4.61) depend crucially[72,184] on the number of quarks, and increase substantially if there are 8 or more quarks.

In view of the failure of this simplest type of grand unified model to have totally disastrous phenomenology, it is reasonable to continue speculating and think about baryon number-violating forces.[182] There is nothing sacred about baryon number conservation: it is believed to be violated by black holes[185] and by nonperturbative weak effects.[186] Baryon number is almost always violated in grand unified models. Indeed we see from the multiplet structure (4.59) that gauge bosons changing quarks into leptons must be present in the SU(5) model.[152] When the multiplets involving charge 2/3 quarks are added to (4.59), one finds transitions of the general form $q+q \to \ell+\bar{q}$ (Fig. 70) which are described by an effective low-energy four-fermi interaction (α,β,γ are colour indices, $u_L = \frac{1}{2}(1-\gamma_5)u$, etc.):

$$2\sqrt{2}\, G_{GUM}\left[\left(\epsilon_{\alpha\beta\gamma}\bar{u}^c_{\alpha_L}\gamma_\mu u_{\beta_L}\right)\left(\bar{e^+}\gamma^\mu\gamma_5 d_\gamma\right) + \left(\epsilon_{\alpha\beta\gamma}\bar{u}^c_{\gamma_L}\gamma_\mu d_{\beta_L}\right)\left(-\bar{e^+_L}\gamma^\mu u_{\alpha_L} + \bar{\nu^c_{e_R}}\gamma^\mu d_{\alpha_R}\right)\right]$$

$$+ \text{ Hermitian conjugate} \qquad (4.62)$$

where $m_{GUM} \simeq m_{X,Y}$ the masses of the baryon-number violating vector bosons
and

$$G_{GUM} \simeq \frac{g^2}{8m_X^2} = \frac{g^2}{8m_Y^2} \qquad (4.63)$$

The interaction (4.62) can give proton decays of the form

$$p \to e^+ + \pi^0, \quad \to \bar{\nu}_e + \pi^0, \quad \to \mu^+ + \pi^0, \quad \to \dots \qquad (4.64)$$

It is easy to see from the form of the interaction (4.62, 463) that the decay rate[182] for $p \to$ anything

$$\Gamma(p \to \text{all}) \propto \frac{1}{m_{GUM}^4} \qquad (4.65)$$

More detailed calculations[72] suggest that

$$\tau(\text{proton}) \sim 10^{30} \left(\frac{m_{GUM}}{10^{14} \text{ GeV}}\right)^4 \text{ years} \qquad (4.66)$$

The present lower limit on the proton lifetime is[187]

$$\tau(\text{proton}) \gtrsim 2 \times 10^{30} \text{ years} \qquad (4.67)$$

Comparing this limit with the estimate (4.57) of the grand unification mass and Eq. (4.66) we see that the SU(5) model makes the proton suffi-ciently stable.

Clearly the estimates (4.57) and (4.66) are very uncertain, even given the speculative nature of the grand unification ideas, and the remote possibility that the specific SU(5) model has anything to do with reality. Nevertheless these results may be generic, and suggest that experiments to improve the lower bound (4.67) by a few orders of magni-tude may be worthwhile. The limit (4.67) was obtained by looking at 20 tons of scintillator underground for about a year, and looking for

electrons with energies of a few hundred MeV, which might come from the decays of muons produced in proton decay. A present-day experiment cannot run for much more than a year, so an improved version would need much more matter to observe decaying. On the other hand, perhaps one could lengthen the time-base by looking in a smaller quantity of matter exposed over a geological epoch for fossil tracks of one of the types (4.64) produced in proton decay.

Regardless of the theoretical ideas discussed here, any experiment to improve the limit on the proton lifetime is of fundamental interest and importance.

References

1.   T. S. Kuhn, The Structure of Scientific Revolutions (University of
     Chicago Press, Chicago, 1970).

2.   E. S. Abers and B. W. Lee, Phys. Reports 9C, 1 (1973); J. C. Taylor,
     Gauge Theories of Weak Interactions (Cambridge University Press,
     1976); J. Iliopoulos, "An Introduction to Gauge Theories," CERN
     Yellow Report 76-11 (1976). For a review and references, see
     H. Quinn, Lectures at this Summer Institute.

3.   J. D. Bjorken, Stanford Linear Accelerator Center preprints SLAC-
     PUB-2062 (1977), SLAC-PUB-2133, -2134 (1978).

4.   H. D. Politzer, Phys Reports 14C, 129 (1974); W. Marciano and
     H. Pagels, Phys. Reports 36C, 137 (1978).

5.   J. D. Bjorken and E. A. Paschos, Phys. Rev. 158, 1975 (1969); S. D.
     Drell, D. J. Levy and T.-M. Yan, Phys. Rev. D_1, 1617 (1970);
     R. P. Feynman, Photon-Hadron Interactions (Benjamin, Reading,
     1972).

6.   For reviews and references see G. Altarelli, 1977 Gif-sur-Yvette
     Summer School Lectures, Rome preprint INFN-ROME-701 (1978);
     C. H. Llewellyn Smith, 1978 Schladning Winter School Lectures,
     Oxford University preprint 47/78 (1978).

7.   It has long been folklore that this is a general feature of renor-
     malizable field theories, hence the need for p_T butchery in the
     naive parton model. Ref. 5. For a discussion in the context of QCD,
     see H. D. Politzer, Phys. Lett. 70B, 430 (1977).

8.   J. Ellis, M. K. Gaillard and G. G. Ross, Nucl. Phys. B111, 253 (1976);
     T. A. DeGrand, Y. J. Ng and S.-H. H. Tye, Phys. Rev. D 16, 3251 (1977).

9.   For reviews and references see C. Quigg, Rev. Mod. Phys. 49, 297
     (1977); R. F. Peierls, T. L. Trueman and L.-L. Wang, Phys. Rev. D 16,
     1397 (1977); L. B. Okun and M. B. Voloshin, Nucl. Phys. B120, 459
     (1977).

10. J. Ellis, M. K. Gaillard and D. V. Nanopoulos, Nucl. Phys. B106,
     292 (1976); for a recent review see M. K. Gaillard, CERN preprint
     TH 2461, to be published in Comments on Nuclear and Particle
     Physics.

11. See for example, H. Georgi and S. L. Glashow, Phys. Rev. Lett. 32,
     438 (1974); H. Georgi, H. R. Quinn and S. Weinberg, Phys. Rev. Lett.
     33, 451 (1974).

12. S. Weinberg, Phys. Rev. Lett. 19, 126- (1967); A. Salam, Proceedings of the 8th Nobel Symposium, ed. by N. Svartholm (Almquist and Wiksell, Stockholm, 1968), p. 367.

13. S. D. Drell, D. J. Levy and T.-M. Yan, Phys. Rev. 187, 2159 (1969) and D 1, 1617 (1970); N. Cabibbo, G. Parisi and M. Testa, Lett. al Nuovo Cim. 4, 35 (1970); J. D. Bjorken and S. J. Brodsky, Phys. Rev. D 1, 1416 (1970).

14. J. D. Bjorken, Phys. Rev. 179, 15-7 (1969).

15. D. H. Perkins, Lectures at this Summer Institute. See also R. E. Taylor, Proc. 1975 Int. Symp. on Lepton and Photon Interactions at High Energies, Stanford, ed. by W. T. Kirk (Stanford Linear Accelerator Center, Stanford, 1975); Y. Watanabe et al., Phys. Rev. Lett. 35, 898, 901 (1975); H. L. Anderson et al., Phys. Rev. Lett. 37, 4 (1976) and 38, 1450 (1977).

16. S. D. Drell and T.-M. Yan, Phys. Rev. Lett. 25, 316 (1970).

17. D. H. Perkins, Proc. 16th Int. Conf. on High Energy Physics, Chicago-Batavia, 1972 (NAL, Batavia, 1973), p. 189.

18. P. C. Bosetti et al., Oxford University preprint "Analysis of Nucleon Structure Functions in CERN Bubble Chamber Neutrino Experiments" (1978).

19. T. A. DeGrand, Y. J. Ng and S.-H. H. Tye, Ref. 5; K. Koller and T. F. Walsh, Phys. Lett. 72B, 227 (1977), E 73B, 504 (1978); H. Fritzsch and K.-H. Streng, Phys. Lett. 7-B, 90 (1978); K. Hagiwara, Nucl. Phys. B137, 164 (1978).

20. S. J. Brodsky, T. G. Coyne, T. A. DeGrand and R. R. Horgan, Phys. Lett. 73B, 203 (1978).

21. A. Zee, Phys. Rev. D 7, 3630 (1973); S. Coleman and D. J. Gross, Phys. Rev. Lett. 31, 45, (1973).

22. D. J. Gross and F. A. Wilczek, Phys. Rev. Lett. 30, 1343 (1973); H. D. Politzer, Phys. Rev. Lett. 30, 1346 (1973).

23. See for example A. M. Polyakov, Nucl. Phys. B121, 429 (1977); C. G. Callan, R. Dashen and D. J. Gross, Phys. Rev. D 17, 2717 (1978).

24. H. Fritzsch, M. Gell-Mann and H. Leutwyler, Phys. Lett. 47B, 365 (1972); D. J. Gross and F. Wilczek, Phys. Rev. D 8, 3633 (1973); S. Weinberg, Phys. Rev. Lett. 31, 494 (1973).

25. J.J.J. Kokkedee, The Quark Model (Benjamin, Reading, 1969).

- 120 -

26. S. L. Adler, Lectures on Elementary Particles and Quantum Field Theory, 1970, ed. by S. Deser, M. Grisaru and H. Pendleton (MIT Press, Cambridge, 1971). K. G. Wilson, Phys. Rev. $\underline{179}$, 1499 (1969).

27. Particle Data Group, Phys. Lett. $\underline{75B}$, 1 (1978).

28. C. Bouchiat, J. Iliopoulos and Ph. Meyer, Phys. Lett. $\underline{38B}$, 519 (1972); D. J. Gross and R. Jackiw, Phys. Rev. D $\underline{6}$, 477 (1972).

29. G. 't Hooft, Nucl. Phys. $\underline{B35}$, 167 (1971).

30. R. Brandelik et al., Phys. Lett. $\underline{76B}$, 361 (1978).

31. G. Alexander et al., DESY preprint 78/30 (1978) and references therein.

32. M. L. Perl, Stanford Linear Accelerator Center preprint SLAC-PUB-2153 (1978) and references therein; J. Kirkby, Talk at this Summer Institute.

33. See for example P.G.O. Freund and S. Nandi, Phys. Rev. Lett. $\underline{32}$, 181 (1974).

34. S. Weinberg, Ref. 24 and Phys. Rev. D $\underline{8}$, 4482 (1973); D. V. Nanopoulos, Lett. al Nuovo Cim. $\underline{8}$, 873 (1973).

35. C. G. Callan, R. Dashen and D. J. Gross, Phys. Lett. $\underline{63B}$, 334 (1976); R. D. Peccei and H. R. Quinn, Phys. Rev. Lett. $\underline{38}$, 1440 (1977) and Phys. Rev. D $\underline{16}$, 1791 (1977).

36. C. G. Callan and D. J. Gross, Phys. Rev. Lett. $\underline{22}$, 156 (1969).

37. See for example Ref. 5, and K. G. Wilson, Ref. 26.

38. A. M. Polyakov, Soviet Phys. JETP $\underline{32}$, 296 (1971), $\underline{33}$, 850 (1971), Proceedings of the 1975 Int. Symp. on Lepton and Photon Interactions at High Energies, Stanford, ed. by W. T. Kirk (Stanford Linear Accelerator Center, Stanford, 1975), p. 855.

39. J. Kogut and L. Susskind, Phys. Rev. D $\underline{9}$, 697, 3391 (1974).

40. See Y. Watanabe et al. and H. L. Anderson et al., Ref. 15; also H. L. Anderson, H. S. Mathis and L. C. Myrianthopoulos, Phys. Rev. Lett. $\underline{40}$, 1061 (1978); and T. Quirk, private communication.

41. C. F. von Weizsäcker, Z. Phys. $\underline{88}$, 612 (1934); E. J. Williams, Phys. Rev. $\underline{45}$, 729 (1934).

42. G. Altarelli and G. Parisi, Nucl. Phys. $\underline{B126}$, 298 (1977).

43. D. J. Gross and F. A. Wilczek, Phys. Rev. D $\underline{8}$, 3633 (1973) and D $\underline{9}$, 980 (1974); H. Georgi and H. D. Politzer, Phys. Rev. D $\underline{9}$, 416 (1974).

44. An alternative means of regularizing $P_{q \leftarrow q}(z)$ is to subtract from it $\delta(z-1) \int_{\epsilon}^{1} dy\ P_{q \leftarrow q}(y)$. The subtracted function $P_{q \leftarrow q}(z)$ has finite moments in the limit $\epsilon \rightarrow 0$, which are identical to those obtained with the regularization (1.43).

45. These calculations are easily done in old-fashioned perturbation theory, keeping initial and final particles on mass-shell, and conserving 3-momentum but not energy.

46. D. Bailin and A. Love, Nucl. Phys. $\underline{B75}$, 159 (1974); M. Glück and E. Reya, Phys. Rev. D $\underline{16}$, 3242 (1977).

47. J. Ellis, "Applications of QCD," Stanford Linear Accelerator Center preprint SLAC-PUB-2121, to appear in Current Trends in the Theory of Fields, to be published by the APS. For previous analyses showing that deep inelastic data favour QCD over other field theories, see V. Baluni and E. Eichten, Phys. Rev. Lett. $\underline{37}$, 1181 (1976) and Phys. Rev. D $\underline{14}$, 3045 (1976); and M. Glück and E. Reya, Ref. 46.

48. S. L. Adler, Phys. Rev. $\underline{143}$, 1144 (1965).

49. D. J. Gross and C. H. Llewellyn Smith, Nucl. Phys. $\underline{B14}$, 337 (1969).

50. D. Robson, Nucl. Phys. $\underline{B130}$, 328 (1977) and references therein.

51. D. K. Choudhury and L.C.F. Vanryckeghem, Phys. Rev. D $\underline{17}$, 1766 (1978); H. Georgi and H. D. Politzer, Nucl. Phys. $\underline{B136}$, 445 (1978); J. F. Owens, Florida State University preprint 78-02-06 (1978).

52. G. Sterman and S. Weinberg, Phys. Rev. Lett. $\underline{39}$, 1436 (1977); see also J. Ellis, M. K. Gaillard and G. G. Ross, Ref. 8. For a recent commentary, see P. M. Stevenson, Imperial College, London preprint ICTP/77-78/25 (1978).

53. A. DeRújula, J. Ellis, E. G. Floratos and M. K. Gaillard, Nucl. Phys. $\underline{B138}$, 387 (1978).

54. E. Farhi, Phys. Rev. Lett. $\underline{39}$, 1587 (1977); see also H. Georgi and M. Machacek, Phys. Rev. Lett. $\underline{39}$, 1237 (1977). Earlier variables such as sphericity[13] are not suitable for computation in perturbative QCD because they are sensitive to the infrared cutoff.

55. A more detailed analysis of this technique has been made by J. Ellis and I. Karliner, Stanford Linear Accelerator Center preprint SLAC-PUB-2191 (1978).

56. K. Shizuya and S.-H. H. Tye, Fermilab preprint Pub-78/54-THY (1978); M. B. Einhorn and B. G. Weeks, Stanford Linear Accelerator Center preprint SLAC-PUB-2164 (1978).

57. See for example E. G. Floratos, Nuovo Cim. $\underline{43A}$, 241 (1978); K. H. Craig and C. H. Llewellyn Smith, Phys. Lett. $\underline{72B}$, 349 (1978); H. Georgi and H. D. Politzer, Phys. Rev. Lett. $\underline{40}$, 3 (1978);

G. Altarelli and M. Martinelli, Phys. Lett. $\underline{76B}$, 89 (1978);
A. Mendez, Oxford University preprint 29/78 (1978).

58.   See the talk by H. Meyer at this Summer Institute, and read between
      the lines.

59.   M. Krammer and H. Krasemann, Phys. Lett. $\underline{73B}$, 58 (1978).

60.   R. P. Feynman and M. Gell-Mann, Phys. Rev. $\underline{109}$, 193 (1958);
      E.G.C. Sudarshan and R. E. Marshak, Phys. Rev. $\underline{109}$, 1860 (1958).

61.   T. D. Lee and C. N. Yang, Phys. Rev. Lett. 4, 307 (1960); B. L.
      Ioffe, L. B. Okun and A. Rudik, Zh. Eksperim. Teor. Fiz. $\underline{47}$, 1905
      (1964) (Soviet Phys. JETP Lett. $\underline{20}$, 1281 (1965)).

62.   Lower limits on $m_{W^\pm}$ of the order of 20 to 30 GeV come from deep
      inelastic neutrinoproduction experiments. For general gauge theory
      bounds on $m_{W^\pm}$, m_{Z0} see J. D. Bjorken, Phys. Rev. D $\underline{15}$, 1330 (1977).

63.   C. H. Llewellyn Smith, Phys. Lett. $\underline{46B}$, 233 (1973); J. S. Bell,
      Nucl. Phys. $\underline{B60}$, 427 (1973); J. M. Cornwall, D. N. Levin and
      G. Tiktopoulos, Phys. Rev. Lett. $\underline{30}$, 1268 (1973) and Phys. Rev.
      D $\underline{10}$, 1145 (1974).

64.   C. N. Yang and R. Mills, Phys. Rev. $\underline{96}$, 191 (1954).

65.   P. Higgs, Phys. Lett. $\underline{12}$, 132 (1964); T. Kibble, Phys. Rev. Lett.
      $\underline{13}$, 585 (1964).

66.   See the lectures by S. Wojcicki at this Summer Institute.

67.   S. Herb et al., Phys. Rev. Lett. $\underline{39}$, 252 (1977); W. R. Innes et al.,
      Phys. Rev. Lett. $\underline{39}$, 1240 (1977); J. K. Yoh et al., Fermilab pre-
      print Pub-78/52-EXP (1978).

68.   C. H. Berger et al., Phys. Lett. $\underline{76B}$, 243 (1978); C. W. Darden
      et al., Phys. Lett. $\underline{76B}$, 246 (1978).

69.   J. Ellis, M. K. Gaillard, D. V. Nanopoulos and S. Rudaz, Nucl. Phys.
      $\underline{B131}$, 285 (1977).

70.   C. E. Carlson and R. Suaya, Phys. Rev. Lett. $\underline{39}$, 908 (1977);
      T. Hagiwara, Y. Kazama and E. Takasugi, Phys. Rev. Lett. $\underline{40}$, 76
      (1978); D. B. Lichtenberg, I. G. Wills and J. T. Kiehl, Phys. Rev.
      Lett. $\underline{39}$, 1592 (1977); S. S. Gershtein et al., Serpukhov preprint
      IFVE 77-11 (1977).

71.   M. S. Chanowitz, J. Ellis and M. K. Gaillard, Nucl. Phys. $\underline{B128}$,
      506 (1977).

72. A. J. Buras, J. Ellis, M. K. Gaillard and D. V. Nanopoulos, Nucl. Phys. B135, 66 (1978).

73. Some physicists have expressed unease about this nomenclature. Similar unease was once felt by the Board of Supervisors of San Francisco, who forbade the display of advertisements containing certain dubious words. This led to the bowdlerization of some signs, so that the North Beach area had a proliferation of "ottomless" bars. Perhaps we should refer to the b and t as the "ottom" and "op" quarks respectively. The San Francisco ordinance has now fallen into disuse.

74. M. Holder et al., Phys. Lett. 69B, 377 (1977). See also the lectures by M. Holder and D. Perkins at this Summer Institute.

75. R. M. Barnett, talk at this Summer Institute. See also L. F. Abbott and R. M. Barnett, Phys. Rev. Lett. 40, 1303 (1978).

76. M. Holder et al., Phys. Rev. Lett. 39, 433 (1977).

77. C. Prescott et al., Stanford Linear Accelerator Center preprint SLAC-PUB-2148 (1978).

78. L. M. Sehgal, Aachen preprint PITHA-102 (1978); see also L. F. Abbott and R. M. Barnett, Ref. 75.

79. For $\Delta S=1$ neutral currents and $\Delta S=2$ K^0-$\bar{K}^0$ mixing, see Ref. 27. For $\Delta C=2$ transitions, see G. J. Feldman, 1977 SLAC Summer Institute lectures.

80. S. L. Glashow, J. Iliopoulos and L. Maiani, Phys. Rev. D 2, 1285 (1970).

81. Y. Hara, Phys. Rev. 134, B701 (1964); Z. Maki and Y. Ohnuki, Progr. Theor. Phys. 32, 144 (1964); D. Amati, H. Bacry, J. Nuyts and J. Prentki, Phys. Lett. 11, 190 (1964) and Nuovo Cim. 34, 1732 (1964); B. J. Bjorken and S. L. Glashow, Phys. Lett. 11, 255 (1964).

82. See the talk by N. Fortson at this Summer Institute.

83. This point of view is not universal. In particular, J. D. Bjorken stresses that the observable effects of "anomalies" at present energies are negligible. The issue is rather one of principle.

84. S. L. Glashow and S. Weinberg, Phys. Rev. D 15, 1958 (1977); E. A. Paschos, Phys. Rev. D 15, 1966 (1977); M. S. Chanowitz et Ref. 71.

85. M. K. Gaillard and B. W. Lee, Phys. Rev. D 10, 897 (1974).

86. J. Rich and D. R. Winn, Phys. Rev. D 14, 1283 (1976). A promising related process: $e^+e^- \to \mu\bar{\mu}\bar{\nu}\bar{\nu}$ is discussed by E. Ma and J. Okada, Phys. Rev. Lett. 41, 287 (1978).

87. For reviews see D. N. Schramm, AIP Conf. Proceedings, APS Div. of Particles and Fields (1978), and Fermi Institute preprint 78-25 (1978).

88. S. Weinberg, Gravitation and Cosmology (J. Wiley and Sons, New York, 1972).

89. B. W. Lee and S. Weinberg, Phys. Rev. Lett. 39, 165 (1977); J. E. Gunn, B. W. Lee, I. Lerche, D. N. Schramm and G. Steigman, Astrophysical Journal, in press (1978).

90. B. W. Lee and S. Weinberg, Phys. Rev. Lett. 38, 1237 (1977).

91. M. Veltman, Nucl. Phys. B123, 89 (1977).

92. M. S. Chanowitz, M. Furman and I. Hinchliffe, Lawrence Berkeley Laboratory preprint LBL-7903 (1978).

93. L. Camilleri et al., CERN Yellow Report 76-18 (1976); particularly section 2.

94. M. L. Perl et al., Phys. Rev. Lett. 35, 1489 (1975).

95. Y. S. Tsai, Stanford Linear Accelerator Center preprint SLAC-PUB-2105 (1978).

96. J.A.M. Vermaseren, Purdue University preprint "Signals for Very Heavy Leptons in e^+e^- Annihilation" (1978).

97. Notice however that the eD parity violation data of Ref. 77 almost exclude an $\begin{pmatrix} E^0 \\ e^- \end{pmatrix}_R$ doublet: no direct evidence against $\begin{pmatrix} M^0 \\ \mu^- \end{pmatrix}_R$ or $\begin{pmatrix} T^0 \\ \tau^- \end{pmatrix}_R$ doublets is yet available. The direct channel production mechanism (2.30) could also be used to produce M^0 or T^0 pairs. Their decay modes would be similar to those of an E^0, with e^- replaced by μ^- or τ^-.

98. J. L. Rosner, Nucl. Phys. B126, 124 (1977).

99. F. Bletzacker and H. T. Nieh, Phys. Rev. D 16, 2115 (1977).

100. B. W. Lee, S. Pakvasa, R. E. Shrock and H. Sugawara, Phys. Rev. Lett. 38, 937 (1977), 38, 1230 (E) (1977).

101. CHEEP--An $e\bar{p}$ Facility in the SPS, ed. by J. Ellis, B. H. Wiik and K. Hübner, CERN Yellow Report 78-02 (1978).

102. M. Kobayashi and K. Maskawa, Progr. Theor. Phys. **49**, 652 (1973).

103. S. Weinberg, Phys. Rev. Lett. **37**, 657 (1976).

104. J. Ellis, M. K. Gaillard and D. V. Nanopoulos, Nucl. Phys. **B109**, 213 (1976). Though calculated using a free quark model, the formula (2.46) is probably not grossly altered by QCD corrections.

105. L. Ryder, Phys. Reports **34C**, 55 (1977).

106. A. Sirlin, Nucl. Phys. **B71**, 29 (1974) and **B100**, 291 (1974); W. Angerson, Nucl. Phys. **B69**, 493 (1974). The analysis in these lectures (see also Ref. 104) may underestimate the uncertainties due to nuclear physics effects, strong interaction effects in (2.42) and so on. However, comparable limits on S_2^L and S_3^L come from the negative results of searches for heavy quarks in neutrinoproduction--see the talk of M. Holder at this Summer Institute.

107. J. Ellis, M. K. Gaillard and D. V. Nanopoulos, Nucl. Phys. **B100**, 313 (1975).

108. R. N. Cahn, Phys. Rev. Lett. **40**, 80 (1978); R. N. Mohapatra and D. P. Sidhu, Phys. Rev. D **17**, 1876 (1978); and B. W. Lee and S. Weinberg, Ref. 90.

109. D. Cutts et al., Phys. Rev. Lett. **41**, 363 (1978); R. Vidal et al., Fermilab preprint "A Search for New Massive Particles" (1978); S. Wolfram, Oxford University preprint "Abundances of Stable Particles Produced in the Early Universe" (1978) argues that the standard "big bang" cosmology would generate more stable fermions of mass ≤ 16 GeV than are allowed by observation.

110. J. Jaros, private communication. I thank M. Perl for interesting discussions about this idea.

111. R. h Barnett, Phys. Rev. Lett. **36**, 1163 (1976).

112. M. Holder et al., Phys. Lett. **77B**, 114 (1978) and CERN preprint "Characteristics of Trimuon Events Observed in High Energy Neutrino Interactions" (1978); see also the talk by M. Holder at this Summer Insitute.

113. M. Holder et al., Phys. Lett. **73B**, 105 (1978); R. J. Loveless et al., University of Wisconsin preprint COO-088-29 (1978).

114. An approach to this problem which combines finite mass effects and the Altarelli-Parisi formalism[12] is being developed by R. C. Brower, A. J. Buras, D. Duke and J. Ellis.

115. The results of this were kindly provided by T. Schalk and A. Seiden.

116. M. K. Gaillard, talk presented at this Summer Institute.

117. A. Ali, CERN preprint TH 2411 (1977).

118. S. Pakvasa and H Sugawara, Phys. Rev. D 14, 305 (1976); L. Maiani, Phys. Lett. 62B, 183 (1976); C. Quigg and J. L. Rosner, Lawrence Berkeley Laboratory preprint LBL-7961 (1978).

119. For a recent discussion of the theoretical value of this quantity in the KM model see J. Ellis and M. K. Gaillard, Fermilab preprint 78/66-THY (1978). Previous calculations--Refs. 104, 118 and E. P. Shabalin, ITEP preprint ITEP-31 (1978) neglected perturbative strong interaction effects and got results which were too low. Ellis and Gaillard also estimate the nonperturbative strong interaction contribution to the neutron electric dipole moment coming from renormalization of the strong interaction θ vacuum parameter by weak interactions in the KM102 model. They find the nonperturbative contribution to be smaller than the perturbative contribution.

120. For a discussion of different models, see A. Ali and Z. Z. Aydin, DESY preprint 78/11 (1978).

121. B. L. Ioffe and V. A. Khoze, Leningrad preprint LINP-274 (1976).

122. J. D. Bjorken, 1976 SLAC Summer Institute Lectures, Stanford Linear Accelerator Center report SLAC-198 (1976) or preprint SLAC-PUB-1866 (1977).

123. F. Halzen and D. M. Scott, University of Wisconsin preprint COO-881-41 (1978).

124. C. H. Llewellyn Smith and B. H. Wiik, DESY preprint 77/38 (1977).

125. O. P. Sushkov, V. V. Flambaum and I. B. Khriplovich, Sov. J. Nucl. Phys. 20, 537 (1975); W. Alles, Ch. Boyer and A. J. Buras, Nucl. Phys. B119, 125 (1977).

126. F. Bletzacker and H. T. Nieh, Nucl. Phys. B124, 511 (1977).

127. D. A. Ross and M. Veltman, Phys. Rev. B95, 135 (1975).

128. J. D. Bjorken, Phys. Rev. D 15, 1330 (1977).

129. I. Hinchliffe and C. H. Llewellyn Smith, Nucl. Phys. B128, 93 (1977); J. Kogut and J. Shigemitsu, Nucl. Phys. B129, 461 (1977).

130. J. D. Bjorken, Proc. of the 1977 Int. Symp. on Lepton and Photon Interactions at High Energies, Hamburg, 1977, ed. by F. Gutbrod (DESY, Hamburg, 1977), p. 960.

131. J. K. Yoh et al., Ref. 67.

132. Yu. L. Dokshitser, D. I. D'yakonov and S. I. Troyan, "Inelastic Processes in Quantum Chromodynamics," Materials of the 13th Winter School of the Leningrad B. P. Konstantinov Institute of Nuclear Physics, Leningrad, 1978, p. 1: available in translation as SLAC TRANS-183 (1978); R. K. Ellis, H. Georgi, M. Machacek, H. D. Politzer and G. G. Ross, MIT preprint CTP-718 (1978); A. H. Mueller, Columbia University preprint CU-TP-125 (1978).

133. G. Altarelli, R. K. Ellis and G. Martinelli, MIT preprint CTP-723 (1978).

134. H. Georgi, Harvard University preprint HUTP 77/A090 (1977).

135. See C. H. Llewellyn Smith, Ref. 6, and references 123, 132 and 134.

136. J. Thaler emphasized this point to me.

137. This oft-used conjecture—see for example B. Combridge, J. Kripfganz and J. Ranft, Phys. Lett. 70B, 234 (1977); R. Cutler and D. Sivers, Phys. Rev. D 17, 196 (1978); R. D. Field, Phys. Rev. Lett. 40, 997 (1978)—has recently been justified in QCD. See C. T. Sachrajda, Phys. Lett. 76B, 100 (1978). W. Furmanski, Jagiellonian University, Kraków preprints 10, 11, 12/78 (1978).

138. R. W. Brown and K. O. Mikaelian, Fermilab preprint Pub-78/49-THY (1978).

139. Radiative corrections reduce this rate by a factor of O(2)—J. D. Bjorken (private communication). A complete programme of calculating weak radiative corrections to e^+e^- processes at these high energies is being undertaken by M. Veltman.

140. M. Veltman, Acta Physica Polonica B8, 475 (1977).

141. P. Darriulat and M. K. Gaillard, LEP physics note "Comments on the Feasibility of Studying the $Z^0W^+W^-$ Vertex in High Energy e^+e^- Collisions" (1978).

142. R. D. Peccei and H. R. Quinn, Ref. 35.

143. S. Weinberg, Phys. Rev. Lett. 40, 223 (1978); F. Wilczek, Phys. Rev. Lett. 40, 279 (1978).

144. J. Ellis and M. K. Gaillard, Phys. Lett. 74B, 374 (1978).

145. E. Bellotti, E. Fiorini and L. Zanotti, Phys. Lett. 76B, 223 (1978).

146. T. W. Donnelly, S. J. Freedman, R. S. Lytel, R. D. Peccei and M. Schwartz, Stanford University preprint ITP-598 (1978).

147. G. 't Hooft, Nucl. Phys. $\underline{B79}$, 276 (1974); A. M. Polyakov, Zh. Eksp. Teor. Fiz. Pis'ma $\underline{20}$, 430 (1974) (JETP Lett. $\underline{20}$, 194 (1974)).

148. T. Richet, private communication from M. J. Perry (1978).

149. H. Georgi and S. L. Glashow, Phys. Rev. Lett. $\underline{28}$, 1494 (1972).

150. Y. Nambu, Nucl. Phys. $\underline{B130}$, 505 (1977).

151. M. B. Einhorn and R. S. Savit, University of Michigan preprint UM HE 78-18 (1978).

152. H. Georgi and S. L. Glashow, Ref. 11.

153. For an alternative approach to grand unified gauge theories, see J. C. Pati and A. Salam, Phys. Rev. D $\underline{8}$, 1240 (1973) and Phys. Rev. D $\underline{10}$, 275 (1974).

154. S. Coleman and E. Weinberg, Phys. Rev. D $\underline{7}$, 1888 (1973).

155. S. Weinberg, Phys. Rev. Lett. $\underline{36}$, 294 (1976); A. D. Linde, Zh. Eksp. Teor. Fiz. Pis'ma Red $\underline{23}$, 73 (1976) (JETP Lett. $\underline{23}$, 64 (1976)).

156. P. H. Frampton, Phys. Rev. Lett. $\underline{37}$, 1378 (1976).

157. A. D. Linde, Phys. Lett. $\underline{70B}$, 306 (1977).

158. E. Gildener and S. Weinberg, Phys. Rev. D $\underline{13}$, 3333 (1976) and references therein.

159. C. E. Vayonakis, Lett. al Nuovo Cim. $\underline{17}$, 383 (1976) and Athens University preprint "New Threshold of Weak Interactions" (1978).

160. B. W. Lee, C. Quigg and H. B. Thacker, Phys. Rev. Lett. $\underline{38}$, 883 (1977); and Phys. Rev. D $\underline{16}$, 1519 (1977). See also D. A. Dicus and V. S. Mathur, Phys. Rev. D $\underline{7}$, 3111 (1973).

161. F. Wilczek, Phys. Rev. Lett. $\underline{39}$, 1304 (1977).

162. P. H. Frampton and W. W. Wada, Ohio State University preprint COO-1595-235 (1978).

163. This process was discussed in Ref. 10 and a cross section given for $e^+ e^- \to Z^0 H$ for light Higgs close to threshold; see also Refs. 121, 122. The exact formula (4.31) is given by B. W. Lee, C. Quigg and H. B. Thacker, Ref. 160. See also Ref. 164. A related process is discussed by K.J.F. Gaemers and G. J. Gounaris, CERN preprint TH 2502 (1978).

164. S. L. Glashow, D. V. Nanopoulos and A. Yildiz, Harvard University preprint HUTP-78/A012 (1978).

165. H. M. Georgi, S. L. Glashow, M. E. Machacek and D. V. Nanopoulos. Phys. Rev. Lett. **40**, 692 (1978).

166. W. W. Wada, private communication (1978).

167. C. Rubbia, CERN $\bar{p}p$ physics note and private communication (1977).

168. J. Lo Secco, Phys. Rev. D **14**, 1352 (1976).

169. J. E. Kim and G Segré, Phys. Lett. B to be published; Y. Tomozawa, University of Michigan preprint UM 77-22 (1977); J. Grifols, Stanford Linear Accelerator Center preprint SLAC-PUB-2108 (1978); L. N. Chang and J. E. Kim, University of Pennsylvania preprint UPR-0097-T (1978); J. F. Donoghue and L.-F. Li, Carnegie-Mellon preprint COO-3066-113 (1978).

170. E. Golowich and T. C. Yang, University of Massachusetts preprint "Charged Higgs Bosons and Decays of Heavy Flavoured Mesons" (1978).

171. This process was suggested to me by R. N. Cahn during the Summer Institute.

172. See Ref. 35, J. Ellis and M. K. Gaillard, Ref. 119, and Ref. 144.

173. V. Baluni, MIT preprint CTP-726 (1978).

174. A. Zepeda, Phys. Rev. Lett. 41, 139 (1978); P. Langacker and H. Pagels, Princeton preprint "Light Quark Mass Spectrum in Quantum Chromodynamics" (1978).

175. H. Faissner et al., Phys. Lett. **60B**, 401 (1976). See also A. F. Rothenberg, Stanford Linear Accelerator Center report SLAC-147 (1972) and Ref. 146.

176. P. Alibran et al., Phys. Lett. **74B**, 134 (1976); T. Hansl et al., Phys. Lett. **74B**, 139 (1978); P. C. Bosetti et al., Phys. Lett. **74B**, 143 (1978).

177. D. A. Dicus, E. W. Kolb, V. L. Teplitz and R. V. Wagoner, University of Texas preprint ORO-3992-337 (1978).

178. For $K^+ \to \pi^+ + a$ see also T. Goldman and C. M. Hoffman, Phys. Rev. Lett. **40**, 220 (1978).

179. See for example T. C. Yang, Phys. Rev. Lett. 41, 523 (1978); H. R. Quinn, private communication (1978); P. Ramond and G. G. Ross, Caltech preprint CALT-68-674 (1978).

180. J. Ellis and M. K. Gaillard, Ref. 119. This analysis supersedes that of Ref. 144. For related remarks see S. Weinberg, unpublished note (1978).

181. H. Georgi, Harvard University preprint 78/A010 (1978); M.A.B. Bég and H.-S. Tsao, Phys. Rev. Lett. $\underline{41}$, 278 (1978).

182. H. Georgi, H. R. Quinn and S. Weinberg, Ref. 11; see also Ref. 71.

183. D. A. Ross, CERN preprint TH 2469 (1978).

184. D.V. Nanopoulos and D. A. Ross, CERN preprint in preparation. For a recent review see D. V. Nanopoulos, CERN preprint TH 2534 (1978).

185. M. J. Perry, Talk at the Ben Lee Memorial Conference (1977).

186. G. 't Hooft, Phys. Rev. Lett. $\underline{37}$, 8 (1976).

187. F. Reines and M. F. Crouch, Phys. Rev. Lett. $\underline{32}$, 493 (1974).
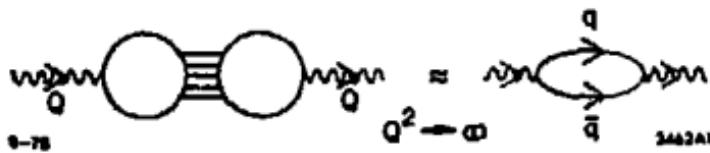
Fig. 1. The quark parton loop diagram for
$e^+e^- \rightarrow$ hadrons at large Q^2s.

8-75   3462A3
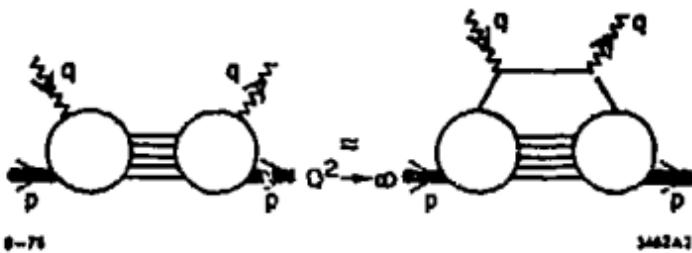
Fig. 2. The quark parton diagram for leptoproduction
         at large $Q^2 = -q^2$.
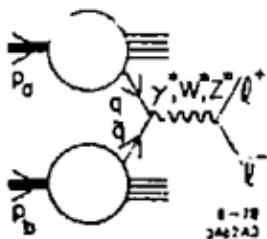
Fig. 3. The quark-antiquark annihilation diagram for hadron + hadron → $\ell^+\ell^- + X$.
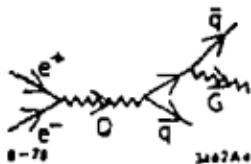
Fig. 4. Gluon bremsstrahlung in e^+e^- annihilation.

T,V;↑

8-78
3462A3
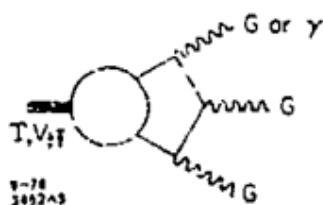
Fig. 5.   The 3 gluon and 2 gluon
+ 1 photon decays of a
heavy quark-antiquark
vector meson.

J_μ^5

g_A^f

e_f

e_f

J_ν

J_ρ

8-78
3462A4
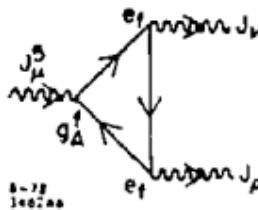
Fig. 6.   The fermion triangle
diagram which gives
anomalies.

τ, λ   ν_τ, ν_λ   τ, λ   ν_τ, ν_λ

Q $Q \to \infty$ $u, c, t \ldots$

$\bar{d}, \bar{s}, \bar{b} \ldots$

9-78
3448A7
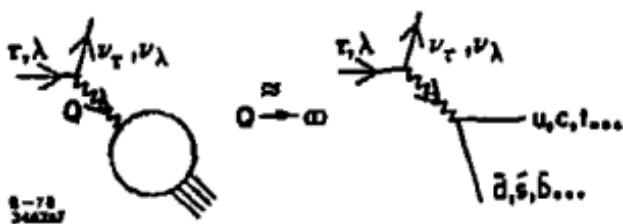
Fig. 7. A parton approximation for semihadronic decays of heavy leptons.

:
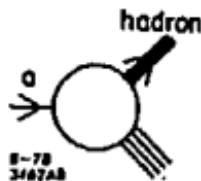
Fig. 8. A quark-parton
         fragmenting into
         hadrons.
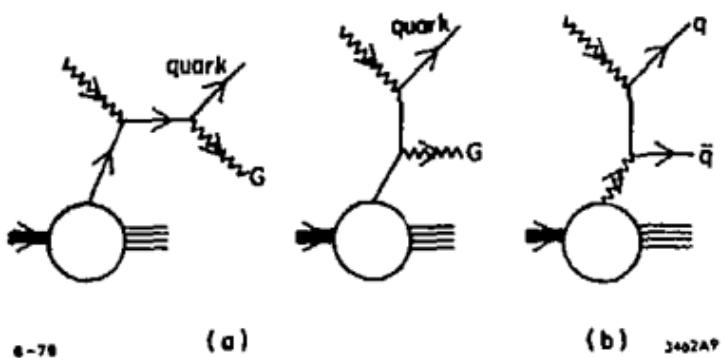
Fig. 9. Strong radiative corrections to leptoproduction cross sections from (a) bremsstrahlung and (b) pair creation.
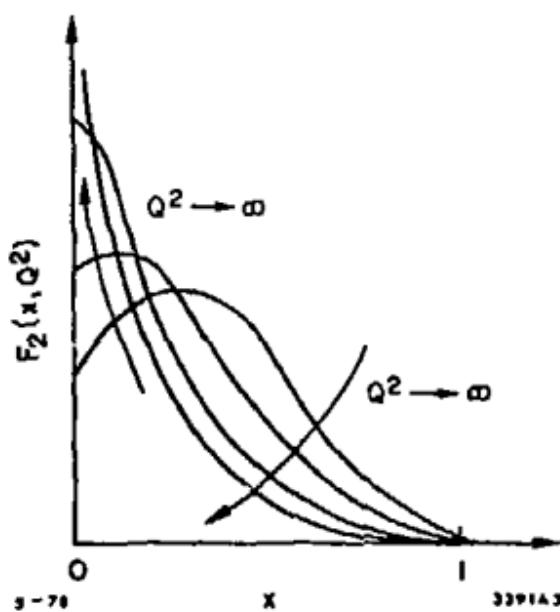
Fig. 10(a). Deviations from scaling in leptoproduction—intuitive expectation.[28,39]
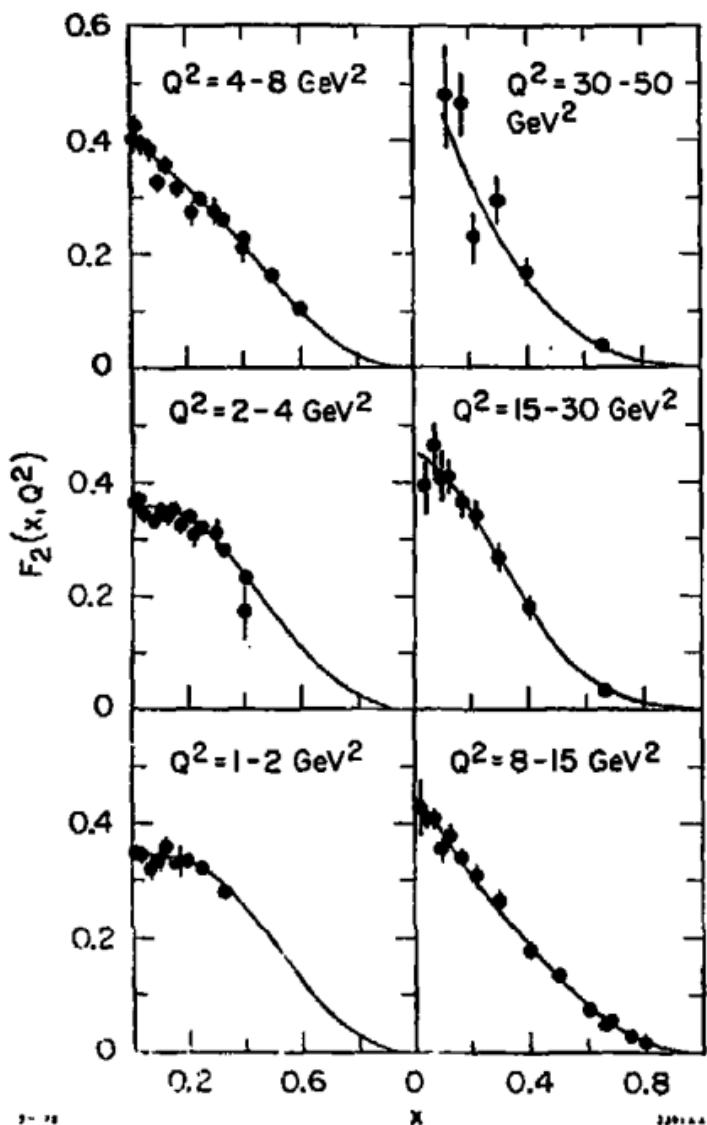
Fig. 10(b). Deviations from scaling in leptoproduction--
experimental data.[40]
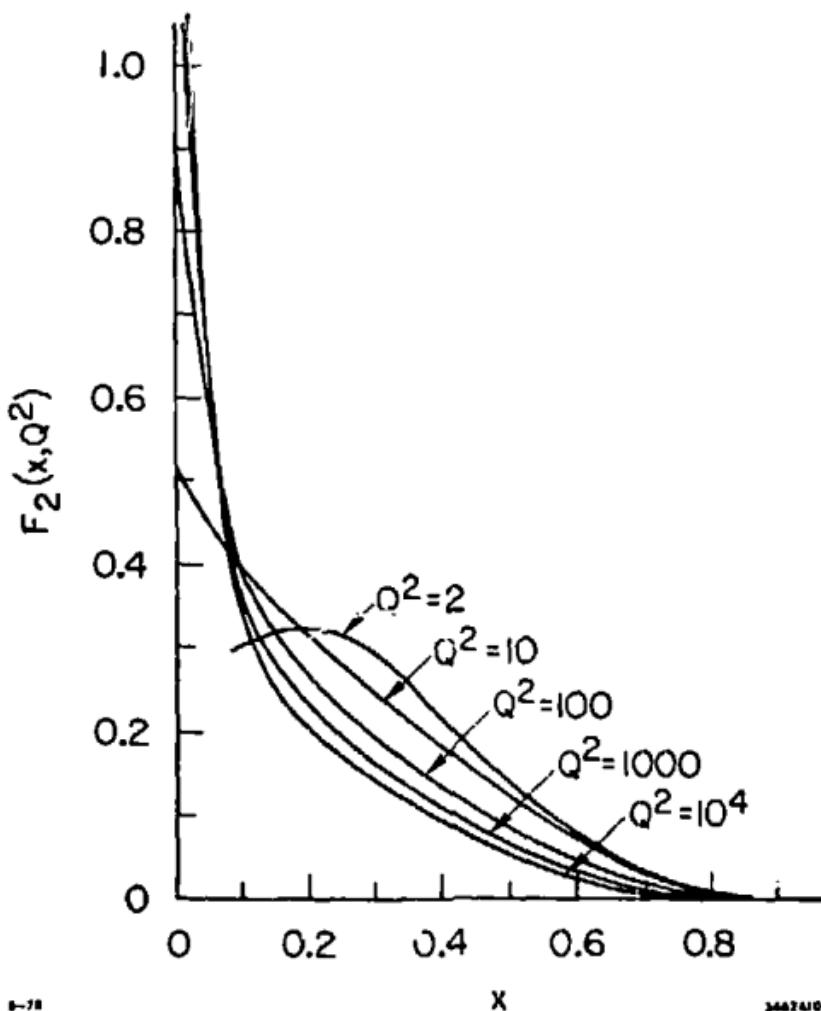
Fig. 10(c). Deviations from scaling in leptoproduction--
a typical QCD calculation.
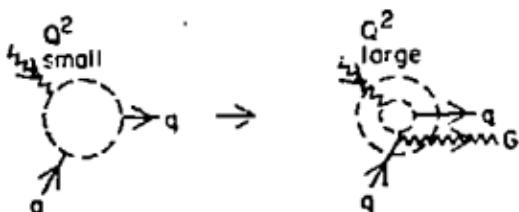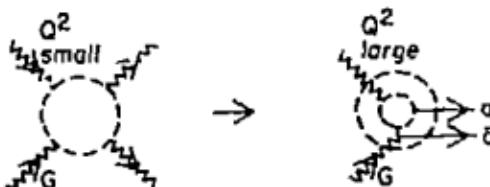
Fig. 11. As Q^2 increases (a) a quark may
be resolved into a quark + gluon,
(b) a gluon may be resolved into
a quark-antiquark pair as the
spatial discrimination of the
probe increases.
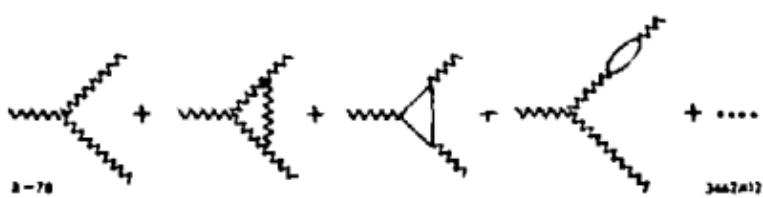
Fig. 12. Some contributions to the 3 gluon vertex g.
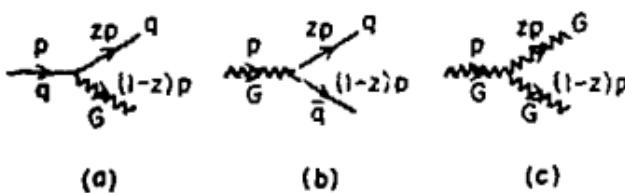
Fig. 13. The basic vertices responsible for the
leading order of scaling violations in
the evolution equations: (a) q → q+G
(b) G → q+q̄ and (c) G → G+G.
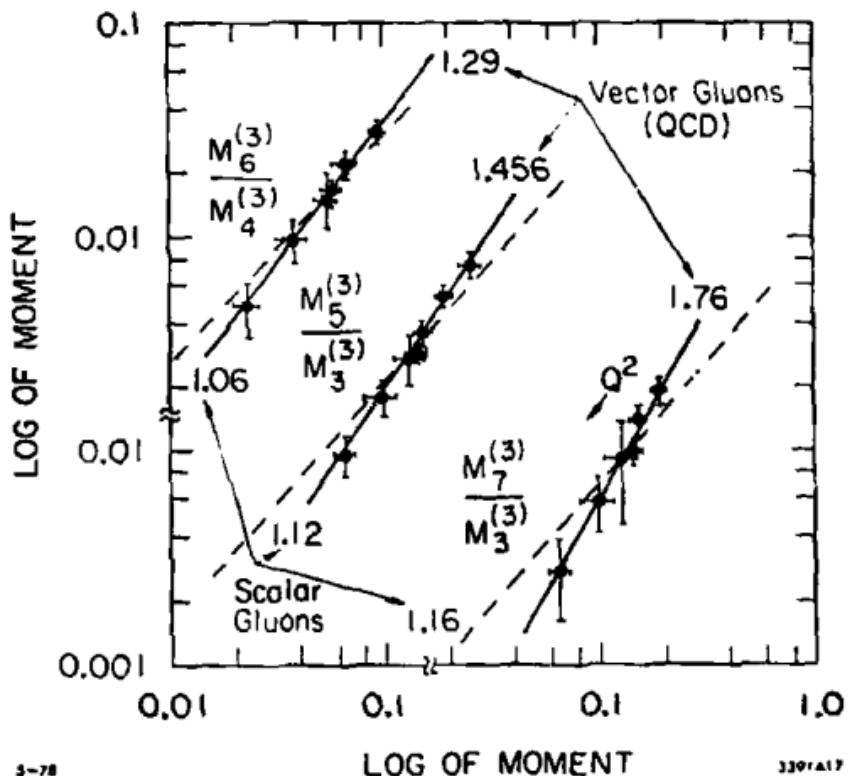
Fig. 14. BEBC[16] data on several moments $M_i^{(3)}(Q^2)$ of the F_1 structure function plotted logarithmically (cf. Eq. (1.51)). Different theories that the data should fall on straight lines with the slopes indicated.
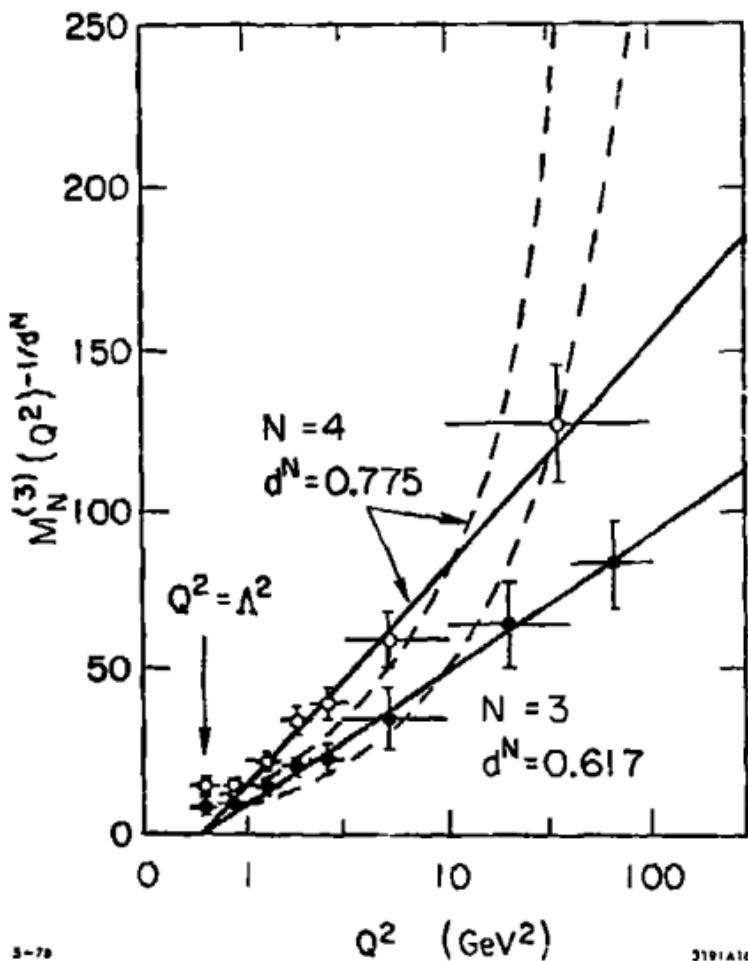
Fig. 15. Suitably chosen powers of $M_n^{(3)}(Q^2)$ [18] which QCD says should vary linearly with $\ln Q^2$ (see text). The curves are attempts to fit the scaling violations with powers of Q^2.
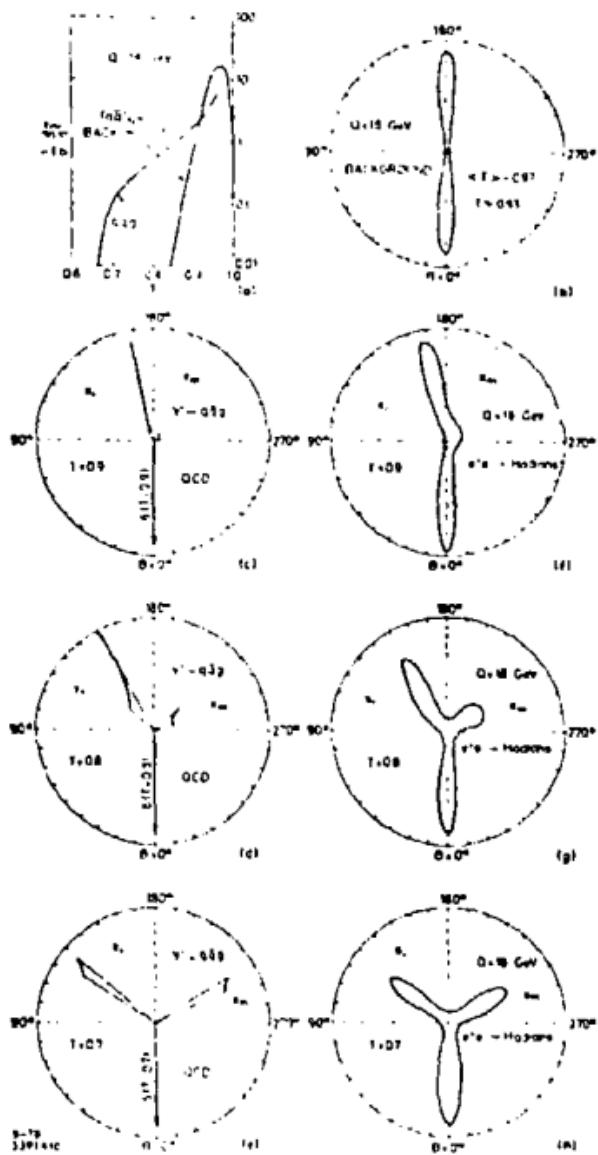
Fig. 16. The distribution of hadronic energy in e^+e^- annihilation expected[53] for different values of the thrust (1.70). (a), (c), (d) and (e) are the results of the perturbative cross section (1.60). (b), (f), (g) and (h) are the results of smearing quark and gluon jets with finite $\langle p_T \rangle$ for the hadrons.
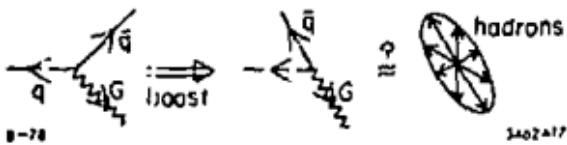
Fig. 17. The effect of the jet boost[53,55] (1.72) which should put the two right-hand jets into their joint centre-of-mass.
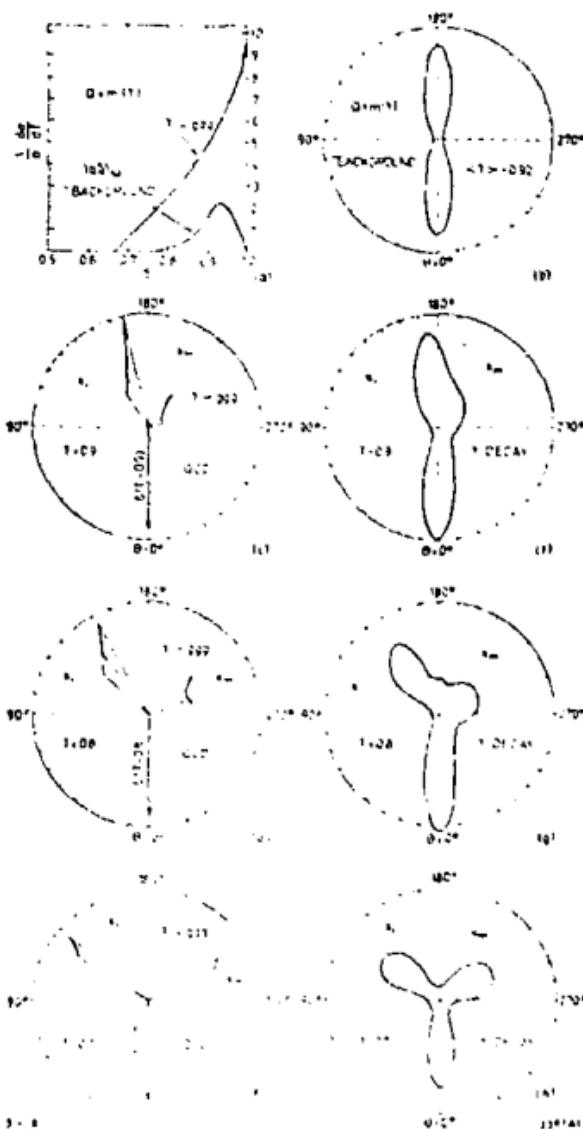
Fig. 18. The distribution of hadronic energy in Υ decay expected for different values of the thrust (1.70). cf. Fig. 16.

σ   σ

~ $\frac{G_F^2 s}{?}$

S   S

1—73   (a)   (b)   3442A10
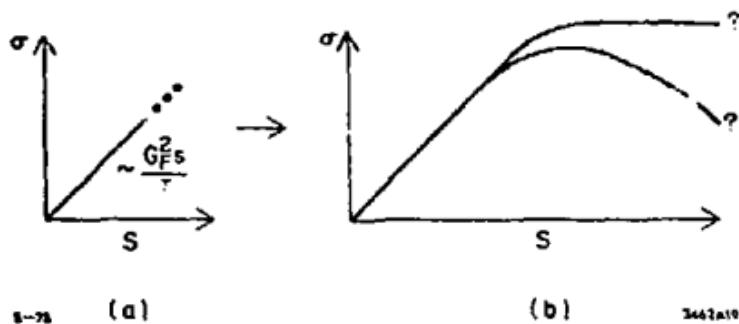
Fig. 19. Weak interaction cross sections (a) rise linearly
with s at low energies, but (b) should either
flatten out or fall at $\sqrt{s} \gtrsim$ several hundred GeV.
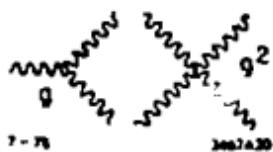
Fig. 20. The 3 and 4 vector boson vertices.
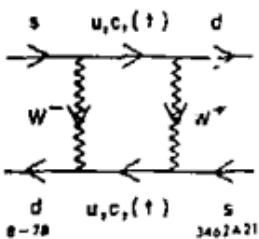
Fig. 21. A box diagram used for calculating the ΔS=2 transition $K^0 \rightarrow \bar{K}^0$.
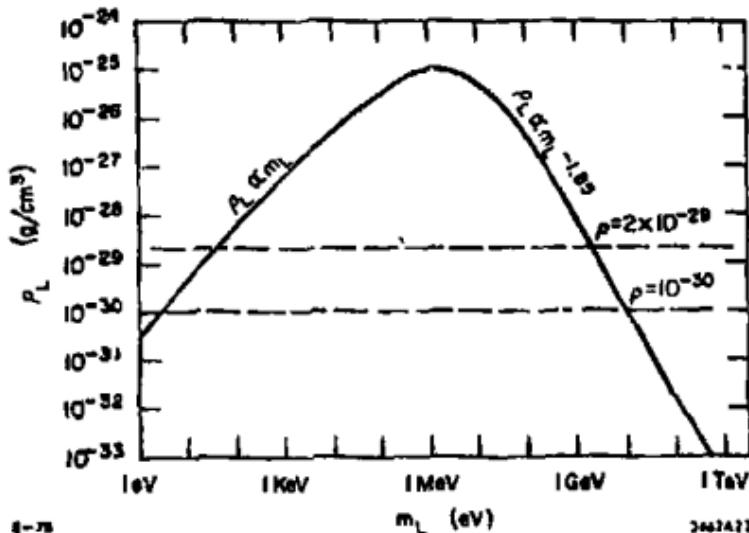
Fig. 22. The mass density of stable neutral leptons expected[87] on the basis of the standard big-bang cosmology[88] compared with the density (2×10^{-29} g/cm³) required to close the Universe and the density ($\sim 10^{-30}$ g/cm³) "observed" in the Universe.
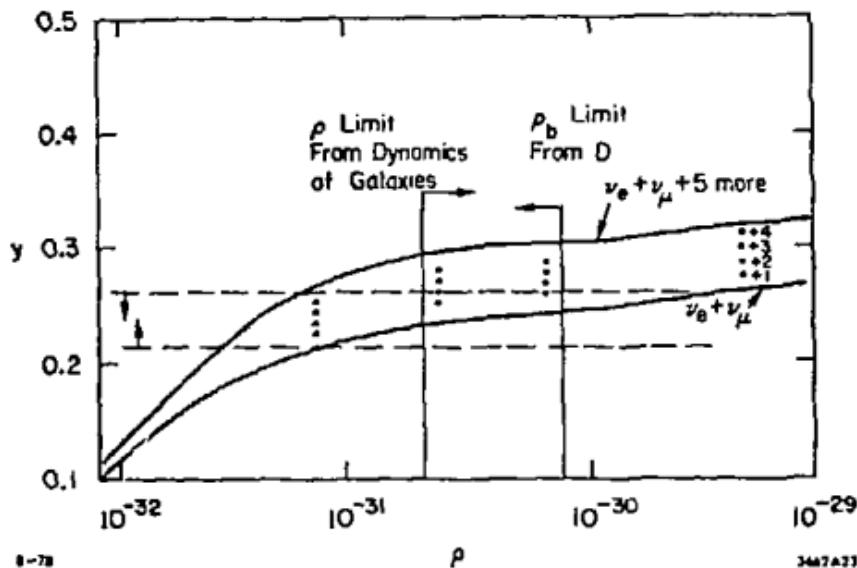
Fig. 23. The Helium abundance Y plotted[87] versus the density of
baryons with the limits imposed by galactic dynamics and
the Deuterium abundance D. The dashed lines are astro-
physical constraints on Y. The curves are the values of
Y obtained with different numbers of neutrinos.
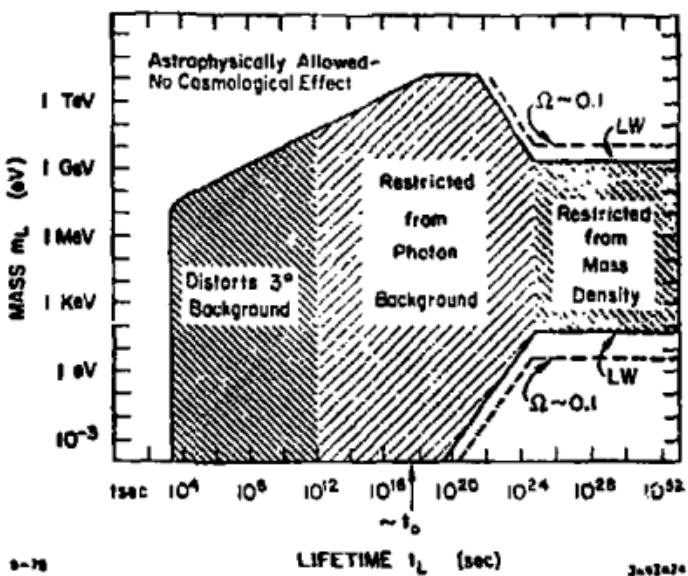
Fig. 24. Cosmologically acceptable and disallowed (the shaded region) ranges of neutral lepton masses and lifetimes.[87]
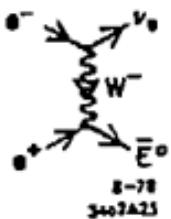
Fig. 25. The process $e^+e^- \to \nu_e \bar{E}^0$
mediated by W^+ exchange.
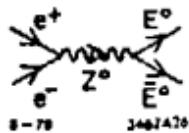
Fig. 26. The process $e^+e^- \to E^0\bar{E}^0$
(or $K^0\bar{K}^0$, $T^0\bar{T}^0$) mediated
by Z^0 exchange.
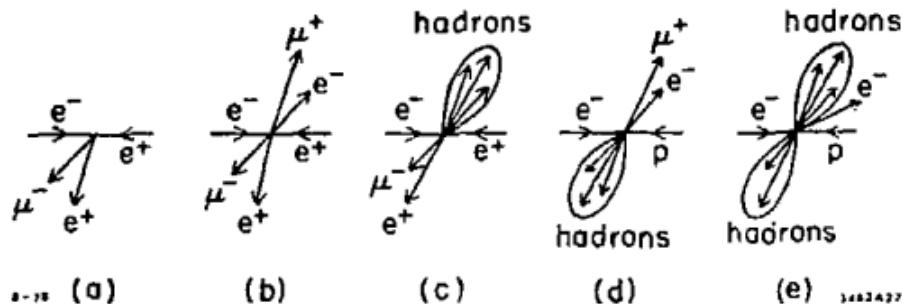
Fig. 27. Possible neutral heavy lepton signatures (a) $e^+e^- \to \mu^-e^+ +$ nothing from $e^+e^- \to \nu_e \bar{E}^0$, (b) $e^+e^- \to \mu^+e^-\mu^-e^+$ from $e^+e^- \to E^0\bar{E}^0$, (c) $e^+e^- \to \mu^-e^+ +$ hadron jet from $e^+e^- \to E^0\bar{E}^0$, (d) $\bar{e}p \to \mu^+e^- +$ hadron jets from $e^-p \to E^0+X$, and (e) $e^-p \to (e^-+jet) +$ hadron jets from $e^-p \to E^0+X$.

Q(e.g: b)   q(e.g: c)

6-78
3483A28

q(e.g: d)

q̄(e.g: ū)
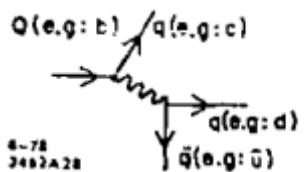
Fig. 28. The class of diagram
          expected to dominate
          heavy quark decay.
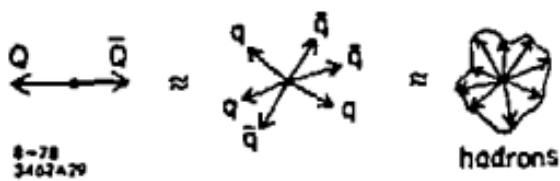
Fig. 29. Heavy quark-antiquark production just above threshold.
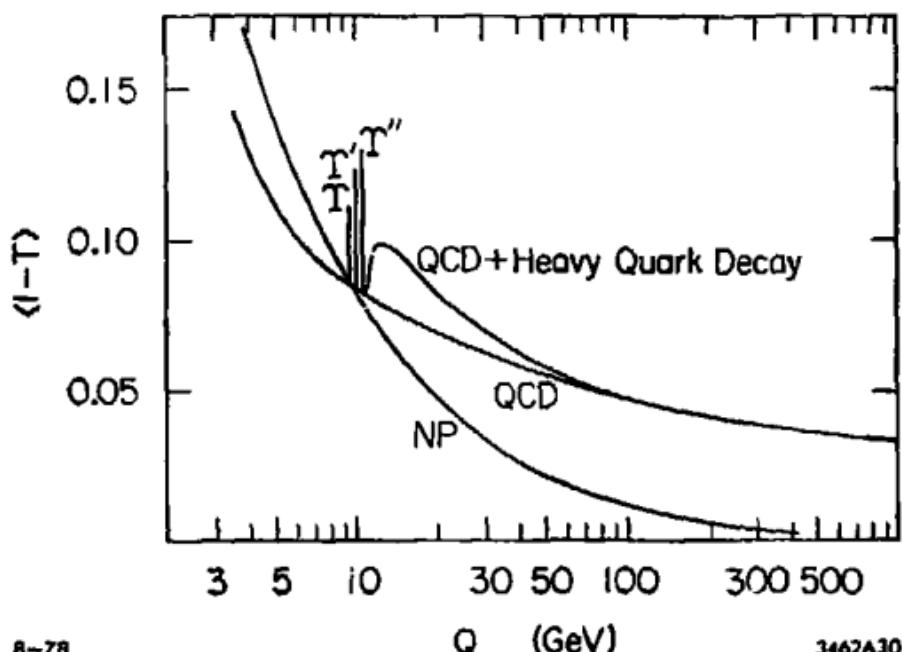
Fig. 30. The quantity <1-T> plotted[53] as a function of centre-of-mass
energy as one crosses the $b\bar{b}$ threshold including naive parton
nonperturbative contributions, QCD radiative corrections, the
narrow resonances Υ, Υ' and Υ'', and the effect of the naked
bottom[73] threshold.
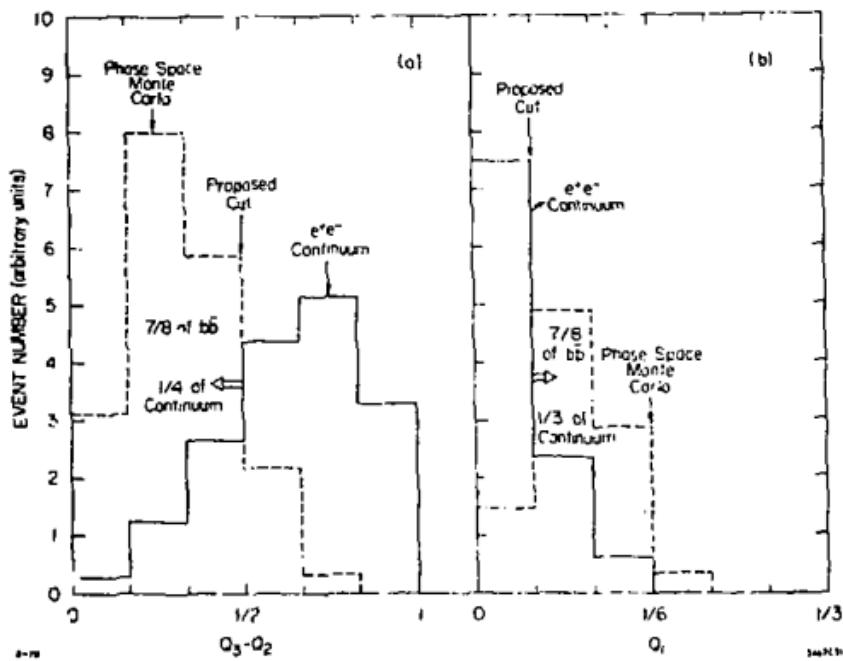
Fig. 31. Distributions (a) in jeticity (see text), and (b) in acoplanarity, comparing PLUTO[58] e^+e^- continuum data with a phase space Monte Carlo[115] expected to mimic heavy $q\bar{q}$ events just above threshold.
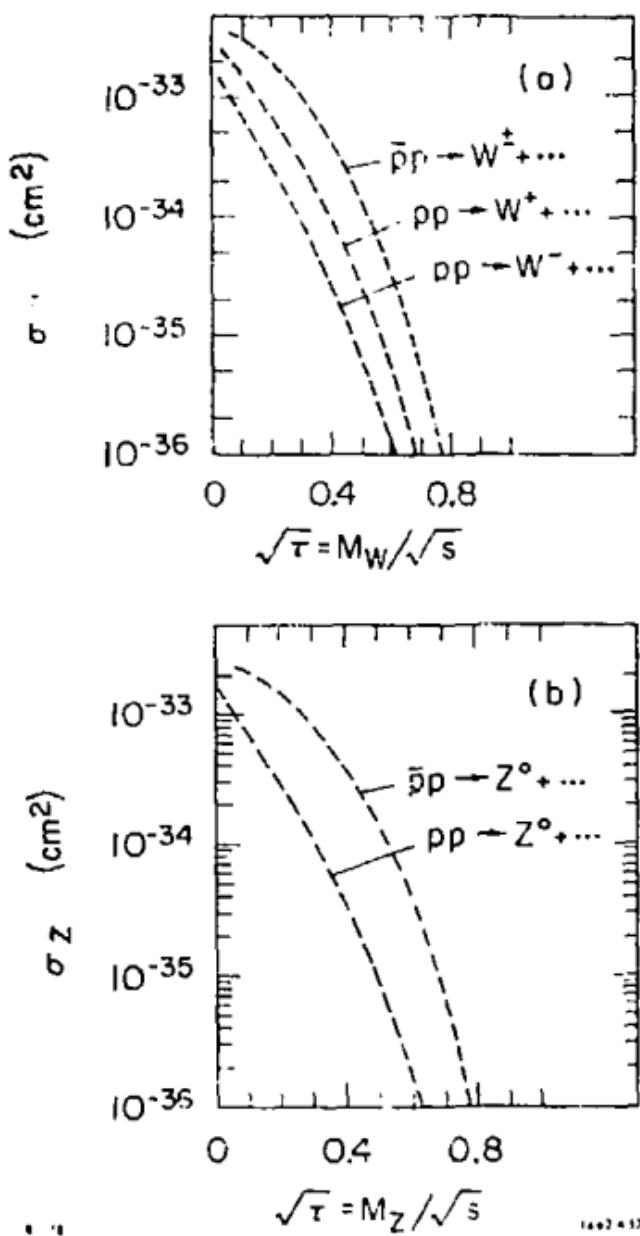
Fig. 32. Cross sections for (a) $W^\pm$ and (b) Z^0 production in pp and $\bar{p}$p collisions as functions of m^2/s, taken from Quigg.[]
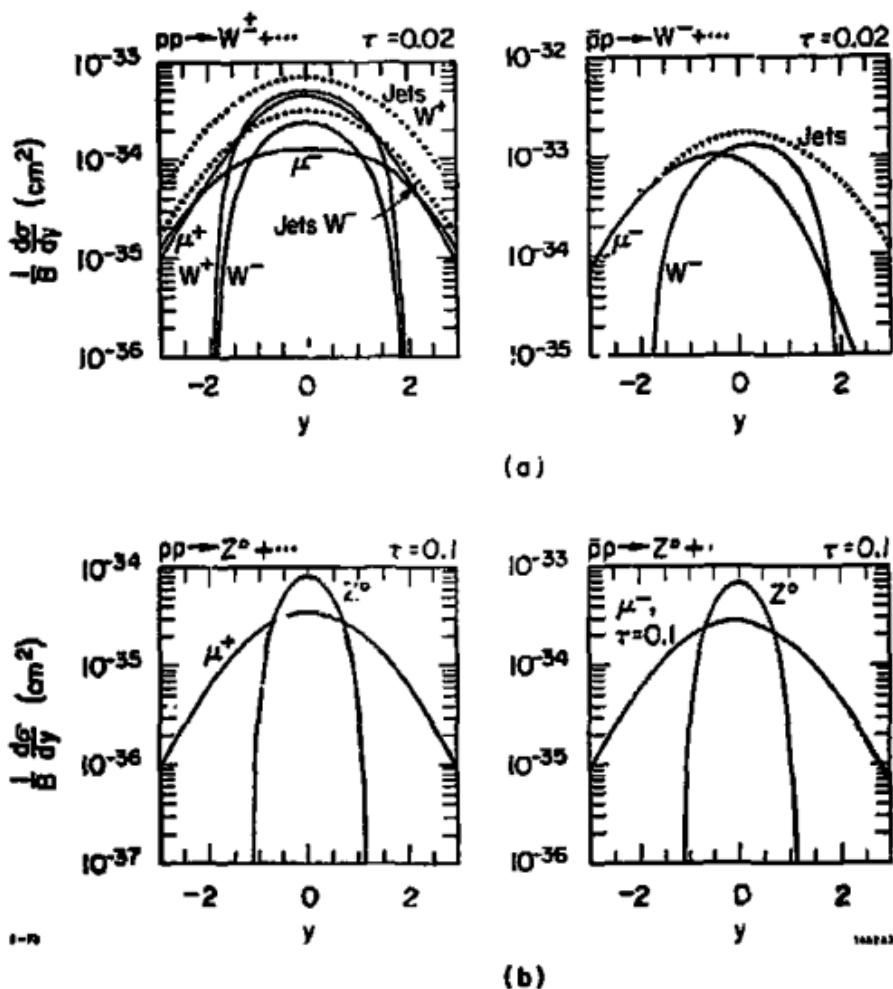
Fig. 33. Differential cross sections in rapidity for decay products of (a) $W^{\pm}$ and (b) Z^0 with $\sin^2 \theta_W = 0.3$, taken from Quigg.[9]
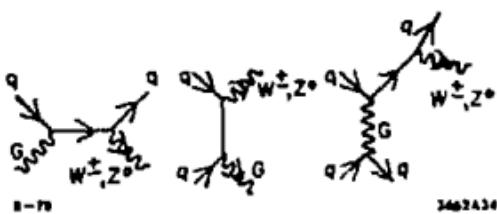
Fig. 34. Subdominant QCD subprocesses
for vector boson production.
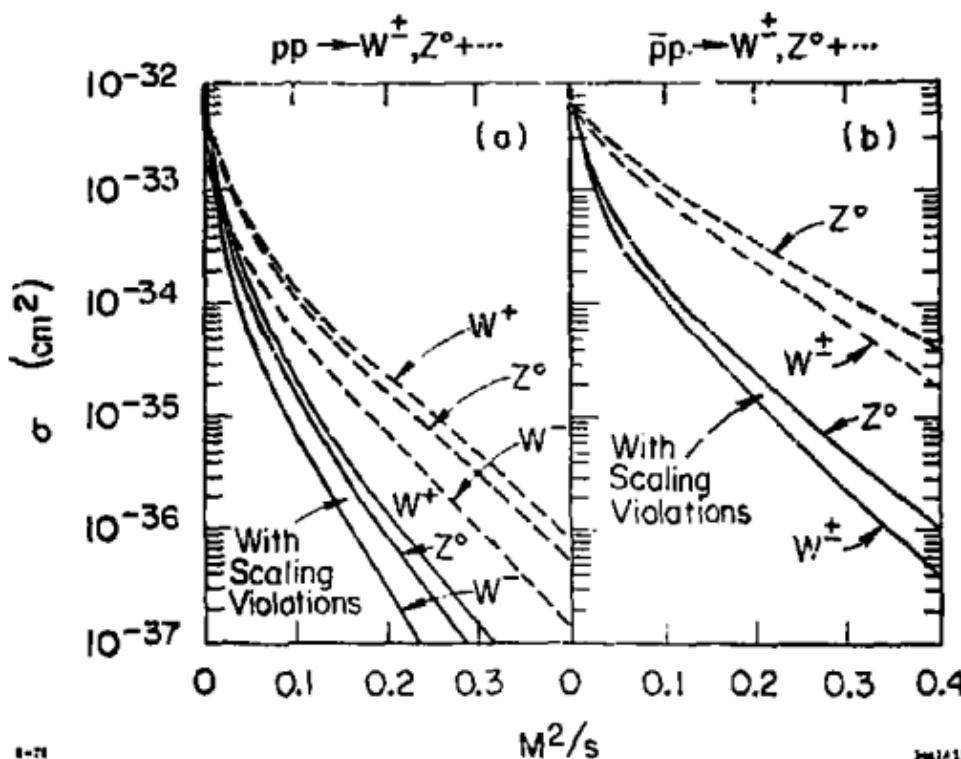
Fig. 35. Estimates[129] of the effects of QCD scaling violations in the quark distributions (3.34) on the vector boson production cross sections in (a) pp, (b) p̄p collisions.
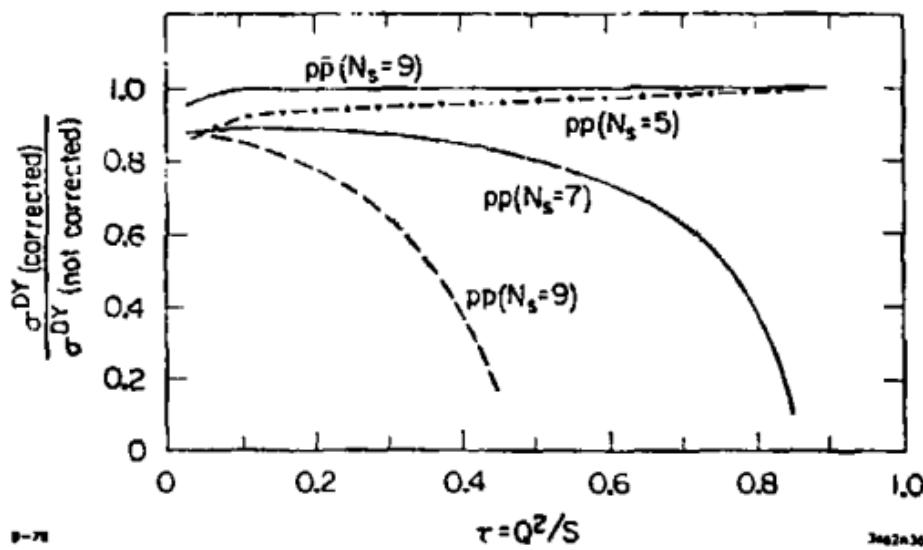
Fig. 36. Estimates[133] of the QCD modifications to the $q\bar{q}$ annihilation cross section contribution (3.32) for $q\bar{q}$ sea distributions $1/x \ (1-x)^{N_S}$.
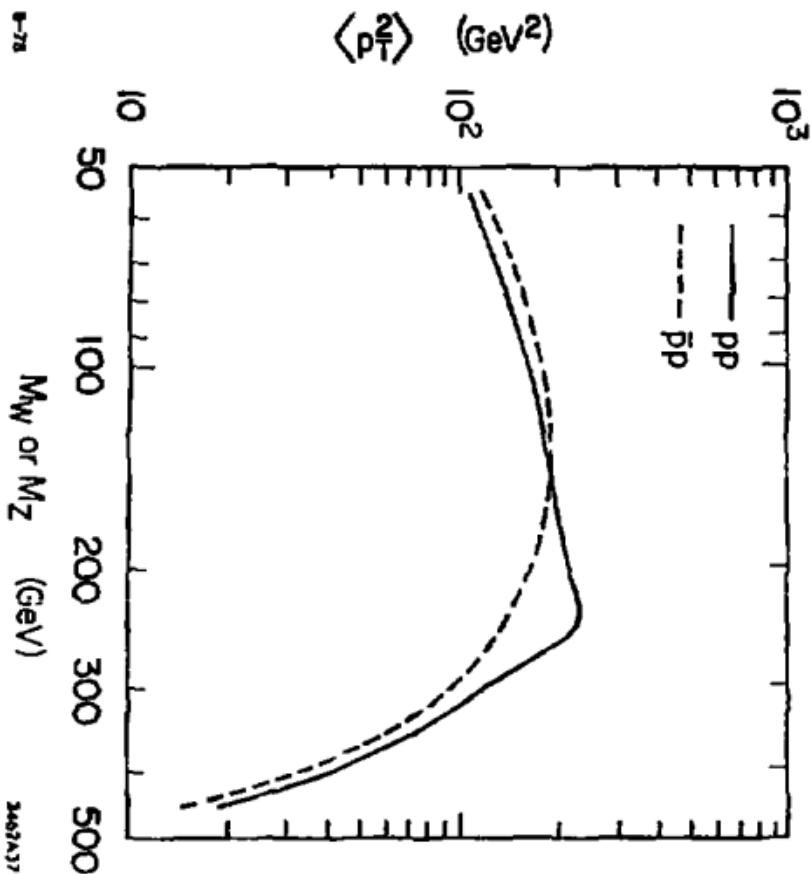
Fig. 37. A calculation[123] of $\langle p_T^2 \rangle$ for different values of the boson mass in pp and $\bar{p}p$ collisions at $\sqrt{s} = 540$ GeV.
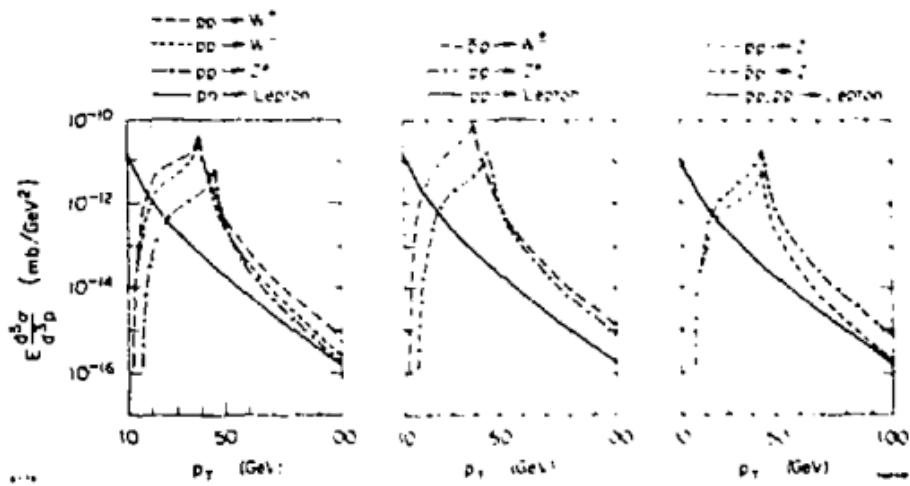
Fig. 38. A calculation[123] of the Jacobian peak with QCD calculations of the p_T smearing and likely lepton backgrounds, using $\sin^2 \theta_W = 0.21$ and $\sqrt{s} = 540$ GeV.
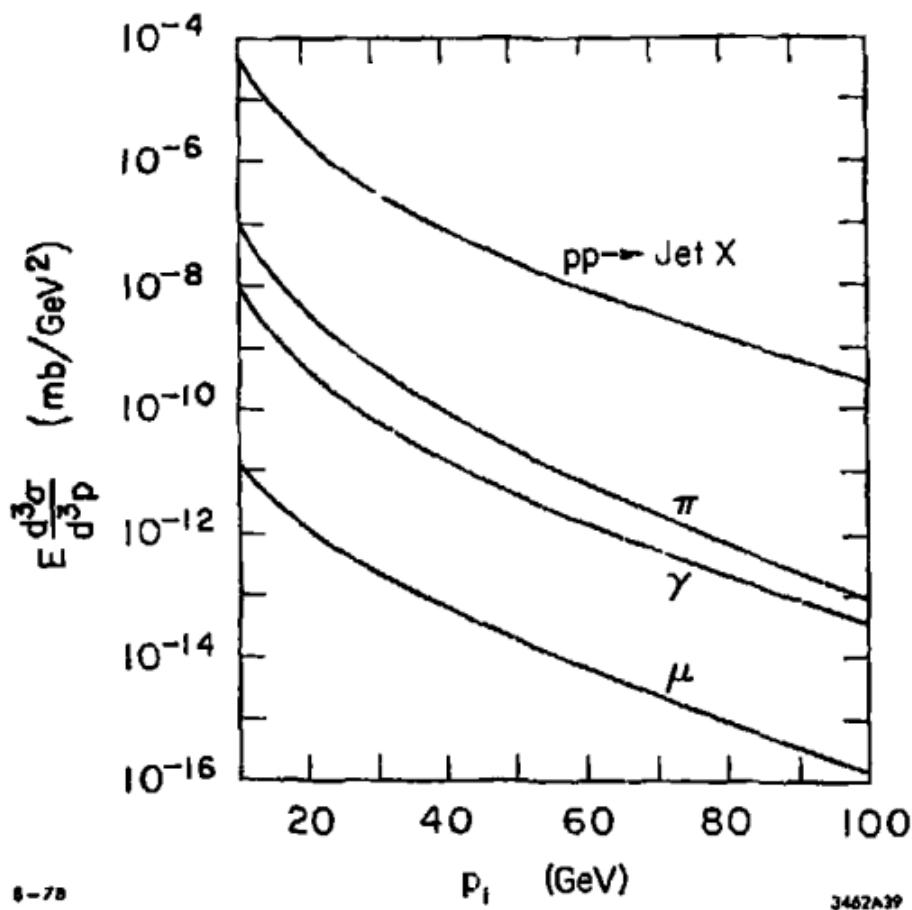
Fig. 39. QCD calculations[123] of jet, π, γ and muon cross sections in pp collisions at √s = 540 GeV.
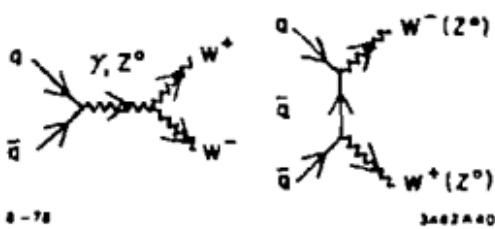
FIG. 40. Diagrams used in calculating
$pp \rightarrow W^+W^-X$ and $Z^0 Z^0 X$.

Fig. 41. Cross sections[138] for $pp \to W^+W^-X$ and Z^0Z^0+X at $\sqrt{s} = 800$ GeV.

The figure shows curves labeled:

$pp \to W^+W^- X$
$pp \to Z^0 Z^0 X$
$\sqrt{s} = 800$ GeV

$M_W = 75$ GeV/c^2
$M_W = 50$ GeV/c^2
$M_Z = 87$ GeV/c^2
$M_Z = 77$ GeV/c^2

Vertical axis: $\frac{d\sigma}{d\tau}$ (10^{-36} cm^2)

Horizontal axis: τ

3462441

8-78
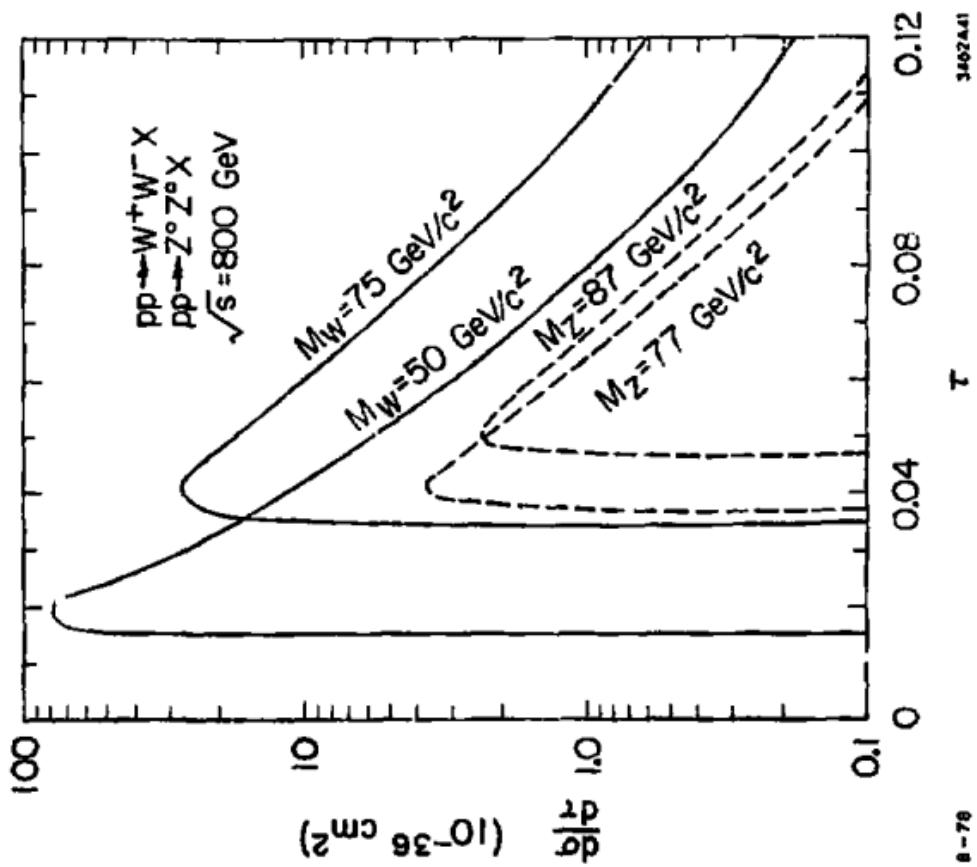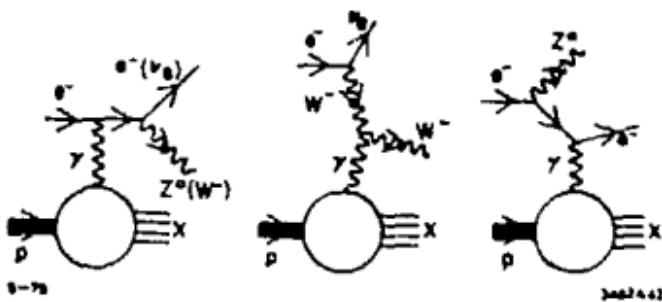
Fig. 42. Diagrams for $e^-p \to \nu W^- + X$ and $e^-p \to e^- Z^0 + X$ involving the lepton vertex.
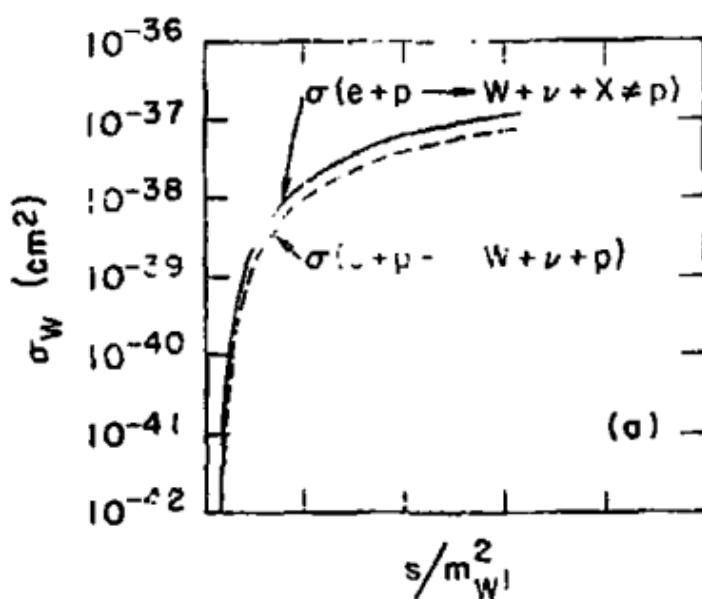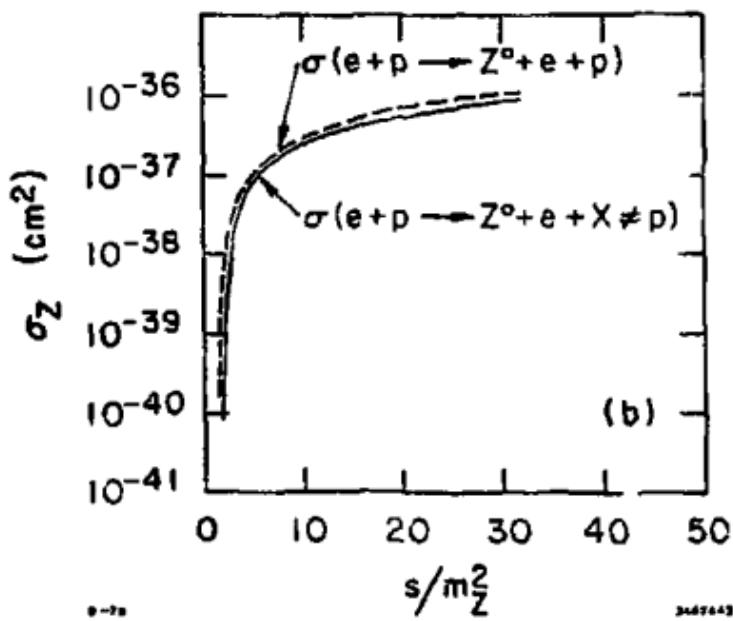
Fig. 43. The cross sections[101,124] for $e^-p \to \nu W^-+X$ and $e^-p \to e^-Z^0+X$ as functions of m^2/s.

$Q^2 = 27,000 \text{ GeV}^2$
$x = 0.25$
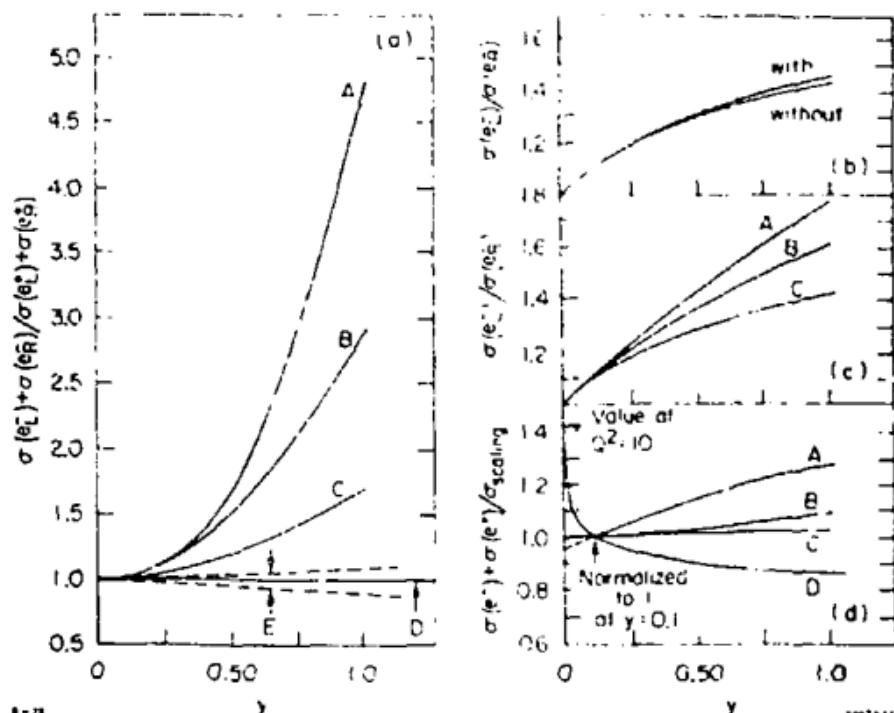
Fig. 44. Various weak electromagnetic interference and strong interaction scaling violation effects[101] in $ep \to e + X$. (a) Charge asymmetries in $\sigma(e_L^-p)/\sigma(e_R^-p)$: A--Weinberg-Salam model with m_Z arbitrarily increased to 150 GeV; B--Weinberg-Salam model with $m_Z = 86$ GeV; C--$SU(2)_L \times SU(2)_R \times U(1)$ model; D--i, std model with $\binom{E^0}{e^-}_R$ doublet; E--estimated uncertainty due to 2γ contributions. (b) Parity violating asymmetry for the Weinberg-Salam model with and without QCD scaling violations. (c) Parity violation in $\sigma(e_L^-p)/\sigma(e_R^-p)$: A--Weinberg-Salam couplings with m_Z taken to ∞; B--Weinberg-Salam with $m_Z = 150$ GeV; C--Weinberg-Salam with $m_Z = 86$ GeV. (d) Apparent scaling violations in $\sigma(e^-p) + \sigma(e^+p)$ coming from strong and weak interaction sources: A--$\binom{E^0}{e^-}_R$ doublet; B--Weinberg-Salam model; C--$SU(2)_L \times SU(2)_R \times U(1)$ model; D--Asymptotic freedom.
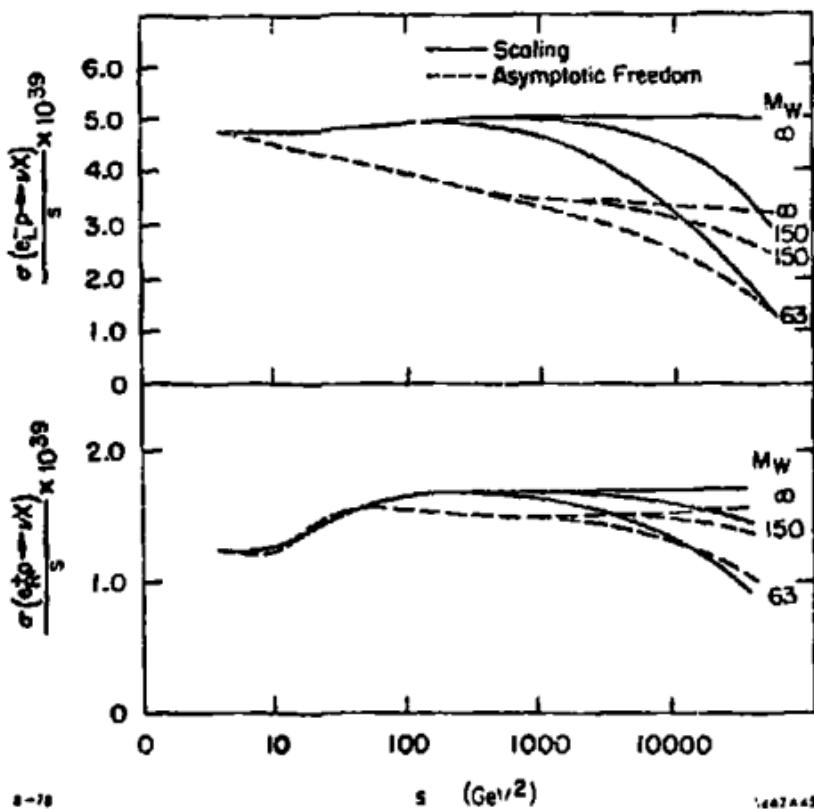
Fig. 45. The effects[69,101,124] on (a) $\sigma(e^-p \to \nu_e + X)$ and (b) $\sigma(e^+p \to \bar{\nu}_e + X)$ cross sections of finite boson masses and QCD scaling violations.
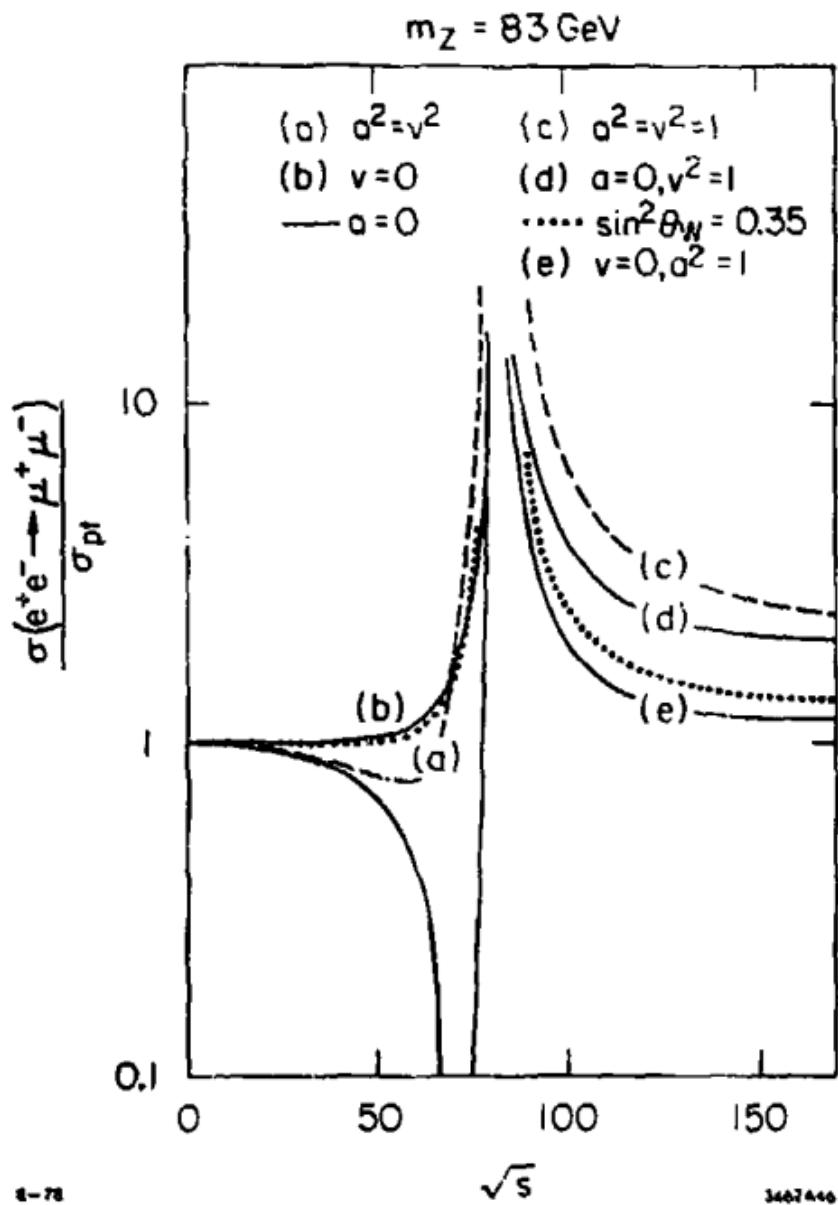
Fig. 46. The shape[93] of the $e^+e^- \to \mu^+\mu^-$ cross section near the Z^0 pole.
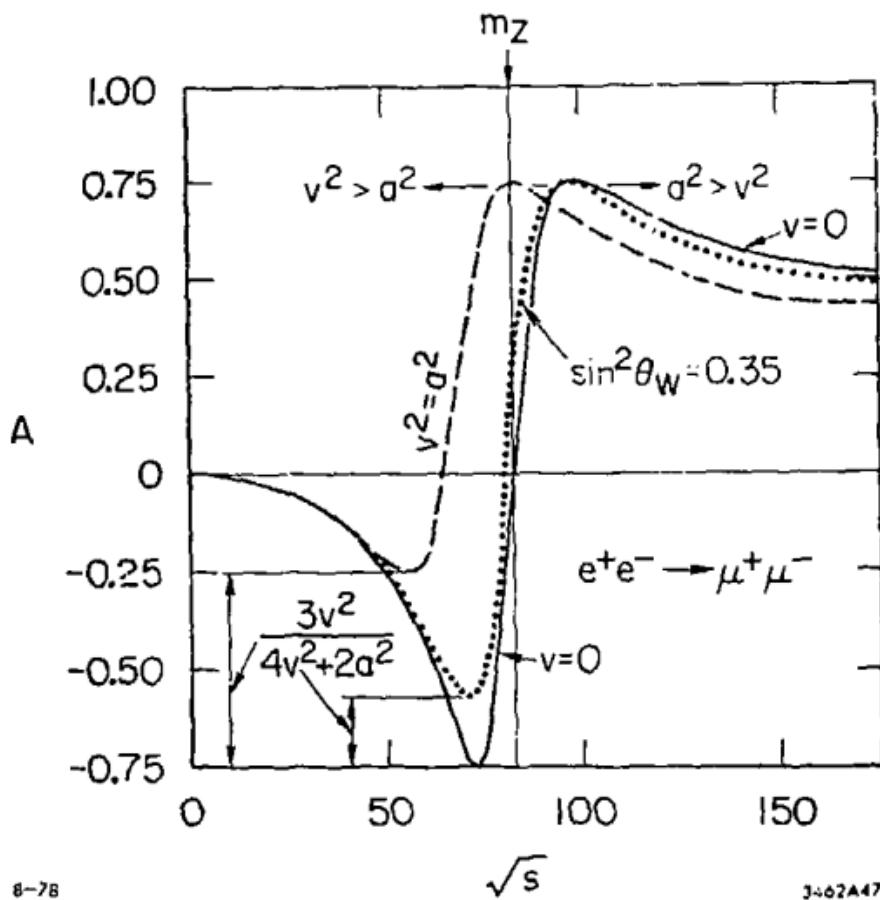
Fig. 47. The shape[93] of the $e^+e^- \to \mu^+\mu^-$ forward-backward asymmetry near the Z^0 pole.
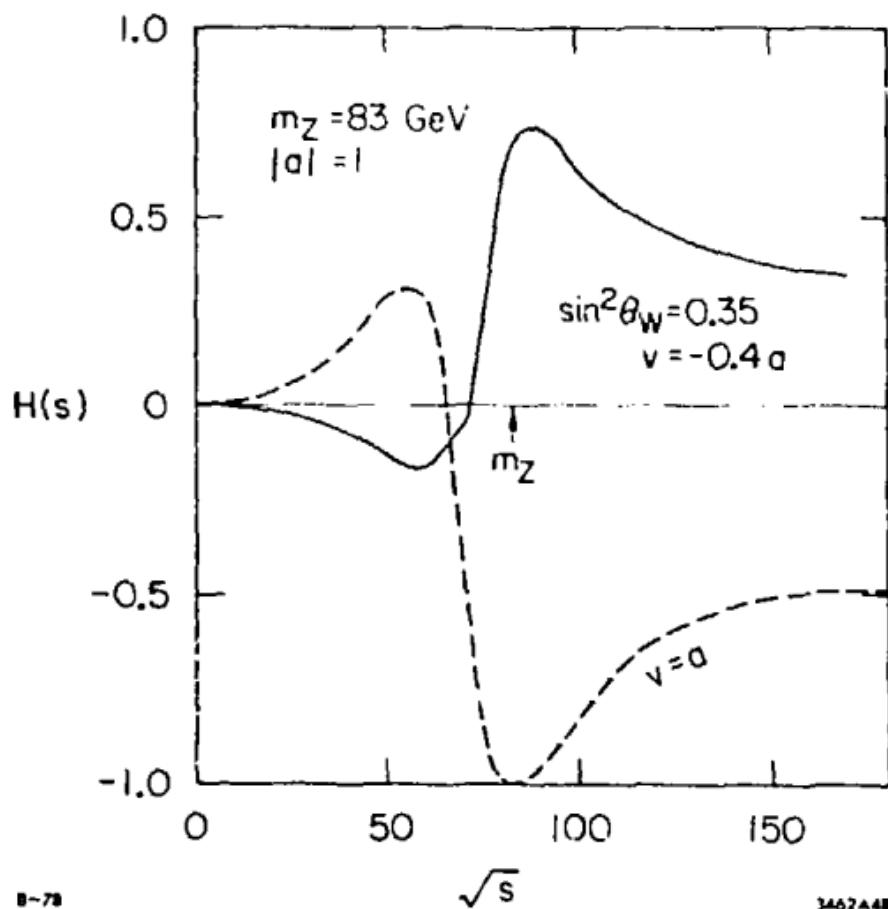
Fig. 48. The average μ (or τ) helicity[93] in $e^+e^- \to \mu^+\mu^-$ (or $\tau^+\tau^-$) near the Z^0 pole.

e^+ W^+

γ, Z^o

e^- W^-

8 – 78

e^+ W^+

ν_e

e^- W^-

3662A49
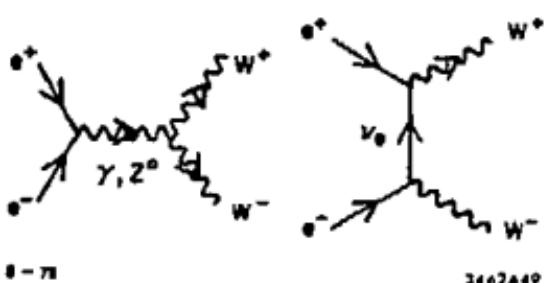
Fig. 49. Diagrams contributing to
$e^+e^- \rightarrow W^+W^-$.
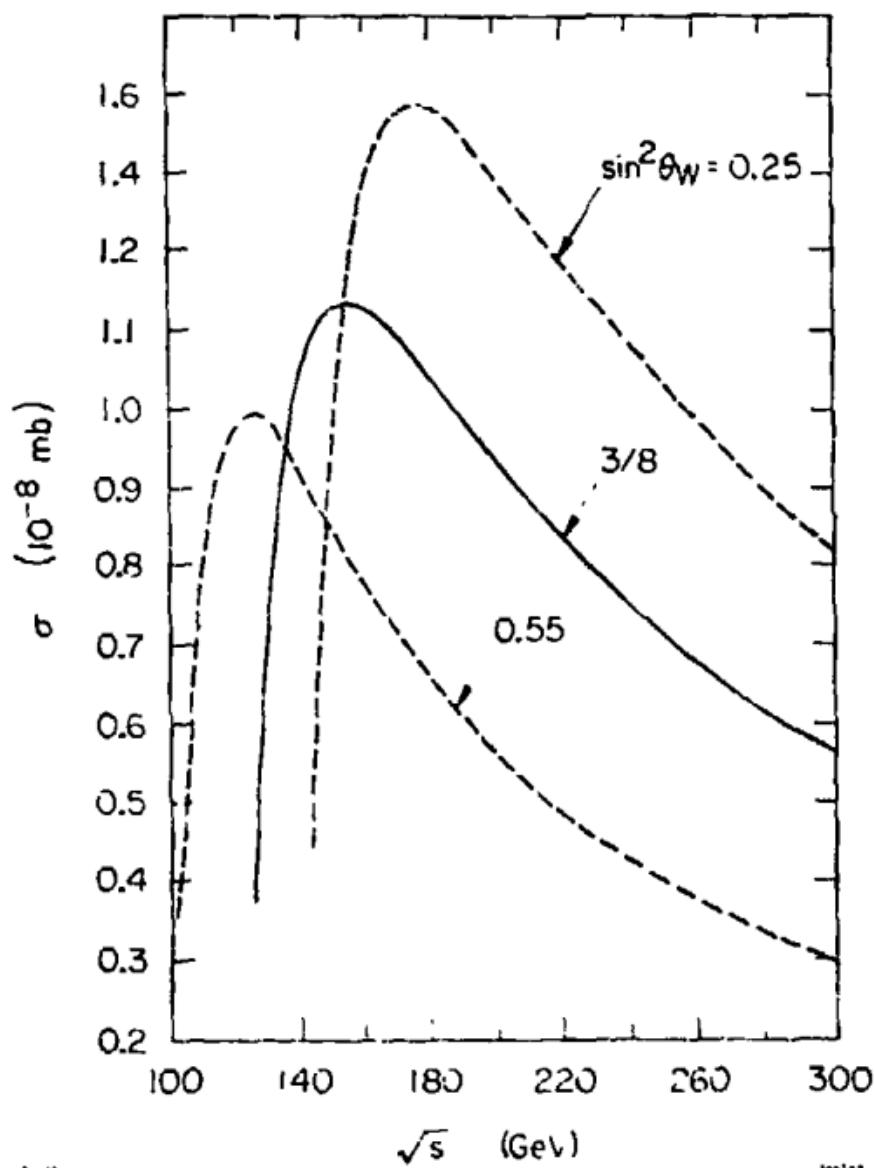
Fig. 50. The total cross section[125] for $e^+e^- \rightarrow W^+W^-$ as a function of the centre-of-mass energy and $\sin^2\theta_W$.
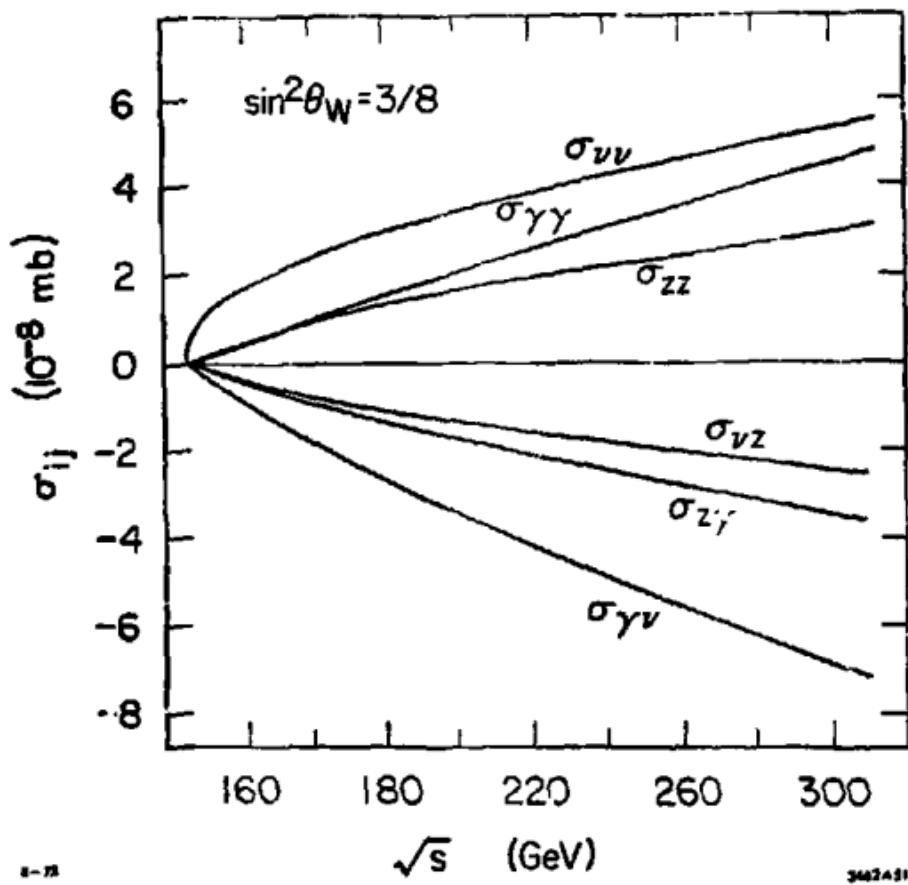
Fig. 5i. The relative magnitudes[125] of different diagrams and their interferences in $e^+e^- \to W^+W^-$.
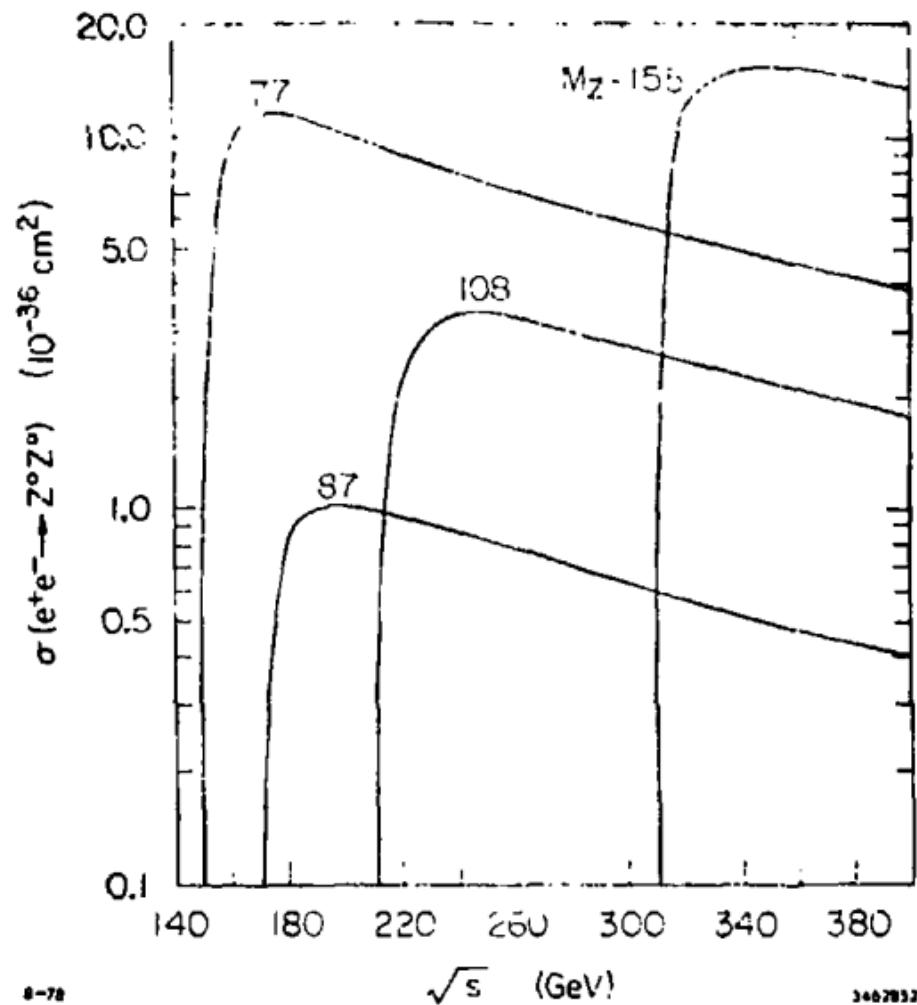
Fig. 52. The cross section of $e^+e^- \to Z^0 Z^0$.
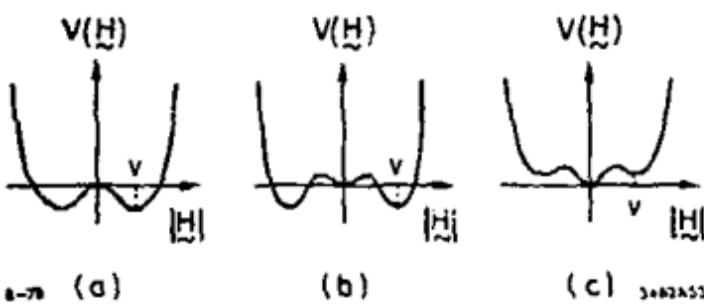
Fig. 53. The Higgs potential (a) in tree approximation,
with radiative corrections and the Universe in
(b) a stable vacuum, and (c) an unstable vacuum.
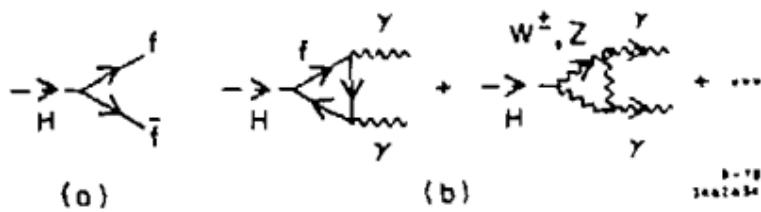
Fig. 54. Higgs decays (a) into $f\bar{f}$, and (b) into $\gamma\gamma$ through virtual fermion and vector boson loops.
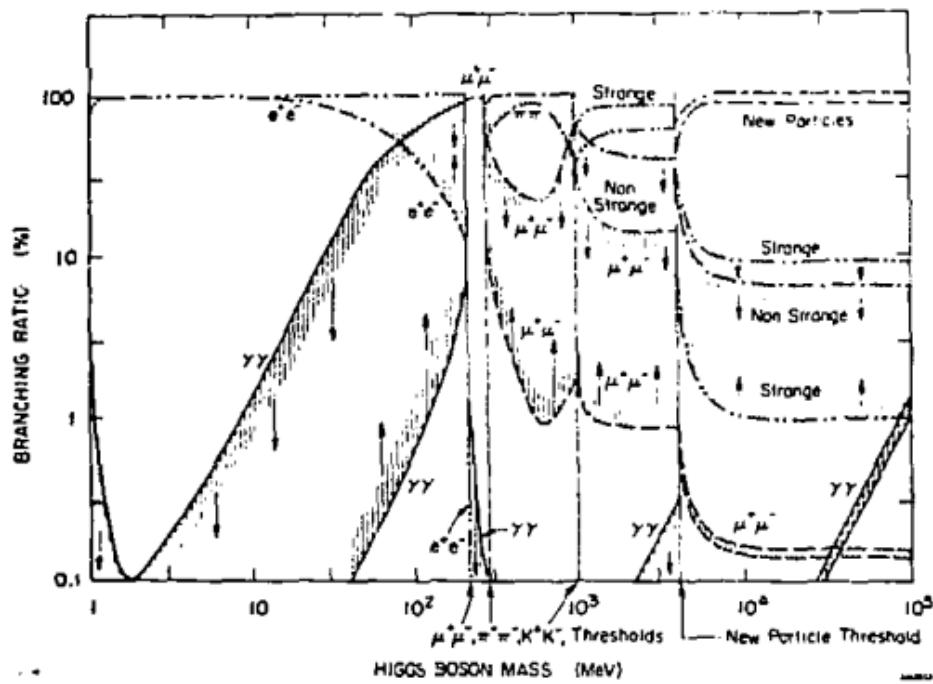
Fig. 55. A compendium[10] of Higgs decay branching ratios for different values of m_H.
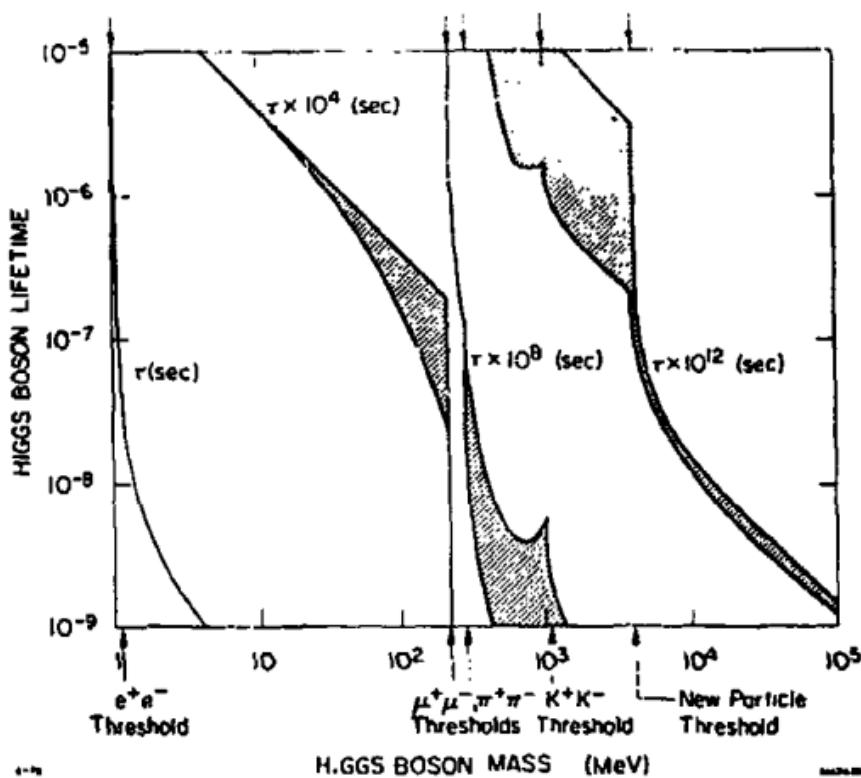
Fig. 56. The Higgs boson lifetime[10] as a function of its mass.

$T, V_{t\bar{t}}$

H

γ

8 — 78   3442A57
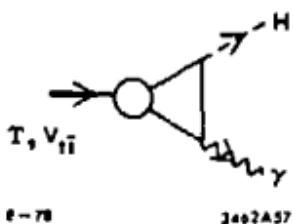
Fig. 57. The decay $V \to H + \gamma$.
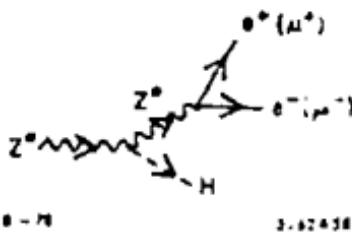
Fig. 58. The decay $Z^0 \to H + \mu^+\mu^-$.
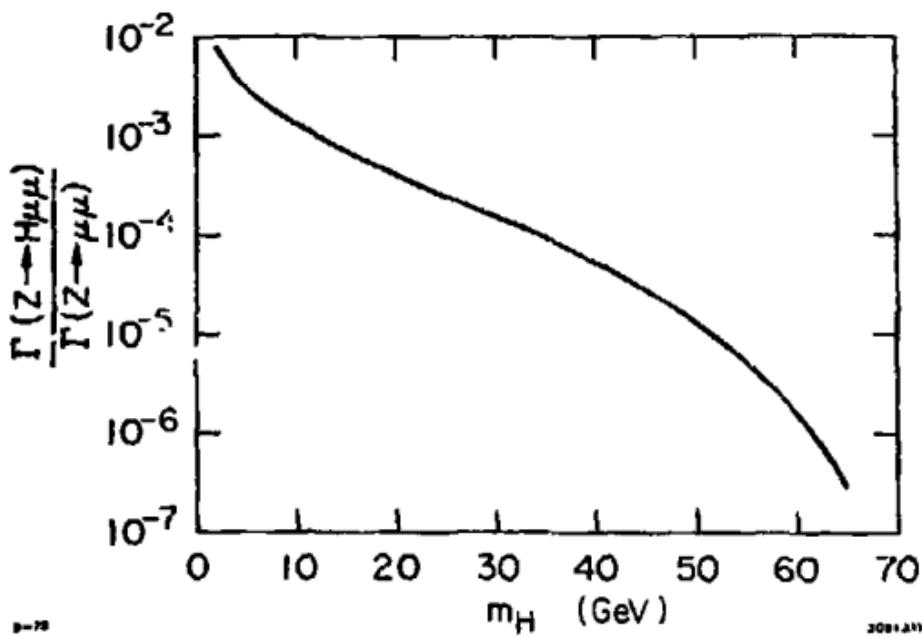
Fig. 59. The rate $\Gamma(Z^0 \to H\mu^+\mu^-)/\Gamma(Z^0 \to \mu^+\mu^-)$ as a function of m_H.[122]
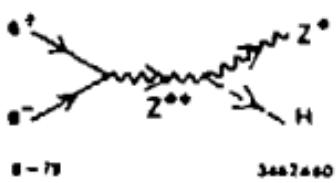
Fig. 60. The process $e^+e^- \to Z^{0*} \to Z^0 + H$.
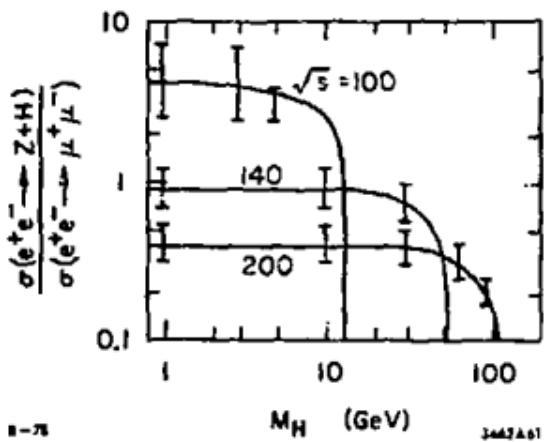
Fig. 61. Calculations[164] of $\sigma(e^+e^- \to Z^0 + H)/\sigma_{pt}$
for different values of $\sqrt{s}$, m_H and
$\sin^2 \theta_W$.
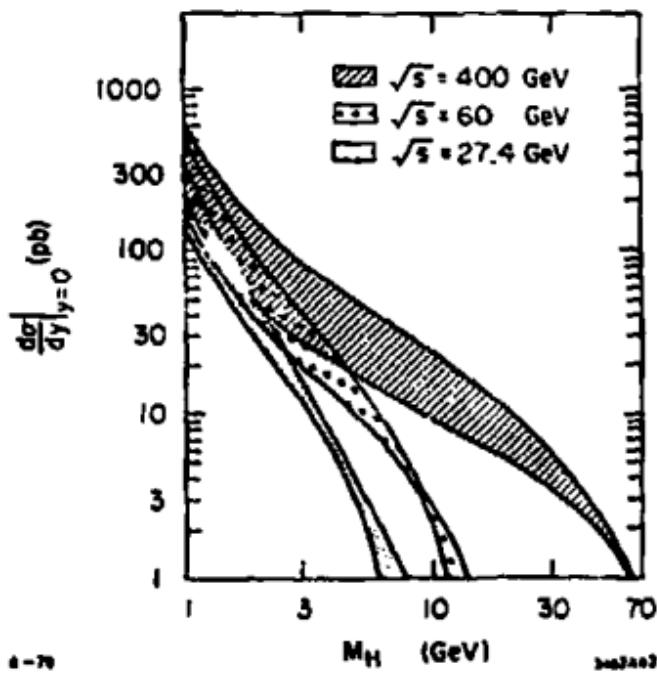
Fig. 62. Calculations[165] of $pp \to H+X$ as functions of m_H and $\sqrt{s}$.
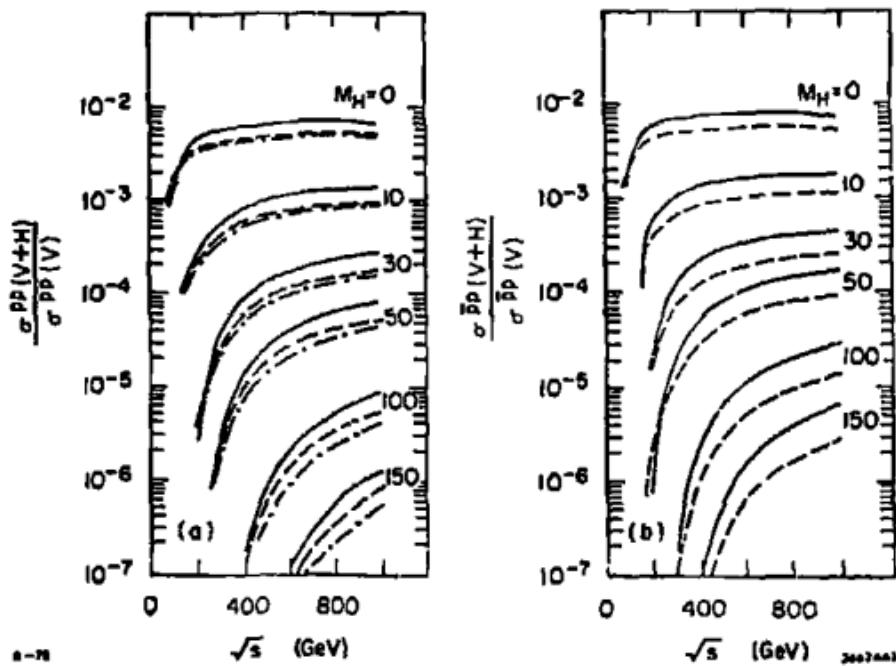
Fig. 63. Calculations[164] of pp or p̄p → $W^{\pm}$ or Z^0 +H+X as functions of m_H at $\sqrt{s}$ = 800 GeV. In (a) the solid/dashed/dot-dashed lines refer to $\sigma(W^++H)/\sigma(W^+)$, $\sigma(W^-+H)/\sigma(W^-)$ and $\sigma(Z+H)/\sigma(Z)$ respectively; in (b) the solid/dashed lines refer to $\sigma(W^{\pm}+H)/\sigma(W^{\pm})$ and $\sigma(Z+H)/\sigma(Z)$ respectively.
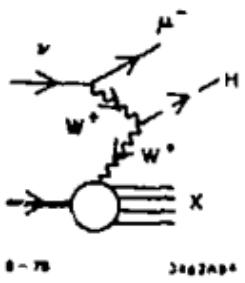
Fig. 64. The dominant diagram[10]
for ν+N → μ⁻+H+X.

ν or σ

Detector

Beam

8-78
3482465
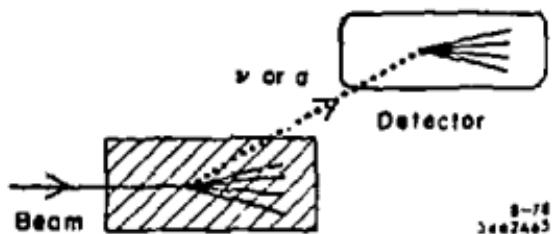
Fig. 65. A schematic sketch of a beam
dump experiment.

(a)   **(b)**

δ∼π   1662440
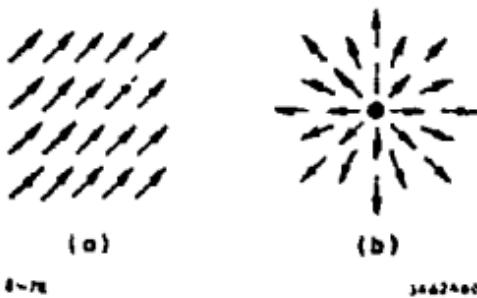
Fig. 66. The spontaneous symmetry breaking
Higgs vacuum expectation value
(a) independent of x as usual, and
(b) in the presence of a monopole.

e^+ e^+ M γ

γ M   M Z^0

γ $\overline{M}$ $W^{\pm}$

e^- e^- $\overline{M}$:

(a)   **(b)**   **(c)**   **(d)**
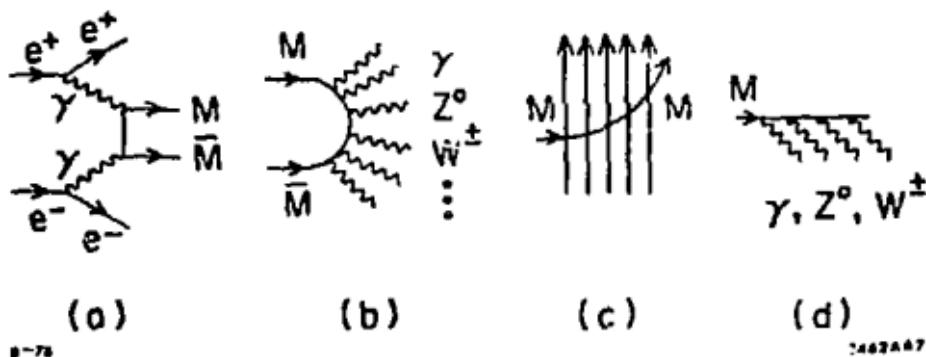
Fig. 67. Monopoles[147] (a) being produced, (b) annihilating to give many γ's, (c) aligning parallel to a magnetic field, and (d) losing energy by radiation.

8 - 79   (o)   (b)   JADJAO0
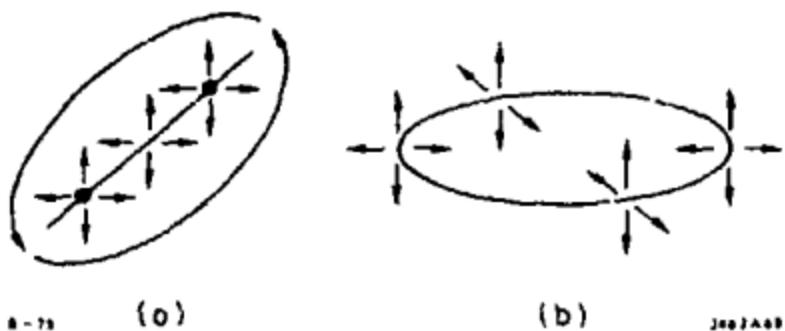
Fig. 68.   Illustrations of possible extended objects in the
            Weinberg-Salam model: (a) a dumb-bell,[150] and
            (b) a flux loop.[151]

α(Q²)   m(Q²)

SU(3)

SU(2)   M_GUM

U(1)   SU(5)

M_q

M_ℓ   M_GUM

M_q=M_ℓ

10   10¹⁵ (GeV)   10   10¹⁵ (GeV)

8-79   (a)   (b)   3442A70
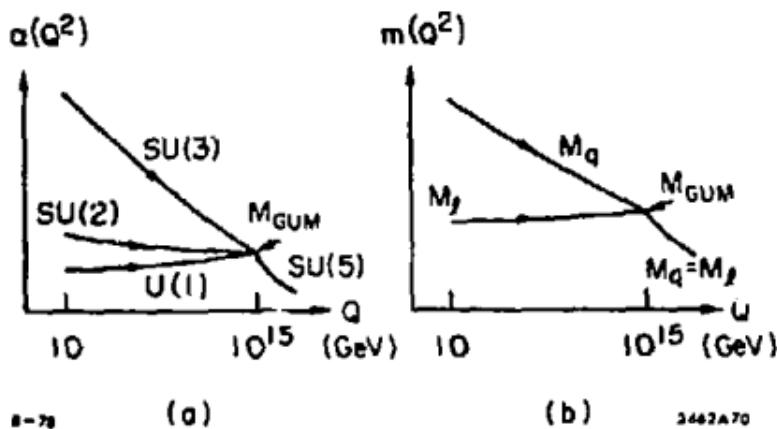
Fig. 49. Qualitative sketches (a) of the
present greatly different weak
and strong coupling constants be-
coming unified at very high ener-
gies, and (b) of quark and lepton
masses which are equal when meas-
ured on the grand unification
mass scale becoming different at
low Q².
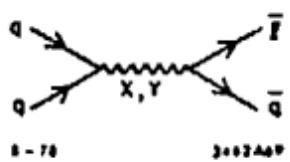
Fig. 70. A typical baryon number violating interaction.